IEEE Access
Multidisciplinary ⋮ Rapid Review ⋮ Open Access Journal

Received 17 June 2024, accepted 3 September 2024, date of publication 6 September 2024, date of current version 27 September 2024.

Digital Object Identifier 10.1109/ACCESS.2024.3455550

RESEARCH ARTICLE

A Modified Bonobo Optimizer With Its Application in Solving Engineering Design Problems

MAALI ALABDULHAFITH[1], (Member, IEEE), HARSHIT BATRA[2,3], NAGWAN M. ABDEL SAMEE[1], MOHAMMED AZMI AL-BETAR[4,5], (Member, IEEE), AMMAR ALMOMANI[5,6], DAVUT IZCI[7,8], SERDAR EKINCI[7], AND FATMA A. HASHIM[9,10]

[1]Department of Information Technology, College of Computer and Information Sciences, Princess Nourah bint Abdulrahman University, P.O. Box 84428, Riyadh 11671, Saudi Arabia
[2]Department of Computer Science and Engineering, Netaji Subhas University of Technology, Dwarka, New Delhi 110078, India
[3]Centre of Excellence in AI, Netaji Subhas University of Technology, Dwarka, New Delhi 110078, India
[4]Artificial Intelligence Research Center (AIRC), Ajman University, Ajman, United Arab Emirates
[5]Department of Information Technology, Al-Huson University College, Al-Balqa Applied University, Al-Huson, Irbid 19117, Jordan
[6]Department of Computer Information Science, Higher Colleges of Technology, Sharjah, United Arab Emirates
[7]Department of Computer Engineering, Batman University, 72100 Batman, Türkiye
[8]Applied Science Research Center, Applied Science Private University, Amman 11931, Jordan
[9]Faculty of Engineering, Helwan University, Cairo 11795, Egypt
[10]MEU Research Unit, Middle East University, Amman 11831, Jordan

Corresponding author: Mohammed Azmi Al-Betar (m.albetar@ajman.ac.ae)

This work was supported by Princess Nourah bint Abdulrahman University, Riyadh, Saudi Arabia, through the Researchers Supporting Project PNURSP2024R407.

ABSTRACT This paper presents a modified bonobo optimizer (MBO) that integrates the Gaussian local mutation, restart strategy, and random contraction strategy into the original bonobo optimizer (BO). BO, inspired by the unique reproductive schemes and fission-fusion social behaviors of bonobos, has previously demonstrated promising results in solving a range of optimization problems. With the new modifications, MBO seeks to improve exploration and exploitation abilities, achieving enhanced convergence speed and solution quality. The Gaussian local mutation aids in fine-tuning solutions by introducing localized variations, the restart strategy provides a mechanism to escape potential local optima, while the random contraction strategy ensures better global search capabilities. The enhanced MBO's performance is critically assessed on the 10 and 100-dimensional CEC 2017 and 10 and 20-dimensional CEC 2022 benchmark suites, along with seven engineering optimization problems, including cantilever beam design, industrial refrigeration system design, welded beam design, speed reducer design, pressure vessel design, multi-product batch plant design, and three-bar truss design. The MBO algorithm exhibits significant improvements in optimization performance, evidenced by highly significant p-values (as low as 1.25E-11) in the Wilcoxon's Signed Rank Test. Preliminary results indicate that the MBO exhibits a marked improvement in both solution accuracy and robustness over its predecessor and other state-of-the-art optimization algorithms such as original bonobo optimizer, sand cat swarm optimization, Chernobyl disaster optimizer, driving training-based optimization, Harris hawk optimizer, Archimedes optimization algorithm, smell agent optimizer, grasshopper optimization algorithm, particle swarm optimization, hybrid sine cosine algorithm with differential evolution, modified capuchin search algorithm, liver cancer algorithm, and modified chameleon swarm algorithm. The algorithm's robust performance can be attributed to its accelerated convergence rate, stability across diverse functions, good exploration-exploitation behavior, and adaptability to high-dimensional and complex solution spaces. The systematic enhancement of proposed algorithm's convergence capabilities positions it as a reliable and efficient tool for addressing challenging engineering optimization problems.

The associate editor coordinating the review of this manuscript and approving it for publication was Okyay Kaynak.

INDEX TERMS Metaheuristics, nature inspired algorithms, modified bonobo optimizer, swarm intelligence, optimization.

I. INTRODUCTION

A. BACKGROUND

Optimization-oriented challenges are pervasive in both our daily activities and professional endeavors. The pursuit of effective and efficient approaches to address such optimization issues has emerged as a crucial focus of research [1]. Optimization involves the identification of the optimal or a satisfactory approximate solution from a myriad of possibilities, given specific conditions for a given problem [2]. As cutting-edge technologies advance, the prevalence and complexity of optimization problems are growing across diverse engineering domains. These encompass fields such as image processing [3], renewable energy [4], artificial intelligence [5], hydrologic and hydraulic modeling [6], production scheduling [7], controller design [8], filter design for system identification [9], aerospace [10], biomedicine and biomedical applications [11], production design [12], vehicle routing [13], vehicle cruise control [14], feature selection [15], mechanical engineering [16], power system engineering [17], fault diagnosis [18], among others. The application of optimization yields substantial enhancements in problem-solving efficiency, reduction of computational burden, and cost savings.

B. RELATED WORKS

Optimization methods can broadly be categorized into mathematical methods and metaheuristic methods. Mathematical methods involve the iterative pursuit of an optimal solution based on a predefined mathematical model and initial conditions. Various mathematical techniques, such as the Nelder-Mead algorithm [19], gradient descent method [20], Hooke and Jeeve algorithm [20], Lagrange multiplier method [21] and Newton's method [22], fall under this category. While these methods are effective for simple problems with low-dimensional solution spaces, practical applications often involve large-scale, nonlinear, and multimodal complex optimization challenges [23]. Mathematical methods rely on gradient information and are sensitive to initial points [24], making them less suitable for addressing complex issues where finding the optimal solution is challenging and local optima are easily encountered. Consequently, mathematical methods face significant limitations in dealing with intricate optimization problems.

Metaheuristic methods constitute an algorithmic framework that transcends specific problems, drawing inspiration from natural phenomena, biological behaviors, or mathematical principles [25], [26], [27], [28], [29]. Serving as an advantageous alternative to mathematical methods, metaheuristic approaches possess qualities such as randomness, straightforward implementation, and a black-box perspective, compensating for the limitations associated with mathematical algorithms. Recently, these methods have gained substantial attention in scholarly works and are frequently utilized to address diverse and intricate engineering challenges.

Within existing literature, three primary methodologies guide the development of metaheuristic algorithms: the creation of novel algorithms, the amalgamation of existing algorithms, and the formulation of hyper heuristics. The processes of introducing new optimization algorithms and synthesizing pre-existing ones are not conflicting; instead, they are mutually beneficial. On one hand, newly devised optimization algorithms serve to address the deficiencies of existing algorithms in specific domains or particular problem instances, offering improved solutions for intricate real-world problems. Many emerging optimization algorithms incorporate strategies or operators with unique search characteristics, presenting a diverse avenue for enhancing the optimization performance of established algorithms. For instance, cuckoo search [30], a relatively recent algorithm, introduced a Levy flight strategy renowned for its effective exploration characteristics. This strategy has been widely integrated into various existing algorithms to enhance their ability to navigate away from local optima [31]. Additionally, numerous new algorithms are fused with established ones to craft hybrid algorithms, capitalizing on the strengths of each constituent algorithm to bolster overall optimization performance.

C. MOTIVATION

As technology advances rapidly and new application requirements emerge, optimization algorithms are increasingly finding application in novel domains such as smart cities [32], smart water management [33], unmanned driving [34], and the internet of things [35]. Concurrently, the rise of key technologies like parallel computing and adaptive computing is enhancing the efficiency and precision of various algorithms, broadening the scope of application for optimization algorithms. Despite this expansion, the utilization of optimization algorithms in diverse fields poses continual challenges and complexities. Many modern engineering problems, characterized by non-separable, nonconvex, and extensive search spaces, present difficulties leading to performance degradation or low convergence for most optimizers [36]. Hence, there is a crucial need to persist in exploring and researching algorithms that enhance these applications, seeking effective optimization technology through practical experimentation.

While numerous optimization algorithms already exist, the imperative of developing new optimizers persists. The no free lunch (NFL) theory [37] posits that no single optimizer can universally excel in solving every optimization problem. This is attributed to three primary reasons. Firstly, the inherent stochastic nature of metaheuristic algorithms can lead to disparities between the discovered optimal solution and the true solution for a given problem, particularly when the solutions are unknown. Consequently, it is challenging to ascertain the optimality of existing algorithms, necessitating the development of new and more efficient optimization algorithms to better tackle such issues and enhance solution accuracy and algorithm efficiency. Secondly, many practical problems exhibit unique characteristics aligned with the search behaviors of specific optimization algorithms, stemming from the inspiration behind their development [38]. While an algorithm may excel in addressing a particular problem due to its tailored search behavior, it may lack robustness when applied to dissimilar problems. Moreover, a new optimization algorithm can introduce distinctive values that complement and extend beyond the capabilities of existing ones. Additionally, the development of a new optimization algorithm presents an opportunity for knowledge sharing and contributes to addressing real-world challenges. Typically, a novel optimization algorithm incorporates specific strategies or operators that can seamlessly enhance the performance of existing methods [39]. Consequently, the continuous need for new optimization algorithms lies in their ability to explore diverse search strategies for specific problems, providing valuable contributions to the optimization community. These considerations constitute the primary motivation behind the current study.

D. NOVELTY AND CONTRIBUTIONS

In light of the above discussion, this paper aims to develop a new metaheuristic algorithm by improving the performance of an existing one. In that sense, one of the recently reported metaheuristic approach named bonobo optimizer [40] is adopted. This optimizer emulates the social behavior and reproductive strategies of bonobos to solve optimization problems. A modified version of the bonobo optimizer is proposed in this work which is prompted by the realization that there are areas of potential improvement in the original algorithm's performance. The proposed version incorporates four pivotal enhancements: a new exploration mechanism, Gaussian local mutation, restart strategy, and random contraction strategy. The exploration mechanism of the snow ablation optimizer [41] is specifically chosen to replace the exploration phase of the bonobo optimizer. This is performed by considering the prowess of the snow ablation optimizer's exploration approach that adeptly harnesses Brownian motion. The Gaussian mutation method ensures a delicate equilibrium between exploration and exploitation which decreases the risk of stagnation. The restart strategy is used to detect a potential entrapment in a local optimum and repositioning it by initiating from a new, randomly chosen point in the solution landscape. The random contraction strategy is used to shrink the search space around promising regions, thus, directing the algorithm's resources towards more probable solution areas and makes the search process more efficient.

In the realm of optimization algorithms, the continuous pursuit of innovative methods to address complex engineering challenges remains an ever-present goal. In this context, the proposed modified version of bonobo optimizer emerges as a promising contender. This study, therefore, delves into its practical efficacy through a comprehensive evaluation against benchmark functions and real-world engineering optimization problems. Benchmarking algorithms against established standards provides a rigorous foundation for assessing their performance. Our investigation begins with an in-depth analysis of the proposed algorithm's capabilities, benchmarking it against a diverse set of nature-inspired algorithms renowned for their versatility and widespread use. The evaluation includes prominent algorithms such as the original bonobo optimizer (BO) [40], sand cat swarm optimization [42], Chernobyl disaster optimizer [43], driving training-based optimization [44], Harris hawk optimizer [45], Archimedes optimization algorithm [46], smell agent optimizer [47], grasshopper optimization algorithm [48], particle swarm optimization [49], hybrid sine cosine algorithm with differential evolution [50], modified capuchin search algorithm [51], liver cancer algorithm [52], and modified chameleon swarm algorithm [53].

The benchmarking process involves extensive experimentation on the CEC 2017 and CEC 2022 test suites, collection of optimization problems showcasing unimodal, multimodal, hybrid, and composite functions. The results garnered from the benchmarking phase underscore the proposed algorithm's notable performance across a spectrum of optimization landscapes. Particularly, it exhibits remarkable efficiency in converging to optimal solutions for unimodal functions, showcasing its competence in navigating singular global optima. In the realm of multimodal functions, characterized by multiple local and global optima, MBO consistently outperforms its counterparts, demonstrating robustness in dealing with diverse optimization landscapes.

Building upon the benchmarking foundation, the study advances to address seven real-world engineering optimization problems. These challenges span cantilever beam design, industrial refrigeration system design, welded beam design, speed reducer design, pressure vessel design, multiproduct batch plant design, and three-bar truss design. The meticulous evaluation involves comparing the proposed algorithm against various optimization algorithms, considering metrics such as the minimum objective function value, standard deviation, and rank. The standout performance of the proposed algorithm in these engineering problems is a testament to its adaptability and reliability in handling intricate real-world scenarios. For instance, in the cantilever beam design problem, where the goal is to minimize the weight of a complex beam structure, the proposed algorithm consistently outshines its competitors, exhibiting not only the lowest minimum objective function value but also a superior convergence rate. Similar trends are observed in other engineering challenges, such as industrial refrigeration system design, welded beam design, and more.

II. BONOBO OPTIMIZER

A. BACKGROUND

The bonobo optimizer (BO) is an algorithm inspired by the unique social behavior and reproductive strategies exhibited by bonobos (scientific name: Pan paniscus), part of the Homininae subfamily, to which humans also belong. This common ancestry makes bonobos the closest living relatives to humans, sharing over 98% of their genetic profile [54]. Discovered initially in 1929 at the Belgian colonial museum [55], these creatures have continued to spark intrigue due to their marked similarity to humans. The divergence in the line of human ancestry and that of the bonobo happened approximately eight million years ago, with a later split between the common chimpanzee and bonobo lineages. Bonobos and chimpanzees form fission-fusion groups, characterized by a large community that splits into smaller societies or subgroups, varying in size and male-female ratio. These subgroups separate and then periodically reassemble based on various activities [55]. These communities display a clear linear dominance hierarchy among both male and female bonobos, determined by the individual's inclusive fitness values. A crucial differentiation between bonobo and common chimpanzee societies lies in their power dynamics: while bonobo societies are predominantly female dominated, some literature alternately refers to females as ''co-dominant'' [56], ''almost co-dominant,'' or'' of the same rank as males'' [57]. The individuals' rank and dominance determine their eligibility for access to resources and participation in reproductive activities.

In these societies, male bonobos typically remain in their natal community, while females migrate to new communities during adolescence, striving to establish themselves there. Four distinct mating strategies have been observed in bonobo societies: promiscuous mating, restrictive mating, consortship mating, and extra-group mating. The choice of a particular mating strategy depends on various factors such as the availability of food, male support, and the dominance hierarchy. These mating strategies aim to maximize reproductive success and maintain genetic diversity.

B. MATHEMATICAL MODEL

The BO emulates the social behavior and reproductive strategies of bonobos to solve optimization problems [58]. Analogous to other metaheuristic approaches, the BO utilizes a fixed population size and initializes the population randomly. In the bonobo hierarchy, the alpha bonobo (bonobo) holds the top rank and is selected as the optimum fitness value achiever among the population. The alpha bonobo is therefore considered the current best solution. After this, BO's parameters (not user-defined) are initialized with their respective initial values. It should be noted that all the random numbers used in this algorithm range from 0 to 1.

1) INITIALIZATION OF NON-USER-DEFINED PARAMETERS

The non-user-defined BO parameters such as probability of phase (*pp*), positive phase count (*ppc*), negative phase count (*npc*), probability of extra-group mating (*pxgm*), change in phase (*cp*), temporary sub-group size factor (*tsgsfactor*), and directional probability (*pd*) are initialized as $ppc = 0$; $npc = 0$; $cp = 0$; $pxgm = pxgm_{initial}$; $tsgsfactor = tsgsfactor_{initial}$; $pp = 0.5$; $pd = 0.5$. Here, $tsgsfactor_{initial}$ and $pxgm_{initial}$ represent the initial values of *tsgsfactor* and *pxgm*, respectively. Further details on these parameters are explored in the following relevant sections.

2) POSITIVE PHASE AND NEGATIVE PHASE

The algorithm considers two phases or states: positive phase (*PP*) and negative phase (*NP*). A *PP* signifies ideal living conditions such as adequate food, successful mating, and protection, leading to the noticeable improvement of fitness in the best solution (alpha bonobo). Conversely, an *NP* is marked by a significant absence of these conditions, with no observable improvement in the current-best solution. As the algorithm iterates, each phase is counted via parameters *ppc* and *npc* for *PP* and *NP*, respectively. These parameters are initially set to zero and incremented when their corresponding phase is active. When one phase count increments, the other resets to zero. It should be noted that in a bonobo community, the status of the alpha bonobo can change. Therefore, a bonobo with higher potential could replace the current alpha bonobo.

3) BONOBO SELECTION USING FISSION-FUSION SOCIAL STRATEGY

Depending on the current phase (*PP* or *NP*), the algorithm applies distinct update mechanisms (or mating schemes) to generate offspring. Another bonobo, chosen based on bonobos' fission-fusion social behavior, participates in mating. In this behavior, bonobos from a larger community form smaller, random-sized temporary sub-groups, which later rejoin the main community. Inspired by this, the mating bonobo is selected. The maximum size of a temporary sub-group (*tsgsmax*) is determined based on the total population size (N) and computed as follows:

$$tsgsmax = max(2, \lceil tsgs_{factor} \times N \rceil) \tag{1}$$

where $tsgs_{factor}$ is the temporary sub-group size factor. If ($tsgs_{factor} \times N$) results in a non-integer, it is rounded up to the nearest integer. To generate a new offspring, the i^{th} bonobo is modified through an exchange of properties with another bonobo (p-bonobo). A temporary subgroup is selected randomly from the population excluding the i^{th} bonobo. From this subgroup, if the fittest bonobo has better fitness than the ith bonobo, it is selected as the p-bonobo. However, if the fittest bonobo has lower fitness, a p-bonobo is randomly chosen from the subgroup. This selection process is repeated every time a bonobo undergoes modification.

4) CREATION OF NEW BONOBO USING DIFFERENT MATING STRATEGIES

The methodology for the creation of a new bonobo revolves around two primary scenarios: positive and negative phases.

In *PP*, the bonobo community is flourishing, characterized by sufficient food re-sources, a safe living environment, an array of genetic variations, and a high success rate of mating. During the *PP*, the probability of implementing promiscuous and restrictive mating strategies is substantially high. The promiscuous mating strategy implies that an estrus female is accessible to both the alpha bonobo and other lower rank males. On the other hand, the restrictive mating strategy allows only the alpha and higher-rank bonobos to mate.

The *NP* represents challenging times in the bonobo community due to factors like scarcity of food, threat from predators or intra-species conflict. During the *NP*, the instances of consortship and extra-group mating increase. In consortship mating, a bonobo couple separates from their group, spends time together, and reenters their group after a few days or weeks. Extra-group mating refers to the event where a female bonobo mates with males from other groups. Despite the higher probability of occurrence, extra-group mating is relatively less frequent compared to consortship mating.

These real-world behaviors are translated into a mathematical model, forming the core of the BO. The BO utilizes a phase-probability (*pp*), initially set at 0.5. This value adjusts at each iteration according to the current phase and phase count. For a positive phase, *pp* varies from 0.5 to 1.0, and for a negative phase, it ranges from 0 to 0.5.

Promiscuous and restrictive mating strategies: To determine the mating strategy, a random number r between 0.0 and 1.0 is generated. If r falls within or equals *pp*, the generation of a new bonobo happens via promiscuous or restrictive mating, following the following definition.

$$new\_bnb_j = bnb_{ij} + r1 \times scab \times (\alpha_{bonobo} - bnb_{ij}) + (1-r1) \times scsb \times flag \times (bnb_{ij} - bnb_{pj}) \tag{2}$$

Here, α_{bonobo} and new_bnb_j represent the j^{th} variables of the alpha bonobo and offspring respectively. The bnb_{ij} and bnb_{pj} represent the j^{th} variable of the i^{th} and p^{th} bonobo respectively. The parameters *scab* and *scsb* are the sharing coefficients for α_{bonobo} and selected p^{th} bonobo. The flag parameter can only be either 1 or −1, depending on the fitness of i^{th} and p^{th} bonobo.

Consortship and extra-group mating strategies: If r is larger than *pp*, then the chosen strategy is either consortship or extra-group mating. The decision between these two strategies relies on another random number $r2$. If $r2$ is within or equals the probability of extra-group mating (*pxgm*), a new bonobo is created through extra-group mating strategy. The generation of a new bonobo through extra-group mating follows a series of equations depending on the comparison between α_{bonobo} and $bonobo_{ij}$ and a third random number $r3$.

$$\beta 1 = e^{(r3^2 + r3 - 2/r3)} \tag{3}$$

$$\beta 2 = e^{(-r3^2 + 2 \times r3 - 2/r3)} \tag{4}$$

The new bonobo is then created according to one of the following equations:

$$new\_bnb_j = bnb_{ij} + \beta 1 \times \left(Var_{maxj} - bnb_{ij}\right), \quad if\, \alpha_{bonobo} \geq bnb_{ij}\ and\ r3 \leq pd \tag{5}$$

$$new\_bnb_j = bnb_{ij} + \beta 2 \times \left(bnb_{ij} - Var_{minj}\right), \quad if\, \alpha_{bonobo} \geq bnb_{ij}\ and\ r3 > pd \tag{6}$$

$$new\_bnb_j = bnb_{ij} + \beta 1 \times \left(bnb_{ij} - Var_{minj}\right), \quad if\, \alpha_{bonobo} < bnb_{ij}\ and\ r3 \leq pd \tag{7}$$

$$new\_bnb_j = bnb_{ij} + \beta 2 \times \left(Var_{maxj} - bnb_{ij}\right), \quad if\, \alpha_{bonobo} < bnb_{ij}\ and\ r3 > pd \tag{8}$$

When $r2$ is greater than *pxgm*, the consortship mating strategy comes into play, and the new bonobo is created using the subsequent equation:

$$new\_bnb_j = bnb_{ij} + flag \times e^{-r4} \times \left(bnb_{ij} - bnb_{pj}\right) \tag{9}$$

If *flag* is 1 or $r5 \leq pd$, then new_bnb_j is computed according to the equation. Otherwise, $new\_bnb_j = new\_bnb_{pj}$.

Updating BO parameters: The parameters in the BO model, namely *pp*, *npc*, *ppc*, *cp*, *pd*, *pxgm*, *tsgsfactor*, undergo updates after each iteration. These updates are based on the change in the fitness of α_{bonobo} from one iteration to another. The updated values of these parameters are then used in the subsequent iteration. The update of parameters is performed as:

- $ppc = 0$,
- $npc = npc + 1$,
- $cp = -min(0.5, npc \times rcpp)$,
- $pp = 0.5 + cp$, $pd = 0.5$,
- $pxgm = min(0.5, pxgm_{initial} + npc \times rcpp^2)$,
- $tsgsfactor = max(0, tsgsfactor_{initial} - npc \times rcpp^2)$.

III. PROPOSED ALGORITHM

The modified BO (MBO) is an improved version of the standard BO, prompted by the realization that there are areas of potential improvement in the original algorithm's performance. This new version incorporates four pivotal enhancements: a new exploration mechanism, Gaussian local mutation, restart strategy, and random contraction strategy. The Gaussian local mutation infuses stochasticity into the optimization process, emulating the natural variations found in evolutionary algorithms. By leveraging a Gaussian distribution, this mutation method ensures a delicate equilibrium between exploration (probing new regions of the solution space) and exploitation (honing in on previously discovered promising solutions). Such a probabilistic approach makes the search more dynamic, decreasing the risk of stagnation. However, in metaheuristic optimization, there's an inherent danger of the search becoming trapped in local optima, solutions that seem optimal in their vicinity but are inferior when the entire search space is considered. To mitigate this, the MBO employs the restart strategy. Upon detecting a potential entrapment in a local optimum, the algorithm strategically repositions its search, initiating from a new, randomly chosen point in the solution landscape. This deliberate reset acts as a countermeasure to stagnation, ensuring a thorough and expansive search while maintaining the algorithm's efficiency. Lastly, the random contraction strategy is an innovative technique to shrink the search space. By dynamically contracting the solution space around promising regions, it ensures that the algorithm's resources are directed towards more probable solution areas, making the search process more efficient. The flowchart in Figure 1 demonstrates the working principle of the proposed MBO.

A. EXPLORATION STAGE

The exploration stage is a pivotal component of optimization algorithms, offering a broad view of the problem space. This extensive survey of the solution space aims to discern regions of interest which likely harbor the optimal solution. Interestingly, in the snow ablation optimizer (SAO) [41], the exploration process is emulated from the natural metamorphosis of snow or liquid water into steam. This steam, due to its diffused and erratic movement, forms an apt analogy for the stochastic traversal of the solution space. To illustrate this, the SAO employs Brownian motion [59] as its exploration paradigm. This motion, typified by the seemingly random ambulation of particles in a fluid, epitomizes the quintessence of a stochastic process.

In a significant update, the exploration mechanism of the SAO has been chosen to replace the exploration phase of the MBO. This decision is rooted in the prowess of the SAO's exploration approach that adeptly harnesses Brownian motion. The standard expression for Brownian motion is encapsulated as:

$$f_{BM}\left(x;0,1\right)=\frac{1}{\sqrt{2\pi}_{ij}}\times exp\left(-\frac{x^{2}}{2}\right) \tag{10}$$

The exploration facet of SAO permits the search agents to roam unconfined in the search expanse, dynamically recalibrating their stances based on the algorithm's trajectory. This movement is mathematically expressed as:

$$Z_i^{(t+1)}=Elite^{(t)}+BM_i^{(t)}\otimes\left(\theta_1\times(G^{(t)}-Z_i^{(t)})+(1-\theta_1)\times(Z^{(t)}-Z_i^{(t)})\right) \tag{11}$$

As previously outlined, each variable in the equation has its designated implication. This strategy ensures an equilibrium between scouting (exploration) and deep diving (exploitation), fostering the algorithm's exemplary competence. Furthermore, this exploration phase capitalizes on the cream of the current population (the elites) and promotes a wide variance among the prospective solutions. Augmented by the capricious nature of Brownian motion, the algorithm is well-equipped to sidestep local optima, amplifying the calibre of the eventual solution. Of particular note is the parameter θ_1, pivotal in directing movement towards either the current best individual or the centroid position of leaders. This suggests that the methodology amalgamates both singular and communal learning paradigms, fully harnessing search intel for a thorough and extensive survey of the solution space.

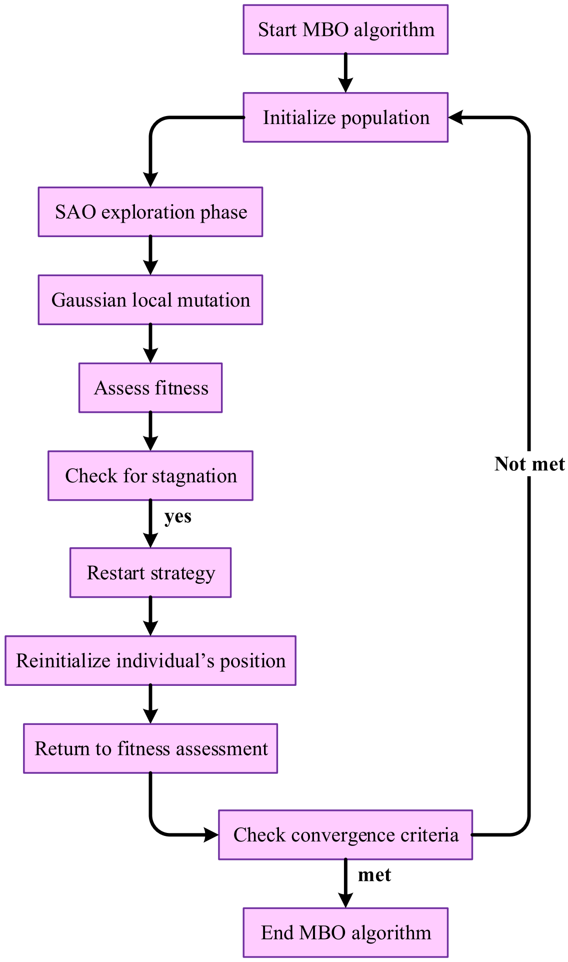

FIGURE 1. Flowchart of the MBO.

B. GAUSSIAN LOCAL MUTATION

The Gaussian local mutation [60] operation introduces some randomness into the algorithm, helping to explore the solution space more thoroughly and reducing the possibility of premature convergence. The importance of maintaining diversity in the population for population-based optimization algorithms cannot be overstated. Diversity helps prevent the algorithm from falling into local optima and boosts the algorithm's ability to explore the problem's search space. The Gaussian mutation helps to achieve this by providing a localized mutation, a form of diversification that allows the algorithm to explore nearby solutions. The localized mutation is achieved mathematically as $X_{new}=X_N+RG\left(X_N-X_t\right)$. Here, RG is a random number generated by a Gaussian probability distribution with mean 0 and standard deviation 0.333. It is crucial to note that Gaussian mutation has proven to be an effective operator in optimization algorithms due to its balanced mix of exploration and exploitation [61]. The variable X_N is determined according to the following rule:

$$X_N = \begin{cases} X_{best2}, \ if \ r1<0.5 \ and \ r2<0.5 \\ X_{best3}, \ if \ r1<0.5 \ and \ r2>0.5 \\ X_{best,otherwise} \end{cases} \quad (12)$$

The selection of the best, second-best, or third-best solution, as defined in Eq. (12), depends on two randomly generated numbers $r1$ and $r2$. This not only brings diversity into the solution but also helps the search process to avoid premature convergence. The motivation to include the second and third-best solutions in the mutation process is to retain a certain degree of diversity in the population. By considering not just the global best but also the runner-ups, we ensure that valuable information from other potential solutions is not lost. By including the Gaussian local mutation in MBO, the aim is to foster diversity and a more comprehensive search of the solution space, thereby increasing the effectiveness of the optimization process. The advantages of this strategy can be summarized as offering an improved balance between exploration and exploitation, reducing premature convergence, and retaining a degree of diversity in the population.

C. RESTART STRATEGY

The restart strategy [62] is designed to circumvent the issue of stagnation in the search process, which is commonly encountered in many optimization algorithms. The primary motive for introducing the restart strategy in MBO is to offer an escape mechanism for search agents which have been trapped in local optima, thereby enhancing the global search capability of the BO. In this way, BO can cover a broader solution space and ensure a more thorough search, improving the likelihood of obtaining the global optimum solution. This strategy becomes highly useful when an individual's position has not improved within a predefined limit. When stagnation is detected, the restart strategy is activated and applied to the stagnant individuals. The restart strategy generates a new position for these individuals by re-initializing their locations in the search space according to Eqs. (13) and (14).

$$X(t+1) = lb + rand \cdot (ub - lb) \quad (13)$$

$$X(t+1) = (ub + lb) - rand \cdot X(t) \quad (14)$$

Here, lb and ub are the lower and upper bound of the problem, respectively. The random opposition-based learning strategy incorporated within this restart strategy enhances the exploration ability of the algorithm, ensuring a more detailed examination of the solution space. The restart strategy provides several advantages. Firstly, it prevents stagnation and encourages continual exploration of the solution space, thereby minimizing the chances of being trapped in local optima. Secondly, it assists in maintaining the diversity of solutions in the population, which is vital for the algorithm's robustness and adaptability. Lastly, by resetting individuals to new, potentially better locations, it increases the algorithm's chance of discovering and converging to the global optimum.

D. RANDOM CONTRACTION STRATEGY

The random contraction strategy (RCS) [63] offers a nuanced approach to optimization algorithms by dynamically contracting the search space. This strategy is particularly useful in handling the intricate balance between exploration, where algorithms are scouting for new potential solutions, and exploitation, where they are refining the current best solutions. A primary challenge in optimization is the propensity of algorithms to prematurely anchor to local optima, especially in the context of multifaceted multi-modal functions. Many algorithms, when confronted with these scenarios, can become too "comfortable" with their present best solutions. They may lack the diversity in their approach to break free and explore beyond these local optima. Incorporating the RCS, we have:

$$X(t+1) = (2 \cdot rand - 1) \cdot X(t) \quad (15)$$

Here, the $2 \cdot rand - 1$ serves a dual purpose. On one hand, it contracts the search domain, which inherently nudges the algorithm to zero in on promising solution areas. On the other hand, the randomness factor ensures that this contraction is not deterministic or uniform, thereby infusing necessary diversity into the search process. What makes RCS unique and effective is its adaptability. Instead of maintaining a static search space or using a predefined reduction sequence, RCS recalibrates the space based on the current solution coupled with a random factor. Such an approach ensures that control parameters are uniformly spread within the interval $[-1, 1]$. This implies that each searching agent has a balanced chance to explore the solution domain between $[-X(t), X(t)]$ as iterations progress. With the element of randomness via $rand$, the strategy makes sure that the agents maintain their dynamism, crucial for dodging the pitfalls of local optima. In essence, RCS introduces a systematic yet adaptable means of contracting the search arena. By doing so, it guides optimization algorithms to veer towards promising regions without being overly deterministic and thereby retains the versatility crucial for tackling complex optimization landscapes.

IV. COMPLEXITY OF MBO

To calculate the time complexity of the MBO with a focus on fitness evaluation time, population size, and the number of iterations, we'll consider each component's complexity in relation to these variables. Let's denote n as population size, k as number of iterations and f as time complexity of evaluating the fitness function for one individual.

1. Initialization: This step involves initializing the population, typically $O(n)$.

2. SAO exploration phase: Assuming a linear complexity with respect to the population size, this step is $O(n)$.

3. Gaussian local mutation: Applying the mutation to each individual is also $O(n)$.

4. Fitness assessment: This is the most critical part in terms of complexity. If the fitness evaluation for one individual has a complexity of f, then for the entire population, it's $(O(n \times f))$.

5. Restart strategy and random contraction strategy: These strategies involve operations on each individual, assumed to be $O(n)$.

6. Convergence check: Typically, $O(n)$, as it involves checking each individual in the population.

Considering these components, the complexity for one iteration of the MBO algorithm can be broken down as follows:

-Initialization, SAO exploration, Gaussian mutation, restart strategy, random contraction strategy, and convergence check: Each $O(n)$.

- Fitness Assessment: $(O(n \times f))$.

Since the algorithm runs for k iterations, the total time complexity for all iterations can be expressed as: $[O(k \times (n + n \times f))]$. Simplifying this, we get: $[O(k \times n \times (1 + f))]$.

This expression represents the time complexity of the MBO in terms of the population size n, the number of iterations k, and the complexity of the fitness evaluation f. It's important to note that f can vary significantly depending on the specific problem and the implementation of the fitness function.

V. RESULTS

This section provides a comprehensive analysis of the MBO's performance, tested against a range of optimization problems, particularly focusing on the CEC 2017 and CEC 2022 test suites, and engineering problems, including cantilever beam design, industrial refrigerator system design, welded beam design, speed reducer design, pressure vessel design, multi-product batch plant design and three-bar truss design. Detailed results from each set of experiments are presented and interpreted in the following relevant subsections.

A. EXPERIMENTAL SETUP

To rigorously assess the efficacy of the proposed MBO, a meticulous experimental design was established. This evaluation involved benchmarking the MBO against a diverse set of nine cutting-edge nature-inspired algorithms, including the original bonobo optimizer (BO) [40], sand cat swarm optimization (SCSO) [42], Chernobyl disaster optimizer (CDO) [43], driving training-based optimization (DTBO) [44], Harris hawk optimizer (HHO) [45], Archimedes optimization algorithm (AOA) [46], smell agent optimizer (SAO) [47], grasshopper optimization algorithm (GOA) [48], particle swarm optimization (PSO) [49], hybrid sine cosine algorithm with differential evolution (SCADE) [50], modified capuchin search algorithm (mCapSA) [51], liver cancer algorithm (LCA) [52], and modified chameleon swarm algorithm (mCSA) [53]. These algorithms were selected for their widespread use and high variability in functionality, ensuring a comprehensive comparison and facilitating an insightful analysis of the MBO's performance.

The benchmarking process comprised 30 independent runs for each algorithm, capped at a maximum of 1000 iterations per run. The population size was kept constant at 50 throughout all experimental runs to maintain uniformity in the experimental conditions. Such a setup aligns well with the recent standards in metaheuristic literature, offering a sufficient exploration of the solution space while avoiding unnecessary strain on computational resources. The problem domain for the experimental investigation was defined within 10 and 100-dimensional hyper-spaces for CEC 2017 along with 10 and 20-dimensional hyper-spaces for CEC 2022. The selection of such an expansive and continuous problem space ensures a thorough and intensive evaluation of the algorithms. It allows the algorithms to explore solutions with wide-ranging magnitudes and orientations, which mimics the complexity and diversity of real-world optimization scenarios. The parameter settings for all the algorithms, including the proposed MBO, were optimized following the guidelines presented in their respective originally reported default values. This was done to ensure the provision of an ideal environment for each algorithm to exhibit its optimal performance.

B. CEC 2017 TEST SUITE

This study utilized twenty-nine benchmark functions from the CEC2017 test suite [64] to conduct the initial statistical assessment. The benchmark functions serve as an effective platform for evaluating the performance of algorithms, as they present difficult challenges. The CEC2017 test suite comprises unimodal (F17-01, F17-03) and multimodal (F17-04 – F17-10) functions that effectively evaluate the algorithms' ability in both exploitation and exploration. In addition to the aforementioned forms, the CEC2017 test suite also encompasses hybrid (F17-11 – F17-20) and composition (F17-21 – F17-30) functions that pose greater challenges for test functions. Further details regarding those test functions can be found in [64].

1) STATISTICAL RESULTS

Table 1 displays the comparative statistical results obtained from 10-dimensional CEC 2017 benchmark functions. The statistical analysis of the CEC2017 test suite (dimension = 10) underscores the efficacy of the MBO algorithm compared to other optimization techniques. In the F17-01 function, MBO exhibited a relatively high performance with a minimum value of 100.0324, ranking third overall, while outperforming several algorithms such as CDO and AOA, which had much higher minimum values of 7.30E+09 and 6.35E+08, respectively. For the F17-03 function, MBO achieved the lowest minimum value of 300, tied with other algorithms but with a notably lower standard deviation, indicating high consistency and reliability. This trend continues with the F17-04 function, where MBO again secured the second rank with a minimum value of 400, demonstrating superior performance over SCSO and CDO with minimum values of 401.8615 and 530.3654, respectively. In the F17-05 function, MBO outperformed other algorithms with a

TABLE 1. Comparative statistical results on CEC2017 test suite (Dimension = 10).

Function	Metric	MBO	BO	SCSO	CDO	DTBO	AOA	PSO	HHO	GOA	SAO	SCADE	mCSA	LCA	mCapSA	SCHO
F17-01	Min	100.0324	100.001	2622.8	7.3E+09	267.2818	6.35E+08	115.0776	84405.85	5.38E+08	3.05E+09	3.66E+08	2913744	5.81E+09	393.1132	483782.7
	Max	10154	1530.345	3.67E+08	1.49E+10	4.87E+08	1.05E+10	11077.21	771678.9	1.26E+10	1.97E+10	1.98E+09	36552297	2.2E+10	35929.43	3.6E+09
	Mean	2849.911	278.8875	24135172	1.3E+10	16732408	5.52E+09	2678.63	382409.1	5.33E+09	1.05E+10	9.41E+08	16992418	1.29E+10	8750.736	4.05E+08
	Std	2813.675	372.378	81987814	2.46E+09	88795140	2.81E+09	2817.298	165301.2	3.45E+09	4.27E+09	3.64E+08	8718636	3.6E+09	7152.989	8.74E+08
	Rank	3	1	8	15	6	12	2	5	11	13	10	7	14	4	9
F17-03	Min	300	300	302.4187	17666.55	364.4036	4163.023	300	300.3243	8384.177	4744.812	1372.627	336.757	13477.16	300.0013	378.0566
	Max	300	300	6027.229	17723.34	5299.743	12756.65	300	304.0174	100782.4	17064.17	5912.592	731.8634	21617.17	311.1743	8575.327
	Mean	300	300	1572.121	17689.61	2030.174	9115.973	300	301.7732	35199.08	10653.97	3565.252	435.9736	19446.41	300.4386	2699.458
	Std	5.17E-14	3.18E-13	1698.377	13.30111	1659.013	1932.31	3.34E-14	0.941775	19861.73	3134.819	1143.365	86.03363	2429.734	2.033254	2510.086
	Rank	1	3	7	13	8	11	2	5	15	12	10	6	14	4	9
F17-04	Min	400	400	401.8615	530.3654	401.1314	457.816	400.0334	400.3587	442.0992	693.1031	424.6767	405.592	571.0641	404.7342	400.2916
	Max	403.9866	403.9866	491.3389	1602.844	528.7269	1224.3	403.5796	436.9228	2557.282	2791.31	478.6732	409.0904	4390.708	478.005	527.8579
	Mean	400.9302	400.5318	434.5204	1298.743	430.1249	642.2112	401.7805	408.18	790.3357	1471.691	444.8084	407.3497	1975.796	416.0239	436.8472
	Std	1.714959	1.378263	29.37869	414.3915	30.62349	172.8515	0.874067	8.138968	526.4735	542.8168	12.14227	0.941282	958.7417	22.98755	35.98361
	Rank	2	1	8	13	7	11	3	5	12	14	10	4	15	6	9
F17-05	Min	502.9849	505.9698	508.9553	567.4061	515.9979	518.9182	509.9496	514.1311	542.5343	564.4448	539.6044	512.597	583.1087	507.9597	508.6866
	Max	519.8991	527.8587	550.9527	590.1205	570.8002	593.5346	553.7274	593.6665	630.6278	657.282	565.1633	549.3312	667.638	533.347	550.8714
	Mean	509.9827	514.2994	529.9066	578.5771	539.3328	549.1384	522.1212	549.8653	583.9026	606.7155	554.1314	526.0347	623.4055	521.0647	530.7832
	Std	4.559341	4.867052	10.66556	5.397957	14.09492	19.96966	10.33219	20.21688	19.40742	24.49755	5.579109	9.256371	19.12295	6.988152	10.73613
	Rank	1	2	6	12	8	9	4	10	13	14	11	5	15	3	7
F17-06	Min	600	600	603.6709	629.8679	609.5657	619.9465	600	610.1855	630.5365	634.9858	612.5705	601.1843	639.0202	600.0001	603.0163
	Max	600	600.0164	642.2387	645.3666	652.4961	650.6112	607.5185	652.4043	687.2439	675.5317	625.1741	605.853	686.5415	600.1491	630.6052
	Mean	600	600.0005	615.4037	634.7192	629.6071	636.2106	601.0586	631.5844	656.8868	653.4864	618.8548	603.3233	667.0417	600.0215	613.5622
	Std	2.62E-07	0.002985	9.136035	3.315272	10.74257	6.501418	1.830085	13.45562	14.50245	10.44498	2.849744	1.192999	9.676901	0.040431	6.572999
	Rank	1	2	7	11	9	12	4	10	14	13	8	5	15	3	6
F17-07	Min	713.6589	719.6492	729.5889	777.4559	720.9254	776.07	710.8654	724.4598	813.8032	797.3529	757.5367	731.6477	802.4344	717.1674	726.7626
	Max	735.2588	744.5314	788.0236	805.9965	800.4548	813.7521	731.8217	809.1088	1107.606	913.6027	799.4852	776.8201	891.9145	754.4309	815.5098
	Mean	722.106	729.9519	756.6191	789.6758	765.7014	794.5025	721.9231	782.841	900.2355	852.9095	776.7233	754.888	852.899	728.6732	760.3612
	Std	5.124448	6.989048	15.20306	6.826965	17.75788	11.32816	5.600992	20.09811	62.2425	24.80109	9.643569	11.58106	26.33294	9.462436	24.51118
	Rank	2	4	6	11	8	12	1	10	15	14	9	5	13	3	7
F17-08	Min	802.9849	802.9849	816.1838	834.3671	813.9294	819.9089	806.9647	810.2632	855.8635	835.4804	836.4835	811.2909	864.1504	805.9697	806.273
	Max	821.8891	830.8437	850.7497	862.3939	833.0849	840.9944	830.8436	855.857	921.4879	891.4456	853.1263	838.4682	906.4195	844.7729	867.3371
	Mean	810.5797	815.1565	830.0305	848.8763	822.6327	830.1058	815.7203	828.625	887.9412	870.376	844.354	822.1196	885.4696	814.6891	827.2474
	Std	5.176434	6.419845	7.074795	8.359668	5.291111	5.797437	6.380993	10.96712	16.1298	12.00996	4.842256	7.934915	12.01728	7.97605	11.91572
	Rank	1	3	9	12	6	10	4	8	15	13	11	5	14	2	7
F17-09	Min	900	900	902.2785	1178.424	963.9569	1099.636	900	922.5594	1540.774	1318.164	957.1327	901.3609	1471.802	900	900.8867
	Max	925.7187	913.1795	1356.164	1396.458	1476.201	1792.871	900.5439	1831.885	4908.659	2499.592	1108.293	930.3999	2797.163	909.3842	1738.934
	Mean	901.048	903.0614	1047.752	1249.186	1174.772	1452.147	900.1058	1450.915	2351.139	1921.535	1026.003	907.3433	2228.033	901.7108	1183.332
	Std	4.687756	3.794417	131.4946	40.89337	131.6581	191.7655	0.187926	242.3213	607.0336	290.8515	35.77671	5.955856	326.8398	2.528611	242.0198
	Rank	2	4	7	10	8	12	1	11	15	13	6	5	14	3	9
F17-10	Min	1068.46	1003.54	1321.844	1742.372	1263.639	1402.171	1249.486	1391.925	1723.946	2174.554	2076.984	1366.557	2671.144	1150.206	1377.706
	Max	2657.053	1914.756	2463.101	2512.207	2104.207	2649.731	2433.108	2269.205	3248.585	3579.432	2548.909	1985.969	3807.383	2304.504	2891.966
	Mean	1481.024	1491.93	1891.892	2192.357	1681.465	2074.495	1791.18	1977.171	2543.077	2791.66	2332.453	1689.104	3231.632	1652.584	1871.349
	Std	493.3796	212.6671	304.6156	202.8859	209.2138	285.5332	301.3832	235.3789	384.2691	364.9863	122.7525	168.6797	301.8119	272.971	294.5106
	Rank	1	2	8	11	4	10	6	9	13	14	12	5	15	3	7
F17-11	Min	1100.995	1102.985	1113.107	1597.483	1106.85	1130.488	1108.959	1116.858	1351.175	1284.237	1176.285	1108.449	1756.133	1102.951	1107.862
	Max	1134.823	1131.56	1264.339	5861.397	1472.588	3096.069	1149.748	1342.602	18738.26	6417.082	1369.04	1150.245	56255.81	1295.719	1412.878
	Mean	1108.094	1115.679	1156.343	5329.762	1172.927	1283.753	1124.126	1179.969	3946.234	2864.956	1271.033	1128.566	11890.39	1118.212	1151.383
	Std	8.166901	9.229274	39.08952	1324.723	77.27654	354.5807	13.0568	70.89599	3362.093	1654.232	47.64485	10.91684	11827.72	34.15757	62.19618
	Rank	1	2	7	14	8	11	4	9	13	12	10	5	15	3	6
F17-12	Min	1752.602	1478.714	21567.67	2950436	3168.478	15491.93	1755.213	32637.15	12219273	12209242	1181217	193262.9	1.12E+08	3539.933	48718.9
	Max	130582.5	46611.79	5794974	9486217	2585055	8284678	34822.59	9539603	1.26E+09	1.29E+09	24813462	16139545	2.95E+09	13832409	4270362
	Mean	22334.83	9958.256	874250.3	5481045	1313425	2125072	12849.45	2798274	3.13E+08	2.94E+08	10609274	2722475	1.1E+09	1010077	1022925
	Std	31133.83	10004.47	1165398	1612343	844550.2	2387419	10467.59	2703734	3.45E+08	3.18E+08	6314430	3202434	8.14E+08	3066796	998289.1
	Rank	3	1	4	11	7	8	2	10	14	13	12	9	15	5	6
F17-13	Min	1308.427	1302.99	2298.524	100031.3	3206.466	3547.618	1520.292	1724.866	23608.66	13417.28	7464.111	1917.218	1331970	1318.771	1939.186
	Max	1421.985	8323.175	35770.07	1.23E+08	23011.39	31931.6	17498.39	56986.99	24548089	65576178	90467.3	34692.54	4.83E+08	32643.92	31858.51
	Mean	1342.217	1548.195	15834.78	36552922	12351.51	13477.63	7072.288	15187.17	3909590	7193516	30625.38	12047.1	95651659	10731.64	11083.52
	Std	29.36116	1279.614	9326.197	48394903	4870.807	9327.541	4121.64	12757.57	5940097	17006114	21942.4	9678.108	1.33E+08	11383.64	9380.151
	Rank	1	2	10	14	7	8	3	9	12	13	11	6	15	4	5
F17-14	Min	1408.039	1405.277	1448.597	1518.27	1459.634	1462.466	1431.742	1466.72	1573.662	1473.812	1477.91	1427.333	1567.52	1417.432	1446.46
	Max	2006.203	1698.027	5160.375	2206.479	5872.87	24100.19	3299.705	1812.624	40835.77	2126.024	1636.504	1533.281	21887.63	4995.425	8463.555
	Mean	1474.557	1447.601	1933.013	1652.755	2030.276	7436.421	1611.202	1562.991	12734.72	1639.916	1549.548	1470.116	4669.065	2364.119	3612.548
	Std	133.5365	56.66406	1163.465	164.2979	1105.863	6646.37	370.1523	90.2913	12686.06	149.6826	29.7691	25.21093	5119.494	1091.681	2164.934
	Rank	3	1	9	8	10	14	6	5	15	7	4	2	13	11	12
F17-15	Min	1501.015	1502.202	1524.047	4361.318	1532.836	2734.433	1508.563	1640.434	4183.18	1760.516	1837.71	1607.732	1567.52	1526.528	1609.049
	Max	1553.929	1528.881	10067.31	7005.122	5876.28	21308.3	2630.538	7028.164	1921321	15202.8	3997.697	3483.615	21887.63	32431.04	22407.53
	Mean	1510.609	1510.727	3079.209	5319.721	3616.463	12940.12	1687.963	3760.856	127926	5122.288	2360.844	1956.234	4669.065	4924.271	7323.294
	Std	10.39516	6.733937	1849.214	673.7667	1648.802	6004.355	260.0572	1706.508	345232.9	3304.893	549.1382	451.4204	5119.494	7017.216	5376.502
	Rank	1	2	6	12	7	14	3	8	15	11	5	4	9	10	13
F17-16	Min	1600.02	1600.231	1615.47	1962.458	1641.686	1750.952	1600.964	1603.194	1686.982	1922.94	1658.881	1604.206	1567.52	1600.683	1603.477
	Max	1934.951	1997.817	2155.576	2203.435	1990.958	2591.708	2051.414	2058.339	2580.811	2372.089	1944.236	1774.079	21887.63	1950.734	2202.951
	Mean	1667.892	1747.418	1781.445	2048.586	1873.071	2040.583	1845.12	1863.284	2128.235	2140.278	1760.96	1667.933	4669.065	1673.623	1824.39
	Std	85.32669	117.2911	124.3484	41.09222	101.8477	152.9057	132.7791	138.9598	240.5707	132.2971	77.99436	58.41366	5119.494	87.07232	159.3702
	Rank	1	4	6	12	10	11	8	9	13	14	5	2	15	3	7
F17-17	Min	1703.107	1701.015	1726.571	1817.1	1726.725	1761.66	1714.738	1734.071	1804.044	1778.653	1761.214	1725.928	1567.52	1705.624	1728.055
	Max	1900.567	1836.2	1824.665	1984.285	1786.613	2066.01	1960.975	1865.759	2471.362	2193.301	1806.428	1773.577	21887.63	1827.433	2041.586
	Mean	1740.081	1737.472	1771.091	1860.358	1757.619	1888.612	1760.516	1775.966	2055.391	1893.763	1780.26	1748.506	4669.065	1738.464	1838.868
	Std	47.33126	38.04815	22.95589	50.88916	15.98508	96.58085	45.69475	37.3742	162.1486	89.94522	12.30535	13.25646	5119.494	23.40819	83.81132
	Rank	3	1	7	11	5	12	6	8	14	13	9	4	15	2	10
F17-18	Min	1802.024	1820.756	2736.27	123708.6	2268.198	2984.527	1903.913	3034.804	14140.92	7574.092	16217.52	2715.444	1567.52	5593.201	2793.284
	Max	11232.94	14368.97	52610.34	1.55E+09	42059.96	32951.78	20856.37	31569.77	2.02E+08	7.13E+08	615485.6	53477.04	21887.63	55243.55	38132.08
	Mean	2622.212	2310.513	21697.86	74251687	13535.62	15522.54	7977.873	11602	12859811	1.3E+08	118364.7	25885.96	4669.065	29786.62	19870.53
	Std	2163.97	2284.567	13874.44	2.85E+08	10930.12	8562.556	5663.915	7912.058	39675749	2.17E+08	119806.2	14569.64	5119.494	14998.84	11534.95
	Rank	2	1	9	14	6	7	4	5	13	15	12	10	3	11	8
F17-19	Min	1900.128	1900.062	1912.416	22161.71	1920.337	1938.622	1911.101	2084.998	5062.87	2320.73	2013.572	1919.346	1567.52	2032.071	1914.598
	Max	1992.637	1908.079	13678.14	1456659	16620.12	84684.14	5507.676	22754.89	19363820	538716.4	18261.69	6056.675	21887.63	32931.39	23401.71
	Mean	1907.054	1902.218	4115.328	1321955	4211.798	30142.76	2796.671	9160.526	1433488	44344.36	5975.058	2242.088	4669.065	11640.71	10221.87
	Std	17.73581	1.774306	4123.343	326453.6	4679.55	21398.65	1150.27	6491.433	4196705	99066.2	4960.207	769.71	5119.494	11405.52	6022.769
	Rank	2	1	5	14	6	12	4	9	15	13	8	3	7	11	10
F17-20	Min	2000	2000	2031.664	2159.691	2041.046	2055.12	2005.599	2030.962	2182.778	2105.28	2059.525	2025.189	1567.52	2001.308	2024.382
	Max	2032.173	2042.435	2249.273	2218.8	2204.739	2293.547	2214.613	2282.755	2557.199	2380.821	2197.011	2065.224	21887.63	2129.419	2301.926
	Mean	2007.518	2014.51	2117.09	2182.334	2115.922	2133.832	2098.709	2156.672	2316.825	2235.821	2117.348	2040.336	4669.065	2027.789	2119.713
	Std	9.327808	10.96475	62.6686	16.16875	54.79899	63.51412	63.38364	71.35391	90.08503	68.13448	29.36758	10.93635	5119.494	22.59699	77.68423
	Rank	1	2	7	12	6	10	5	11	14	13	8	4	15	3	9
F17-21	Min	2200	2200	2200.456	2352.251	2201.456	2227.52	2200	2200.398	2223.994	2258.087	2215.354	2201.137	1567.52	2101.001	2215.677
	Max	2329.546	2346.535	2349.993	2375.079	2331.263	2397.672	2341.877	2388.301	2404.739	2434.331	2257.766	2207.01	21887.63	2333.41	2389.268
	Mean	2297.698	2313.275	2273.124	2365.53	2218.607	2312.697	2301.391	2285.076	2333.454	2381.602	2234	2203.68	4669.065	2209.109	2338.359
	Std	44.16879	31.58108	64.02981	5.781563	24.47882	40.3192	46.66913	72.42123	58.65984	39.62522	10.5653	1.577866	5119.494	38.08955	36.87657
	Rank	7	10	5	13	3	9	8	6	11	14	4	1	15	2	12

TABLE 1. *(Continued.)* **Comparative statistical results on CEC2017 test suite (Dimension = 10).**

	Min	2300.289	2300.78	2235.05	2504.414	2242.548	2470.429	2300.289	2306.66	2422.625	2427.844	2328.219	2231.713	1567.52	2215.56	2307.733
	Max	2303.198	2310.43	2332.646	4065.379	2330.444	3309.954	2302.96	3545.083	4473.708	4812.433	2422.054	2315.005	21887.63	2313.579	3439.771
F17-22	Mean	2301.476	2303.164	2309.166	3198.266	2301.133	2767.583	2301.632	2355.509	2884.326	3202.967	2365.584	2297.891	4669.065	2293.929	2411.392
	Std	0.697092	2.335855	20.33694	344.2408	18.99022	185.7403	0.713652	224.7354	356.9823	487.4303	23.523	27.25996	5119.494	29.92779	216.525
	Rank	4	6	7	13	3	11	5	8	12	14	9	2	15	1	10
	Min	2606.365	2609.596	2611.44	2728.32	2615.567	2647.984	2607.055	2612.527	2641.677	2687.072	2634.113	2616.714	1567.52	2614.833	2617.147
	Max	2644.571	2641.645	2685.512	2993.685	2704.8	2772.274	2641.515	2719.713	2712.503	2839.42	2664.539	2643.424	21887.63	2657.175	2697.717
F17-23	Mean	2618.229	2621.478	2639.217	2830.403	2654.881	2710.213	2623.683	2669.365	2677.181	2773.242	2649.06	2626.979	4669.065	2632.821	2661.001
	Std	8.800494	7.200791	18.01101	63.92209	24.21339	37.01991	10.33285	26.75173	18.72359	27.07137	7.508022	7.401149	5119.494	10.56734	21.34514
	Rank	1	2	6	14	8	12	3	10	11	13	7	4	15	5	9
	Min	2500	2602.584	2503.882	2712.708	2501.077	2639.303	2500	2500.952	2661.462	2678.787	2548.251	2506.077	1567.52	2500	2510.832
	Max	2766.676	2825.554	2815.263	2937.959	2744.488	2923.772	2782.834	2904.345	2889.875	3073.07	2796.718	2789.303	21887.63	2802.086	2891.955
F17-24	Mean	2739.356	2759.896	2751.804	2905.751	2545.544	2812.602	2726.107	2787.551	2796.083	2922.112	2649.282	2684.757	4669.065	2694.381	2788.073
	Std	45.94838	34.81426	67.72586	40.57754	58.18222	65.83985	77.40169	106.0321	34.36201	87.05542	86.60329	115.7433	5119.494	130.2197	61.7898
	Rank	6	8	7	13	1	12	5	9	11	14	2	3	15	4	10
	Min	2897.746	2897.94	2899.599	3332.165	2911.971	2958.41	2897.743	2612.969	2982.334	3268.779	2936.651	2899.951	1567.52	2898.525	2904.274
	Max	3009.483	3025.353	3024.639	3609.739	3025.337	3645.943	2947.66	2948.708	3933.748	4356.598	3057.371	2952.088	21887.63	3024.22	3063.913
F17-25	Mean	2938.448	2945.008	2934.674	3585.96	2946.728	3199.507	2924.823	2916.237	3276.482	3858.317	2971.708	2934.547	4669.065	2935.14	2948.3
	Std	28.76749	31.384	25.49435	67.91731	26.00352	137.0106	23.11685	61.68579	224.2573	267.3099	28.08238	21.47333	5119.494	41.13811	39.50232
	Rank	6	7	4	13	8	11	2	1	12	14	10	3	15	5	9
	Min	2800	2600	2832.941	4021.619	2601.095	3169.93	2600	2815.664	3169.533	3152.71	3031.979	2907.32	1567.52	2983.512	2611.906
	Max	3457.784	3421.24	3643.766	4080.867	4102	4245.334	2947.149	4276.613	4931.262	5130.908	3234.648	3011.427	21887.63	3161.449	4203.208
F17-26	Mean	3024.748	3031.689	3052.558	4043.232	3193.512	3724.675	2894.715	3486.463	3842.959	4379.996	3141.506	2931.812	4669.065	3052.788	3224.235
	Std	140.7512	158.8584	154.063	14.62954	344.7454	289.0565	57.485	502.9087	544.5553	479.2555	48.88412	29.4447	5119.494	62.81564	393.3935
	Rank	3	4	5	13	8	11	1	10	12	14	7	2	15	6	9
	Min	3071.208	3071.778	3091.074	3229.231	3087.347	3156.396	3090.001	3103.058	3102.3	3168.697	3100.458	3090.974	1567.52	3089.573	3094.166
	Max	3200.002	3200.002	3182.905	3313.848	3183.053	3306.539	3182.517	3216.461	3224.746	3500.023	3108.976	3099.973	21887.63	3103.721	3281.482
F17-27	Mean	3095.198	3088.363	3104.682	3276.018	3122.296	3208.563	3108.783	3149.157	3134.062	3293.204	3104.349	3095.186	4669.065	3095.445	3134.971
	Std	44.60497	35.44208	21.44794	26.4894	31.14261	39.37212	27.50518	39.46037	33.73676	92.21703	1.77354	2.206545	5119.494	2.749137	40.11707
	Rank	3	1	6	13	8	12	7	11	9	14	5	2	15	4	10
	Min	3100	3100	3100.068	3594.06	3162.971	3279.906	3100	3101.937	3258.205	3487.122	3266.3	3108.967	1567.52	3176.684	3167.275
	Max	3300.002	3300.002	3457.645	3599.241	3473.681	3889.889	3446.48	3583.218	3838.812	4208.036	3466.523	3412.078	21887.63	3411.826	3726.098
F17-28	Mean	3258.087	3263.127	3325.225	3596.33	3331.91	3676.068	3288.748	3392.319	3505.684	3887.405	3381.962	3207.35	4669.065	3315.822	3373.881
	Std	45.16098	50.75037	101.2264	1.30836	85.00814	153.9342	135.7358	99.30679	164.8514	173.1805	62.62618	81.8808	5119.494	90.13287	126.6634
	Rank	2	3	6	12	7	13	4	10	11	14	9	1	15	5	8
	Min	3150.372	3150.809	3148.064	3258.295	3174.336	3198.988	3155.165	3193.053	3201.594	3243.663	3210.112	3151.069	1567.52	3140.414	3177.651
	Max	3355.436	3375.256	3398.985	3557.191	3385.252	3629.636	3313.347	3471.755	3613.428	3786.501	3324.308	3262.094	21887.63	3295.962	3430.706
F17-29	Mean	3200.072	3208.611	3236.549	3349.516	3252.349	3370.296	3210.206	3314.318	3358.974	3505.595	3261.673	3190.396	4669.065	3188.63	3264.544
	Std	51.58033	46.1016	68.51594	63.36751	50.82952	110.7029	40.809	62.12146	102.0331	127.9914	29.66273	29.45276	5119.494	43.63519	61.25425
	Rank	3	4	6	11	7	13	5	10	12	14	8	2	15	1	9
	Min	3215.16	3210.262	4919.214	87938.88	3803.213	61285.4	4604.857	24407.87	164126.3	39153.9	253935.6	5808.337	1567.52	4408.43	8777.378
	Max	3555.706	4927.996	2519426	659669.2	1825062	61188547	1251785	7448713	15226156	80405449	1628925	1049391	21887.63	2446311	7787474
F17-30	Mean	3324.124	3433.262	708018.7	256555.4	281759.6	10666020	213386.2	1486478	3397713	15800033	736856	200159.3	4669.065	713624.4	1620083
	Std	105.8388	358.9385	756101.4	128511.7	442537.2	14843022	429772.1	2070598	4124724	16621012	265550.5	338313.3	5119.494	579185.5	1752984
	Rank	1	2	8	6	7	14	5	11	13	15	10	4	3	9	12
Friedman Rank		2.3793	2.931	6.7586	12.1034	6.7586	11.1724	4.0345	8.3448	12.931	13.2414	8.3448	4.1379	13.4138	4.6897	8.7586
Mean Rank		1	2	6	10	6	9	3	7	11	12	7	4	13	5	8

minimum value of 502.9849 and maintained the highest rank. Similarly, MBO exhibited a strong performance in the F17-06 and F17-07 functions, where it ranked first and second, respectively, showcasing its robustness and effectiveness. The MBO algorithm also consistently performed well across various other functions, securing top ranks and maintaining low standard deviations, which indicates stability in optimization results.

Table 2 presents the comparative statistical results on the CEC2017 test suite with a dimension of 100, highlighting the performance of multiple optimization algorithms. Notably, the MBO algorithm exhibits significant achievements across various metrics. For example, MBO consistently ranks high in terms of minimum, maximum, mean, and standard deviation values for most functions, indicating robust performance and reliability. In particular, MBO ranks 2nd in F17-01 and F17-04, demonstrating its superior ability to find optimal solutions compared to other algorithms. Additionally, MBO achieves the lowest standard deviation in several instances, suggesting consistent performance and minimal variation in results. These achievements underscore the efficacy of MBO in handling high-dimensional optimization problems, positioning it as a highly competitive algorithm in the field of metaheuristic optimization.

In Table 3, which considers a dimension of 10, MBO consistently outperforms or shows comparable performance to many other algorithms across various functions. Especially, for functions like F17-01, F17-03, F17-05, and F17-11, MBO achieves significantly better results compared to most other methods, as indicated by very low p-values (e.g., 1.16E-07, 1.55E-09, 0.001589, 0.000446) in the Wilcoxon's Signed Rank Test. This demonstrates MBO's robustness and effectiveness in finding optimal solutions.

Table 4 considers a higher dimension of 100 and MBO continues to demonstrate strong performance here, as well. While some functions show less significant improvements (e.g., F17-01 with p-value 0.529782), others like F17-03, F17-04, and F17-25 still show MBO's ability to compete effectively with other methods. For instance, in function F17-03, MBO significantly outperforms most other methods with a very low p-value of 8.84E-07, demonstrating its robustness across different dimensions.

2) CONVERGENCE AND BOXPLOT ANALYSIS

Figure 2 demonstrates the convergence curves of MBO on functions from the CEC 2017 benchmark suit with a dimension of 10. On the other hand, Figure 3 demonstrates a boxplot analysis for 10-dimensional CEC 2017 test suite. The illustrations verify the effectiveness of the MBO discussed earlier. This is further supported by the convergence curves in Figure 4 and boxplot analysis Figure 5 which present the respective illustrations for 100-dimensional CEC 2017 test suite.

TABLE 2. Comparative statistical results on CEC2017 test suite (Dimension = 100).

Function	Metric	MBO	BO	SCSO	CDO	DTBO	AOA	PSO	HHO	GOA	SAO	SCADE	mCSA	LCA	mCapSA	SCHO
F17-01	Min	2709175	505115.9	6.35E+10	1.61E+11	1.04E+11	2.49E+11	7034450	1.85E+10	2.69E+11	2.62E+11	2.15E+11	3.18E+10	2.66E+11	8.74E+09	7.44E+10
	Max	3.54E+09	2.99E+09	1.19E+11	1.73E+11	1.69E+11	2.89E+11	3.13E+08	3.45E+10	4.04E+11	3.02E+11	2.46E+11	5.67E+10	2.95E+11	2.52E+10	1.32E+11
	Mean	8.06E+08	8.44E+08	9.05E+10	1.67E+11	1.42E+11	2.67E+11	63676650	2.71E+10	3.32E+11	2.86E+11	2.31E+11	4.31E+10	2.85E+11	1.55E+10	1.05E+11
	Std	1E+09	8.73E+08	1.26E+10	2.9E+09	1.86E+10	1.08E+10	76580894	3.44E+09	3.83E+10	7.34E+09	7.56E+09	5.32E+09	6.28E+09	4.14E+09	1.26E+10
	Rank	2	3	7	10	9	12	1	5	15	14	11	6	13	4	8
F17-03	Min	542696.5	378885.2	258692	315591.6	267117.4	305762.8	327041.7	285207.7	425753.1	344952.5	326474.7	449835	359048.5	449816.8	338828
	Max	3556905	1356212	341450.7	371322.1	338302.1	519307.1	715806	460466.2	4.54E+08	635836.1	358273.9	849418.6	3499716	999987.6	810150.7
	Mean	1391051	664145.5	301644.8	350142.6	306832.2	361453.7	465543.3	327933.1	16413225	471452.5	347202.9	611757.6	639972.2	681134.4	433953.7
	Std	772272.6	247834.7	20156.49	10815.41	18549.95	44027.29	97677.05	29702.56	82655352	70975.08	8244.553	89097.77	711728	152888.4	116054.1
	Rank	14	12	1	5	2	6	8	3	15	9	4	10	11	13	7
F17-04	Min	719.1026	664.8419	5124.341	46417.18	13974.85	62247.04	669.5773	3619.188	93294.1	90148.7	51459.37	3905.586	107995.6	1484.742	9345.671
	Max	1467.319	1577.653	14968.68	51105.42	42567.96	123417.7	914.5458	7823.724	207679.8	158560.1	77626.07	7059.185	155367.6	3040.554	25678.54
	Mean	987.5603	1130.251	10319.74	48695.01	23832.68	93063.66	795.2529	5441.773	133780.6	135026.4	61823.56	5444.564	132329.2	2113.467	15791.91
	Std	158.4299	180.3657	2720.735	1109.342	6974.268	14932	62.53699	1082.148	31479.65	16086.86	6608.407	844.6287	12511.08	448.4253	4145.544
	Rank	2	3	7	10	9	12	1	5	14	15	11	6	13	4	8
F17-05	Min	942.3111	1104.189	1467.436	1872.686	1427.679	1931.745	956.9567	1489.588	2195.063	2103.464	2005.258	1655.603	2126.772	1158.034	1596.965
	Max	1524.968	1374.229	1778.745	2031.56	1691.938	2159.686	1314.449	1696.832	2663.174	2324.166	2126.041	2143.235	2323.91	1588.943	2014.355
	Mean	1174.317	1220.539	1596.906	1947.737	1577.199	2057.41	1136.51	1617.837	2373.918	2234.2	2064.735	1873.866	2230.421	1364.181	1772.561
	Std	113.4997	77.06933	69.2676	37.08829	71.99706	64.89611	88.13139	53.61125	108.2684	56.38116	26.99073	93.62078	46.51019	94.07302	88.71961
	Rank	2	3	6	10	5	11	1	7	15	14	12	9	13	4	8
F17-06	Min	607.566	611.0985	673.7539	698.5734	669.9158	700.9877	633.6331	677.0228	722.4022	711.6075	705.4355	664.6059	713.333	645.3419	676.1892
	Max	629.9758	631.3306	692.9225	710.5721	678.4492	716.0739	659.2529	694.9961	746.5976	726.9701	713.6136	700.8676	731.0582	671.5233	718.4987
	Mean	618.9435	618.6498	683.2602	704.9246	674.0235	708.9252	647.7702	688.586	731.6653	719.2775	709.8648	681.812	720.8213	658.5428	691.4893
	Std	5.659709	4.746469	4.47825	3.178767	2.146343	4.179282	7.010531	3.683312	6.228994	3.912272	2.38702	8.266658	4.644488	6.683477	9.539793
	Rank	2	1	7	10	5	11	3	8	15	13	12	6	14	4	9
F17-07	Min	1438.14	1557.93	2965.348	3278.99	3120.609	3803.697	1271.948	3587.698	4211.028	4052.434	3650.323	2702.749	3949.559	2135.131	2831.078
	Max	2305.639	2456.371	3621.158	3625.703	3542.907	4085.967	2221.085	3932.823	7135.106	4661.342	3995.179	3427.812	4296.881	3305.139	3783.014
	Mean	1771.533	1887.814	3356.423	3377.565	3406.944	3954.346	1584.335	3787.292	5072.425	4249.365	3819.639	2921.745	4168.419	2624.872	3187.793
	Std	189.2684	211.9278	174.4788	66.20839	85.21087	62.589	194.1671	105.8472	711.1813	147.4953	84.18575	165.1127	73.91267	279.7022	178.7751
	Rank	2	3	7	8	9	12	1	10	15	14	11	5	13	4	6
F17-08	Min	1259.935	1342.515	1923.035	2325.505	1884.23	2350.211	1299.728	1978.874	2440.3	2612.003	2407.023	1986.321	2612.591	1434.91	1949.47
	Max	1775.658	1693.485	2211.412	2495.898	2120.073	2628.086	1680.214	2234.764	3124.082	2818.498	2572.757	2323.958	2805.78	1970.543	2330.773
	Mean	1468.4	1529.212	2050.197	2405.066	1987.75	2486.464	1479.098	2072.549	2837.264	2704.088	2497.226	2163.712	2713.529	1676.559	2179.141
	Std	116.0499	89.38307	84.41481	50.76473	62.01317	73.24395	90.5145	60.61998	147.2819	54.26989	43.61542	75.21734	43.13354	116.5612	110.856
	Rank	1	3	6	10	5	11	2	7	15	13	12	8	14	4	9
F17-09	Min	17457.64	11367.84	32889.97	63604.63	25416.58	58773.53	14412.91	55135.35	85021.76	74392.93	73403.74	66552.69	81153.02	16793	74829.08
	Max	54547.19	23759.58	55707.49	75769.26	32684.13	84394.18	37780.18	73482.04	215272.1	111082.5	83668.47	127812.9	104430.3	61788.42	102399.3
	Mean	33922.57	17903.39	42380.7	70903.47	28839.25	70436.38	22729.76	63755.42	132097.1	88919.33	78039.91	95125.1	92222.29	40187.51	92478.73
	Std	9888.143	2950.01	6352.157	3592.114	2154.643	6608.972	5543.526	4517.661	26908.28	8085.59	2687.078	19381.74	5137.071	10143.68	6747.99
	Rank	4	1	6	9	3	8	2	7	15	11	10	14	12	5	13
F17-10	Min	32468.82	11815.74	19382.42	30709.9	14672.76	28925.8	12399.64	20100.28	31694.09	30449.03	30891.59	30167.83	33379.53	17214.93	24914.47
	Max	35252.3	17389.98	24627.24	33855.09	18751.94	32754.45	18154.98	27311.68	35854.33	37084.81	33173.27	34472.78	36487.22	25040.68	31654.51
	Mean	34149.41	14116.03	21679.63	32424.14	17098.37	30730.4	15089.7	24007.08	33624	33026.12	32280.58	32187.48	35034.48	20578.93	28174.3
	Std	704.7494	1408.049	1163.143	759.0283	788.0061	941.168	1755.147	1779.32	820.0488	1255.63	565.8577	883.4936	802.4112	1863.59	1572.21
	Rank	14	1	5	11	3	8	2	6	13	12	10	9	15	4	7
F17-11	Min	4016.671	5177.299	56553.78	137196.1	60837.4	121857.7	8081.836	60694.8	387421.8	201433.6	154201.3	28255.43	332037.5	75235.98	65164.6
	Max	72074.94	32083.36	122609.1	216545.7	126244	229327.2	26221.73	145506.9	1541823	517746.7	270152.2	79457.46	534078.9	265445.3	133304.8
	Mean	18846.99	14838	82297.77	165684.1	96647.42	170811.7	13751.87	100419.2	676750.5	308036.8	208032.8	54521.38	435032.4	141837.1	103980.6
	Std	12564.61	6910.77	18797.01	17651.54	14738.88	24119.78	3954.96	19205.7	216122	70785.51	30772.82	14786.14	50284.64	46267.81	19501.22
	Rank	3	2	5	10	6	11	1	7	15	13	12	4	14	9	8
F17-12	Min	0	0	0	0	0	0	0	0	0	0	0	0	0	0	0
	Max	9277986	15346590	1.08E+10	1.03E+11	2.02E+10	1.4E+11	4687260	2.28E+09	1.63E+11	1.82E+11	1.1E+11	6.16E+09	2.03E+11	9.3E+08	3.09E+10
	Mean	7.6E+08	3.06E+08	4.18E+10	1.1E+11	8.7E+10	2.34E+11	1.17E+08	1.02E+10	2.68E+11	2.61E+11	1.44E+11	1.32E+10	2.58E+11	3.46E+09	7.31E+10
	Std	97293267	1.01E+08	2.47E+10	1.07E+11	5.39E+10	1.8E+11	27888564	4.55E+09	2.17E+11	2.32E+11	1.27E+11	8.95E+09	2.31E+11	1.98E+09	4.66E+10
	Rank	1.39E+08	80813654	8.23E+09	1.8E+09	1.75E+10	2.36E+10	20961973	1.89E+09	2.77E+10	1.82E+10	1.09E+10	1.6E+09	1.4E+10	7.37E+08	1.07E+10
F17-13	Min	2	3	7	10	9	12	1	5	13	15	11	6	14	4	8
	Max	2419.272	2623.185	2.62E+08	2.73E+10	1.54E+09	3.48E+10	3869.101	19882001	1.94E+10	4.19E+10	1.39E+10	4.5E+08	4.16E+10	1330956	1.58E+09
	Mean	143352.3	1579908	6.45E+09	2.86E+10	2.18E+10	5.7E+10	27659.75	78783053	7.71E+10	6.11E+10	3.18E+10	1.57E+09	6.24E+10	3.28E+08	1.79E+10
	Std	27505.88	144708.6	2.15E+09	2.78E+10	1.01E+10	4.58E+10	10571.45	44336484	4.85E+10	5.57E+10	2.4E+10	9.12E+08	5.49E+10	68033070	8.21E+09
	Rank	38361.65	304370.7	1.46E+09	3.27E+08	4.98E+09	6.46E+09	6007.468	15253637	1.28E+10	4.77E+09	3.75E+09	2.65E+08	4.31E+09	1.07E+08	4.26E+09
F17-14	Min	2	3	7	11	9	12	1	4	13	15	10	6	14	5	8
	Max	238282	301602.4	2351232	21633026	1594363	48969320	331206.3	2743604	71014527	18975871	22929754	3809332	64859166	2071666	2777645
	Mean	3638085	2599760	27714271	38833931	9129736	2.02E+08	1955504	14261976	5.39E+08	2.11E+08	67876132	55115249	3.15E+08	22896611	49204892
	Std	1181012	1110849	11145209	29455728	4007315	94370551	1008984	7466735	2.31E+08	87719173	34019464	20829268	2.02E+08	10628339	15349890
	Rank	768479.9	692041.9	6081757	4004902	2053952	45728677	459684.2	2459273	1.09E+08	46354629	8522372	10986704	73922408	5015811	9995598
F17-15	Min	3	2	7	10	4	13	1	5	15	12	11	9	14	6	8
	Max	2034.766	2643.886	23889243	1.91E+10	6358767	1.25E+10	2070.583	2941945	8.31E+09	2.2E+10	4.42E+09	60300437	2.45E+10	178389.7	48783574
	Mean	50468.45	165454.3	5.47E+09	2.63E+10	6.67E+09	3.23E+10	18700.63	13323775	3.32E+10	4.02E+10	1.14E+10	4.6E+08	4E+10	1.07E+08	1.17E+10
	Std	9497.634	16456.42	7.61E+08	2.6E+10	2.16E+09	2.37E+10	5619.268	6533414	2.06E+10	3.14E+10	7.43E+09	1.95E+08	3.1E+10	13782117	3.59E+09
	Rank	10300.28	30437.44	1.12E+09	1.3E+09	1.91E+09	4.88E+09	4317.688	2479980	7.67E+09	4.62E+09	1.62E+09	74581716	3.85E+09	29353032	2.57E+09
F17-16	Min	2	3	7	13	8	12	1	4	11	15	10	6	14	5	9
	Max	4710.79	4518.034	7081.48	17026.7	6841.914	16018.55	3711.952	7929.272	16157.94	19519.02	13920.37	9993.468	17931.17	6051.449	7653.729
	Mean	12909.81	6868.295	13683.04	19825.43	15578.43	24502.36	7097.188	13200.66	32500.89	34358.05	18557.01	13217.19	34271.64	9455.528	14920.8
	Std	8722.205	5510.206	10008.12	18746.25	9642.122	19893.32	5188.379	9485.69	22166.33	27785.85	16251.28	11507.47	28226.41	7681.914	10565.15
	Rank	3161.273	550.5985	1586.86	722.92	1886.553	2350.971	864.7741	1030.782	4252.66	3124.146	1059.563	700.3233	3408.582	777.3043	1553.056
F17-17	Min	4	2	7	11	6	12	1	5	13	14	10	9	15	3	8
	Max	4057.262	4325.887	6634.149	5626602	6321.561	697426.8	3814.477	5200.506	80266.44	3044088	14300.73	7453.188	1354109	5662.609	6375.095
	Mean	9286.767	6998.22	23041.61	11381845	198119.7	15587995	6352.239	8342.498	65283839	64508727	444332.9	9565.164	1.1E+08	8889.586	72589.6
	Std	6544.295	5441.127	9997.411	10833775	25039.26	5363535	5004.134	7202.708	8007840	22594049	99026.98	8461.346	39613258	7217	19232.39
	Rank	1915.072	540.7241	4350.915	1004564	39202.03	3880110	648.2413	687.1572	15493916	15123617	87727.44	485.3365	32709164	803.9285	18469.5
F17-18	Min	3	2	7	13	9	11	1	4	12	14	10	6	15	5	8
	Max	527700.4	758371.9	2503504	31426821	1253301	37774813	272216.6	3293216	1.16E+08	31955527	36615634	12080794	99187298	3924154	5815993
	Mean	18775370	3811526	37935596	44792595	14219924	6.6E+08	4744423	17780656	7.14E+08	6.27E+08	1.35E+08	45407052	1.3E+09	33482182	39355338
	Std	3667304	1875545	10947528	37560393	5086286	1.97E+08	1588945	7229589	3.25E+08	2.02E+08	82533520	24791077	7.4E+08	19373449	20245039
	Rank	3947957	775103.4	8515224	3192625	3191089	1.6E+08	944691.5	3032174	1.42E+08	1.29E+08	24800697	8081927	3.52E+08	7965948	8860290
F17-19	Min	3	2	6	10	4	12	1	5	14	13	11	9	15	7	8
	Max	2083.839	2447.634	51281990	2.26E+10	28390430	1.42E+10	2269.414	10200765	1.22E+10	2.35E+10	4.05E+09	1.02E+08	2.02E+10	267403.8	1E+08
	Mean	48078.99	33315.76	2.57E+09	2.29E+10	9.6E+09	3.44E+10	21647.49	43922331	4.22E+10	3.89E+10	1.28E+10	3.93E+08	4E+10	1.56E+08	8.94E+09
	Std	11109.69	8668.618	6.44E+08	2.27E+10	2.04E+09	2.28E+10	7057.547	22279159	2.29E+10	3.24E+10	6.92E+09	2.32E+08	3.13E+10	19452763	2.68E+09
	Rank	12105.45	7745.885	6.8E+08	43399455	2.29E+09	4.42E+09	4710.866	7863027	7.83E+09	4.18E+09	1.74E+09	67642830	4.74E+09	34417728	2.67E+09
F17-20	Min	3	2	7	11	8	12	1	5	13	15	10	6	14	4	9
	Max	5257.381	3721.215	4956.992	6387.374	4671.898	5910.278	3726.033	5212.806	7767.795	6972.773	6791.428	6713.276	7822.88	4540.443	5383.166
	Mean	9051.553	5841.444	7043.461	8125.408	5711.642	7918.055	6444.882	7205.532	9545.421	8736.473	8146.792	8757.553	9864.881	8455.294	7654.327
	Std	8234.54	4718.726	6124.862	7683.419	5396.86	7327.729	5186.348	6168.626	8920.227	8016.835	7615.18	7709.993	8986.911	5798.054	6545.015
	Rank	667.6393	524.3103	444.9006	345.5009	282.7253	416.1212	607.7621	508.091	394.4175	430.5011	289.8578	564.8578	475.6289	753.3794	506.8891
F17-21	Min	13	1	5	10	3	8	2	6	14	12	9	11	15	4	7
	Max	2850.107	2992.58	3455.045	3897.319	3510.877	4421.605	2824.566	3944.267	4489.178	4821.865	3948.424	3573.398	4947.492	3146.652	3711.48
	Mean	3412.558	3487.693	4101.919	4110.485	4292.187	5041.094	3315.717	4577.397	5325.36	5494.898	4403.323	3911.719	5546.681	3755.471	4186.157
	Std	3063.832	3184.278	3656.284	3987.713	3907.69	4665.888	3106.546	4281.216	4846.189	5127.347	4137.814	3750.828	5196.801	3339.069	3961.962
	Rank	131.4835	120.4388	144.0155	58.37697	176.6468	163.9591	108.4282	169.9484	214.0202	160.5031	100.1251	89.95278	133.9034	130.4982	132.2735

TABLE 2. *(Continued.)* Comparative statistical results on CEC2017 test suite (Dimension = 100).

	Min	1	3	5	9	7	12	2	11	13	14	10	6	15	4	8
	Max	34799.49	14600.18	21997.3	33496.43	19623.01	32370.62	16076.65	24359.18	31879.23	34209.79	32930.41	32758.1	35746.71	19935.75	28271.85
F17-22	Mean	37479.94	19093.15	29344.8	35697.62	24491.44	35665.99	21173	30439.66	37530.72	39523.5	35539.48	35956.86	39632.48	33001.66	34179.83
	Std	36165.23	16443.85	25549.45	34778.94	22397.2	33937.72	18938.22	26819.73	35098.74	35928.87	34449.25	34428.78	37828.82	22765.28	31342.59
	Rank	621.51	1135.093	1908.024	712.6208	1254.551	962.9382	1431.709	1420.487	1313.208	1249.187	669.3546	1026.685	839.519	2246.069	1462.323
	Min	14	1	5	11	3	8	2	6	12	13	10	9	15	4	7
	Max	3249.502	3318.195	4148.7	5900.704	4574.457	6152.76	3502.101	5001.171	4814.357	6171.138	4931.135	4071.352	7433.074	3607.888	4658.144
F17-23	Mean	3761.905	3782.028	4865.567	6659.489	5925.514	8130.55	4367.956	7355.101	6409.523	8155.437	5587.088	4460.776	8573.388	4106.146	5760.338
	Std	3460.336	3589.833	4448.913	6293.265	5127.239	7185.951	3879.655	5783.145	5401.478	7024.124	5228.364	4296.754	8070.103	3718.206	5118.229
	Rank	127.7544	119.2356	171.2191	177.3861	338.9086	522.6792	201.99	445.9741	421.5629	485.7392	150.0674	94.88711	366.4355	110.0895	336.4095
	Min	1	2	6	12	8	14	4	11	10	13	9	5	15	3	7
	Max	3989.237	4519.841	5032.931	8902.541	6475.199	8926.924	3897.193	6281.005	5379.189	9927.977	6646.153	4791.903	10414.64	4121.804	5787.543
F17-24	Mean	5033.417	5258.205	6244.335	10845.15	9311.787	14378.21	4959.894	9451.81	10164.05	14810.77	7927.269	5391.79	14297.46	4602.238	7307.985
	Std	4425.856	4767.345	5457.243	9425.105	7765.348	11308.13	4256.941	7722.014	7255.666	11858.53	7225.265	5082.325	13302.49	4323.407	6610.744
	Rank	228.3768	193.085	309.4011	388.573	622.0512	1195.915	234.3797	705.5963	1233.408	1234.816	312.4904	146.497	890.2282	135.2503	352.2169
	Min	3	4	6	12	11	13	1	10	9	14	8	5	15	2	7
	Max	3363.068	3494.053	6173.028	16607.81	9828.195	22387.19	3324.186	5130.982	28946.36	28447.67	16227.78	5788.247	29507.71	4527.215	7723.691
F17-25	Mean	3910.449	4031.98	12804.81	19482.62	16586.3	33426.07	3601.876	6671.104	98006.87	37141.66	24647.37	8428.413	35065.22	6889.282	16003.96
	Std	3659.988	3717.249	8748.793	17310.95	12606.02	28587.2	3465.264	5735.374	42803.02	32304.94	21523.54	7013.881	32979.81	5370.321	10734.64
	Rank	168.4045	164.322	1342.403	538.1716	1706.203	2833.058	62.43167	388.7365	14235.63	2117.325	1867.544	611.5533	1668.346	534.4174	2108.045
	Min	2	3	7	10	9	12	1	5	15	13	11	6	14	4	8
	Max	11106.45	16815.36	21703.6	42349.42	27147.54	45512.71	4503.788	23956.95	35952.07	50788.22	33698.98	20982.89	51780.17	15452.58	25702.15
F17-26	Mean	20655.76	25833.79	37748.26	46917.86	37933.87	60144.9	21394.72	34263.83	67123.39	59423.16	46800.09	26305.38	58922.1	21883.45	35107.87
	Std	16204.79	20331.19	30204.71	44057.05	34372.98	52191.87	15612.94	29593.63	51759.39	55857.45	40652.64	23327.14	56662.64	18452.55	30608.39
	Rank	2170.924	2284.162	3529.601	1018.062	2017.955	3699.269	3843.879	2454.671	9673.213	2040.144	3426.173	1352.767	2153.33	1591.14	2274.984
	Min	2	4	7	11	9	13	1	6	12	14	10	5	15	3	8
	Max	3200.024	3200.022	4627.179	8967.107	5051.677	9650.264	3590.053	4741.338	5423.459	10539.89	7302.089	4281.123	13216.11	3500.221	5048.477
F17-27	Mean	3200.025	3200.024	5944.559	10331.51	10434.2	15760.96	4331.997	8453.065	14610.6	19971.71	10753.73	5562.683	19112.58	4466.343	7927.828
	Std	3200.024	3200.023	5285.845	9674.859	7410.742	12793.22	3811.365	6079.491	7575.376	15862.78	8775.938	4711.815	16620.92	3818.863	6260.255
	Rank	0.000268	0.000517	409.8524	364.103	1363.671	1370.346	162.0372	1003.514	2071.208	2015.923	743.8558	257.9007	1483.138	198.2632	700.9884
	Min	2	1	6	12	9	13	3	7	10	14	11	5	15	4	8
	Max	3300.024	3300.024	8569.973	32083.04	11187.44	26827.68	3439.956	6009.219	32096.71	27652.68	22788.29	6738.697	29578.63	4767.728	9870.593
F17-28	Mean	5912.343	5612.726	15202.42	33858.58	15387.24	40906.04	3676.515	10359.59	58138.38	42983.35	27294.28	10377.18	33560.57	17264.21	19489.74
	Std	3732.93	4202.567	11495.28	32718.39	13403.44	34133.32	3555.152	7773.152	44005.66	32038.03	25576.22	8624.095	32161.22	8448.959	15010.98
	Rank	663.6496	575.8303	1636.686	439.8639	1146.22	3131.898	47.38271	949.9976	5919.349	2355.826	1253.65	939.5972	1101.941	2743.433	2175.024
	Min	2	3	7	13	8	14	1	4	15	11	10	6	12	5	9
	Max	5000.015	5521.395	10659.34	150781.5	11910.73	28243.94	5903.872	9332.836	24337.35	334700.9	21324.48	9956.366	183786.9	8361.448	9990.431
F17-29	Mean	7763.017	8832.049	20320.53	178843.3	25691.65	1486043	8411.102	14380.41	5943406	3996481	119407	14145.78	7696986	11145.41	30909.96
	Std	6386.403	6685.175	13343.94	166216.1	15624.97	598603.1	7109.629	12057.79	1156276	1092209	55902.85	11707.79	2392354	9467.868	14344.4
	Rank	587.6397	715.9652	2191.376	8059.549	2978.327	332624.5	558.9492	1264.432	1237860	711811.3	26414.24	878.1503	1935414	792.1272	4596.288
	Min	1	2	7	11	9	12	3	6	14	13	10	5	15	4	8
	Max	3516.169	3925.704	3.56E+08	2.96E+10	1.15E+09	2.29E+10	12570.69	1.23E+08	1.99E+10	3.59E+10	1.53E+10	4.52E+08	3.68E+10	16973864	1.05E+09
F17-30	Mean	74824.2	69610.85	1.14E+10	3.14E+10	1.94E+10	5.27E+10	140372.8	6.34E+08	6.13E+10	5.82E+10	2.86E+10	1.31E+09	5.82E+10	1.76E+08	1.61E+10
	Std	17132.2	14164.53	3.28E+09	3.05E+10	8.2E+09	4.18E+10	24888.76	3.38E+08	3.64E+10	5.01E+10	1.99E+10	6.94E+08	4.82E+10	95234779	6.87E+09
	Rank	18443.59	14091.3	2.63E+09	4.22E+08	4.59E+09	7.47E+09	23480.4	1.37E+08	9.99E+09	5.59E+09	3.28E+09	1.9E+08	6.41E+09	40617116	4.23E+09
Friedman Rank		3.8276	2.6207	6.2069	10.4828	6.8276	11.3793	1.8276	6.1724	13.3448	13.3448	10.2069	7	14.0345	4.6552	8.069
Mean Rank		3	2	6	11	7	12	1	5	13	13	10	8	14	4	9

TABLE 3. Wilcoxon's signed rank test on CEC 2017 test suite (Dimension = 10).

Function	MBO vs BO	MBO vs SCSO	MBO vs CDO	MBO vs DTBO	MBO vs AOA	MBO vs PSO	MBO vs HHO	MBO vs GOA	MBO vs SAO	MBO vs SCADE	MBO vs mCSA	MBO vs LCA	MBO vs mCapSA	MBO vs SCHO
F17-01	1.16E-07	7.38E-10	3.02E-11	0.006669	3.02E-11	0.935192	3.02E-11	3.02E-11	3.02E-11	3.02E-11	3.01986E-11	3.02E-11	2.13273E-05	3.02E-11
F17-03	1.55E-09	1.25E-11	1.25E-11	1.25E-11	1.25E-11	0.000404	1.25E-11	1.25E-11	1.25E-11	1.25E-11	1.25223E-11	1.25E-11	1.25223E-11	1.25E-11
F17-04	0.060429	6.07E-11	3.02E-11	4.62E-10	3.02E-11	0.000399	3.2E-09	3.02E-11	3.02E-11	3.02E-11	3.01986E-11	3.02E-11	3.01986E-11	4.62E-10
F17-05	0.001589	6.66E-10	2.99E-11	3.65E-11	3.31E-11	9.68E-08	6.63E-11	2.99E-11	2.99E-11	2.99E-11	8.03196E-10	2.99E-11	1.05967E-07	1.28E-09
F17-06	0.500156	1.59E-11	1.59E-11	1.59E-11	1.59E-11	2.89E-10	1.59E-11	1.59E-11	1.59E-11	1.59E-11	1.5945E-11	1.59E-11	1.5945E-11	1.59E-11
F17-07	2.6E-05	6.7E-11	3.02E-11	2.15E-10	3.02E-11	0.935192	6.07E-11	3.02E-11	3.02E-11	3.02E-11	4.07716E-11	3.02E-11	0.005084222	1.78E-10
F17-08	0.004017	6.64E-11	3E-11	1.4E-09	3.66E-11	0.003004	1.54E-09	3E-11	3E-11	3E-11	2.01808E-07	3E-11	0.019860779	5.43E-09
F17-09	1.04E-06	4.71E-11	2.58E-11	2.58E-11	2.58E-11	0.306576	2.85E-11	2.58E-11	2.58E-11	2.58E-11	6.4387E-10	2.58E-11	1.24659E-05	3.49E-11
F17-10	0.024157	3.16E-05	3.83E-06	0.000141	5.86E-06	8.15E-05	1.75E-05	1.31E-08	2.44E-09	2.32E-06	3.36814E-05	3.02E-11	0.000691252	1.64E-05
F17-11	0.000446	2.37E-10	3.02E-11	2.03E-09	3.69E-11	1.25E-07	1.09E-10	3.02E-11	3.02E-11	3.02E-11	5.96442E-09	3.02E-11	0.001517566	2.92E-09
F17-12	0.115362	1.07E-09	3.02E-11	8.1E-10	2.67E-09	0.706171	7.39E-11	3.02E-11	3.02E-11	3.02E-11	3.01986E-11	3.02E-11	0.046755842	1.21E-10
F17-13	4.35E-05	3.02E-11	3.02E-11	3.02E-11	3.02E-11	3.02E-11	3.02E-11	3.02E-11	3.02E-11	3.02E-11	3.01986E-11	3.02E-11	2.87158E-10	3.02E-11
F17-14	0.750574	6.05E-07	5.53E-08	3.35E-08	2.61E-10	1.75E-05	1.6E-07	6.07E-11	6.01E-08	1.25E-07	6.35604E-05	4.2E-10	1.59641E-07	2.67E-09
F17-15	0.520145	4.5E-11	3.02E-11	3.34E-11	3.02E-11	5.57E-10	3.02E-11	3.02E-11	3.02E-11	3.02E-11	3.01986E-11	3.02E-11	4.97517E-11	3.02E-11
F17-16	0.004427	4.12E-06	3.02E-11	1.56E-08	5.49E-11	4.12E-06	9.53E-07	4.62E-10	3.69E-11	3.16E-05	0.063532651	3.16E-05	0.190730333	5.09E-06
F17-17	0.77312	2.6E-05	1.69E-09	0.000189	6.52E-09	0.001518	1.64E-05	6.7E-11	1.29E-09	6.74E-06	0.000769729	0.000318	0.031465633	1.07E-07
F17-18	0.750587	2.87E-10	3.02E-11	2.44E-09	2.87E-10	6.01E-08	1.17E-09	3.02E-11	3.69E-11	3.02E-11	1.61323E-10	0.233989	8.99341E-11	2.87E-10
F17-19	0.118817	5.07E-10	3.02E-11	5.57E-10	3.69E-11	1.61E-10	3.02E-11	3.02E-11	3.02E-11	3.02E-11	2.37147E-10	0.028129	3.01986E-11	6.07E-11
F17-20	0.012712	3.33E-11	3.01E-11	3.01E-11	3.01E-11	2.87E-10	3.33E-11	3.01E-11	3.01E-11	3.01E-11	6.67933E-11	0.090472	1.2843E-06	4.07E-11
F17-21	0.027086	0.620404	3.02E-11	1.75E-05	0.08771	0.228101	0.099258	0.009883	3.5E-09	9.51E-06	2.87897E-06	0.662735	6.76501E-05	8.48E-09
F17-22	0.000132	1.25E-07	3.02E-11	0.030317	3.02E-11	0.293852	3.02E-11	3.02E-11	3.02E-11	3.02E-11	0.00039881	0.662735	0.000212646	3.02E-11
F17-23	0.020681	3.01E-07	3.02E-11	2.23E-09	3.02E-11	0.036439	1.29E-09	3.34E-11	3.02E-11	9.92E-11	1.86817E-05	1	8.1975E-07	8.1E-10
F17-24	6.36E-05	1.17E-05	5.07E-10	2.03E-09	1.16E-07	0.564161	1.87E-07	5.07E-10	5.07E-10	0.003671	0.217016825	1	0.02150618	2.39E-08
F17-25	0.056492	0.77312	3.02E-11	0.206205	3.69E-11	0.001405	0.035137	3.69E-11	3.02E-11	3.32E-06	0.297271689	0.446419	0.899995037	0.728265
F17-26	0.359247	0.387027	3E-11	0.059389	1.09E-10	1.02E-06	3.82E-05	1.94E-10	6.03E-11	2.76E-05	0.004421149	0.420315	0.162310824	0.003334
F17-27	0.818746	8.29E-06	3.02E-11	6.28E-06	1.1E-08	7.22E-06	1.39E-06	4.42E-06	1.46E-10	9.51E-06	9.51394E-06	0.379036	9.51394E-06	4.74E-06
F17-28	0.001999	0.013319	1.79E-11	0.002225	2.98E-11	0.065633	2.79E-07	3.2E-10	1.79E-11	8.3E-10	0.000304174	0.201009	0.009885772	2.73E-05
F17-29	0.149449	0.016285	7.38E-10	6.36E-05	4.57E-09	0.162375	3.08E-08	5.97E-09	8.99E-11	2E-06	0.994101921	0.297272	0.297271689	1.34E-05
F17-30	0.510598	3.02E-11	3.02E-11	3.02E-11	3.02E-11	3.02E-11	3.02E-11	3.02E-11	3.02E-11	2.63E-11	3.01986E-11	0.137323	3.01986E-11	3.02E-11

C. CEC 2022 TEST SUITE

Both the proposed method and other approaches were subjected to additional testing on the CEC2022 test suite with 10 and 20-dimensional search spaces. This suite has 12 distinct test functions, each of which can be categorized as unimodal, multimodal, hybrid, or composition [65]. The details can be found in [66].

1) STATISTICAL RESULTS

In Table 5 and Table 6, the performance of the MBO algorithm on the CEC2022 test suite is evaluated and compared with several other optimization algorithms. The MBO algorithm consistently shows competitive performance across the CEC2022 test suite, especially notable in minimizing the objective function values. In Table 5 (dimension = 10), MBO

TABLE 4. Wilcoxon's signed rank test on CEC 2017 test suite (Dimension = 100).

Function	MBO vs BO	MBO vs SCSO	MBO vs CDO	MBO vs DTBO	MBO vs AOA	MBO vs PSO	MBO vs HHO	MBO vs GOA	MBO vs SAO	MBO vs SCADE	MBO vs mCSA	MBO vs LCA	MBO vs mCapSA	MBO vs SCHO
F17-01	0.529782	3.02E-11	3.02E-11	3.02E-11	3.02E-11	0.001004	3.02E-11	3.02E-11	3.02E-11	3.02E-11	3.02E-11	3.02E-11	3.02E-11	3.02E-11
F17-03	8.84E-07	3.02E-11	3.02E-11	3.02E-11	3.02E-11	1.33E-10	3.02E-11	0.395267	1.09E-10	3.02E-11	5.53E-08	6.01E-08	8.2E-07	1.46E-10
F17-04	0.001114	3.02E-11	3.02E-11	3.02E-11	3.02E-11	2.2E-07	3.02E-11	3.02E-11	3.02E-11	3.02E-11	3.02E-11	3.02E-11	3.02E-11	3.02E-11
F17-05	0.030317	4.5E-11	3.02E-11	6.07E-11	3.02E-11	0.185767	3.34E-11	3.02E-11	3.02E-11	3.02E-11	3.02E-11	3.02E-11	4.31E-08	3.02E-11
F17-06	0.935192	3.02E-11	3.02E-11	3.02E-11	3.02E-11	3.02E-11	3.02E-11	3.02E-11	3.02E-11	3.02E-11	3.02E-11	3.02E-11	3.02E-11	3.02E-11
F17-07	0.033874	3.02E-11	3.02E-11	3.02E-11	3.02E-11	0.000141	3.02E-11	3.02E-11	3.02E-11	3.02E-11	3.02E-11	3.02E-11	4.98E-11	3.02E-11
F17-08	0.016955	3.02E-11	3.02E-11	3.02E-11	3.02E-11	0.630876	3.02E-11	3.02E-11	3.02E-11	3.02E-11	3.02E-11	3.02E-11	3.08E-08	3.02E-11
F17-09	9.76E-10	0.000356	3.02E-11	0.028129	3.02E-11	7.74E-06	3.02E-11	3.02E-11	3.02E-11	3.02E-11	3.02E-11	3.02E-11	0.016285	3.02E-11
F17-10	3.02E-11	3.02E-11	1.55E-09	3.02E-11	3.34E-11	3.02E-11	3.02E-11	0.010315	1.25E-05	1.46E-10	1.69E-09	7.66E-05	3.02E-11	3.02E-11
F17-11	0.166866	7.39E-11	3.02E-11	3.34E-11	3.02E-11	0.063533	3.69E-11	3.02E-11	3.02E-11	3.02E-11	5.57E-10	3.02E-11	3.02E-11	3.34E-11
F17-12	0.501144	3.02E-11	3.02E-11	3.02E-11	3.02E-11	1.86E-06	3.02E-11	3.02E-11	3.02E-11	3.02E-11	3.02E-11	3.02E-11	3.02E-11	3.02E-11
F17-13	0.096263	3.02E-11	3.02E-11	3.02E-11	3.02E-11	0.137323	3.02E-11	3.02E-11	3.02E-11	3.02E-11	3.02E-11	3.02E-11	3.02E-11	3.02E-11
F17-14	0.750587	3.69E-11	3.02E-11	8.89E-10	3.02E-11	0.630876	3.69E-11	3.02E-11	3.02E-11	3.02E-11	3.02E-11	3.02E-11	4.08E-11	3.34E-11
F17-15	0.111987	3.02E-11	3.02E-11	3.02E-11	3.02E-11	0.115362	3.02E-11	3.02E-11	3.02E-11	3.02E-11	3.02E-11	3.02E-11	3.02E-11	3.02E-11
F17-16	0.001236	0.610008	3.02E-11	0.77312	3.02E-11	3.83E-05	0.935192	3.02E-11	3.02E-11	3.02E-11	0.002499	3.02E-11	0.589451	0.115362
F17-17	0.245814	0.001236	3.02E-11	1.43E-05	3.02E-11	0.011711	0.599689	3.02E-11	3.02E-11	3.02E-11	0.001004	3.02E-11	0.428963	7.74E-06
F17-18	0.028129	1.03E-06	3.02E-11	0.002499	3.02E-11	0.002891	2.49E-06	3.02E-11	3.02E-11	3.02E-11	6.7E-11	3.02E-11	5.07E-10	4.62E-10
F17-19	0.923442	3.02E-11	3.02E-11	3.02E-11	3.02E-11	0.706171	3.02E-11	3.02E-11	3.02E-11	3.02E-11	3.02E-11	3.02E-11	3.02E-11	3.02E-11
F17-20	4.5E-11	5.07E-10	1.16E-07	2.61E-10	7.77E-09	8.99E-11	5.07E-10	5.19E-07	0.007617	5.09E-08	0.000117	1.19E-06	1.41E-09	7.38E-10
F17-21	0.00062	3.02E-11	3.02E-11	3.02E-11	3.02E-11	0.12597	3.02E-11	3.02E-11	3.02E-11	3.02E-11	3.02E-11	3.02E-11	2.92E-09	3.02E-11
F17-22	3.02E-11	3.02E-11	1.55E-09	3.02E-11	1.78E-10	3.02E-11	3.02E-11	0.000318	0.145319	1.96E-10	7.12E-09	1.2E-08	3.02E-11	3.02E-11
F17-23	0.000301	3.02E-11	3.02E-11	3.02E-11	3.02E-11	5.07E-10	3.02E-11	3.02E-11	3.02E-11	3.02E-11	3.02E-11	3.01E-11	7.12E-09	3.02E-11
F17-24	5.6E-07	3.34E-11	3.02E-11	3.02E-11	3.02E-11	0.002266	3.02E-11	3.02E-11	3.02E-11	3.02E-11	8.15E-11	3.02E-11	0.059428	3.02E-11
F17-25	0.19073	3.02E-11	3.02E-11	3.02E-11	3.02E-11	2.68E-06	3.02E-11	3.02E-11	3.02E-11	3.02E-11	3.02E-11	3.02E-11	3.02E-11	3.02E-11
F17-26	4.69E-08	3.02E-11	3.02E-11	3.02E-11	3.02E-11	0.864994	3.02E-11	3.02E-11	3.02E-11	3.02E-11	3.02E-11	3.02E-11	5.61E-05	3.02E-11
F17-27	1.46E-10	3.02E-11	3.02E-11	3.02E-11	3.02E-11	3.02E-11	3.02E-11	3.02E-11	3.02E-11	3.02E-11	3.02E-11	3.02E-11	3.02E-11	3.02E-11
F17-28	0.002499	3.02E-11	3.02E-11	3.02E-11	3.02E-11	0.077272	3.02E-11	3.02E-11	3.02E-11	3.02E-11	3.02E-11	3.02E-11	6.07E-11	3.02E-11
F17-29	0.118817	3.02E-11	3.02E-11	3.02E-11	3.02E-11	2.13E-05	3.02E-11	3.02E-11	3.02E-11	3.02E-11	3.02E-11	3.02E-11	3.02E-11	3.02E-11
F17-30	0.818746	3.02E-11	3.02E-11	3.02E-11	3.02E-11	0.004856	3.02E-11	3.02E-11	3.02E-11	3.02E-11	3.02E-11	3.02E-11	3.02E-11	3.02E-11

achieves the minimum value (300) across many functions, which is on par with or better than several other algorithms. For instance, on F22-01, MBO ranks 2nd in minimum value and 1st in mean value, indicating its strong performance in finding the global optimum consistently. Moreover, the standard deviation (Std) for MBO is often lower than other methods, suggesting robustness and stability in its solutions.

In Table 6 (dimension = 20), MBO continues to demonstrate competitive performance, particularly in achieving low minimum values across various functions. For example, on F22-01, MBO achieves the minimum value of 300, showing its ability to find the global optimum effectively. The mean values for MBO are also competitive, demonstrating its ability to achieve good solutions consistently across different test functions

The Wilcoxon's Signed Rank Test results underscore the exceptional performance of the MBO algorithm across the CEC 2022 test suite functions. In the 10-dimensional tests, MBO exhibited remarkable superiority over numerous state-of-the-art algorithms. Especially, on Function F22-01, MBO achieved highly significant p-values of 2.53E-10 against BO, 1.25E-11 against SCSO, CDO, DTBO, AOA, and other algorithms, demonstrating its effectiveness in producing superior solutions. Similarly, on Function F22-05, MBO achieved p-values as low as 6.04E-10 against BO, highlighting its robust performance. These results were consistent across various functions, reaffirming MBO's efficacy in optimizing complex problems. In higher dimensions, such as 20, MBO continued to outperform competitors, achieving significant p-values across functions like F22-01 and F22-02. These findings underscore MBO as a highly competitive algorithm for solving challenging optimization tasks.

2) CONVERGENCE AND BOXPLOT ANALYSIS

Figure 6 demonstrates the convergence curves of MBO on functions from the CEC 2022 benchmark suit with a dimension of 10. On the other hand, Figure 7 demonstrates a boxplot analysis for 10-dimensional CEC 2022 test suite. The illustrations verify the effectiveness of the MBO discussed earlier. This is further supported by the convergence curves in Figure 8 and boxplot analysis Figure 9 which present the respective illustrations for 20-dimensional CEC 2022 test suite.

D. EXPLORATION–EXPLOITATION ANALYSIS

Figure 10 provides a clear explanation of the exploration-exploitation dynamics demonstrated by MBO when dealing with the CEC 2022 test suite. The displayed curves demonstrate a sophisticated and harmonious exploration-exploitation behavior exhibited by MBO on 10-dimensional CEC 2022 functions. More precisely, the algorithm devotes a significant portion of its time to exploring, especially in the beginning of its operation. The intentional focus on exploration during the initial stages enhances the algorithm's effectiveness in thoroughly navigating the solution space, which may aid in identifying and converging towards the best possible answers. This analysis of exploration-exploitation provides vital insights into how the MBO algorithm strategically allocates computational efforts. It highlights the flexible and effective approach of the algorithm in navigating difficult optimization landscapes.

E. ENGINEERING PROBLEMS

As part of the performance evaluation of the proposed MBO, seven different real-world engineering optimization problems were also considered. The following subsections provide a

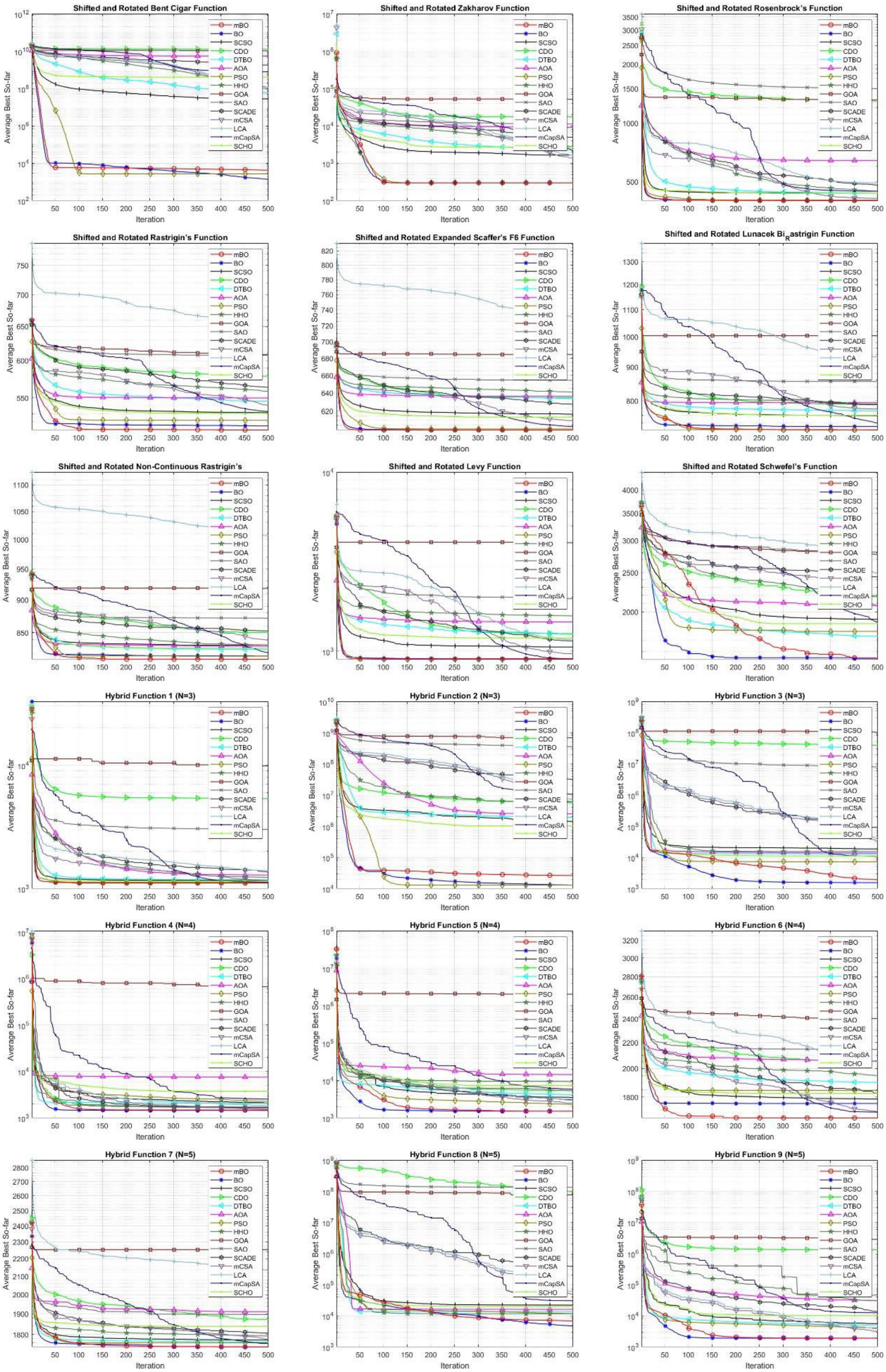

FIGURE 2. Convergence curves of test functions from CEC2017 test suite (dimension = 10).

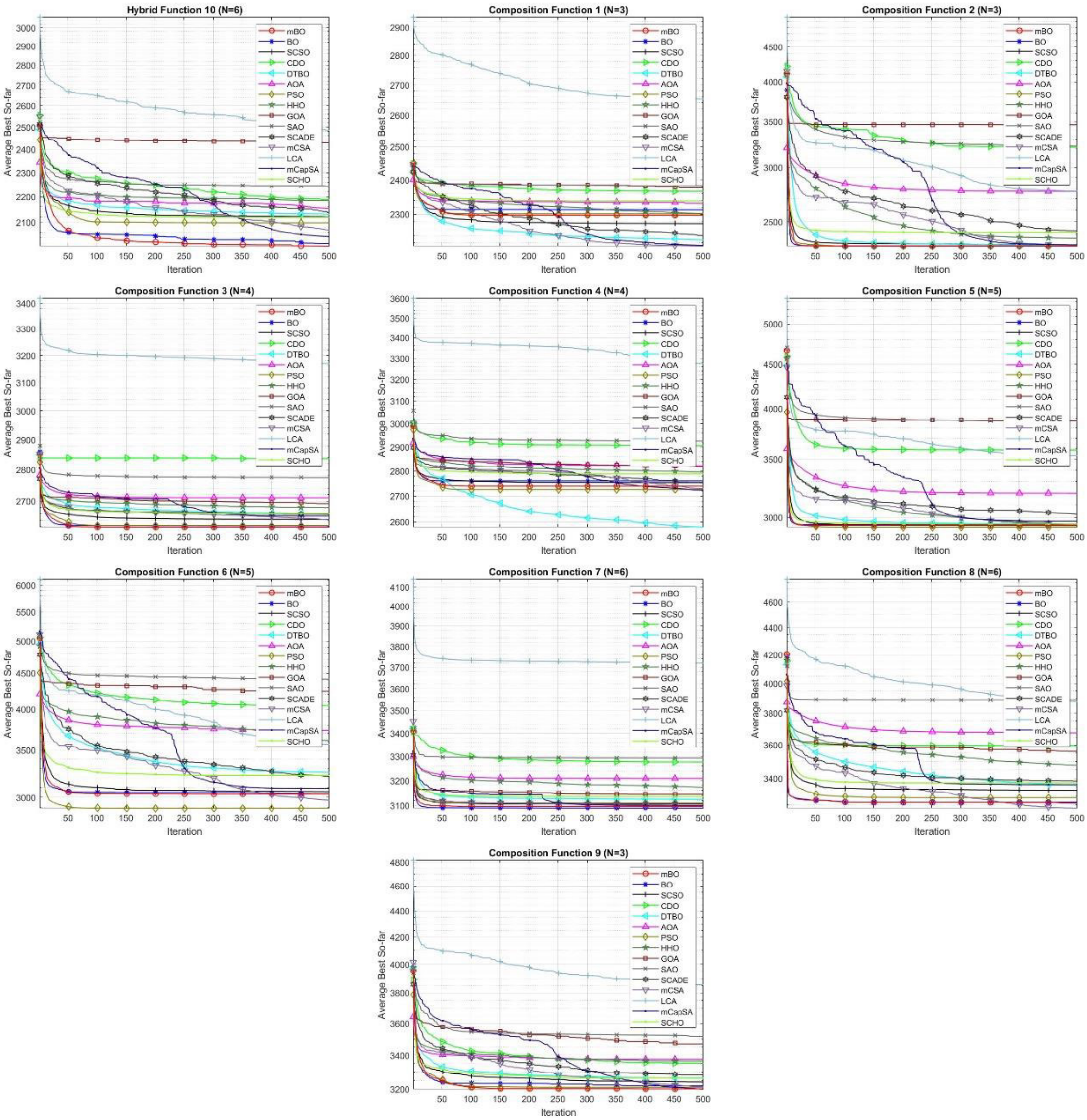

FIGURE 2. ***(Continued.)*** **Convergence curves of test functions from CEC2017 test suite (dimension = 10).**

detailed description of the problems and demonstrate the efficacy of the MBO comparatively.

1) CANTILEVER BEAM DESIGN

The first considered challenge for the performance evaluation of MBO is related to the optimal design of a cantilever beam. This problem constitutes a significant engineering challenge that requires determining the optimal dimensions for the components of a cantilever beam. The overarching objective is to minimize the overall weight of the beam structure, while simultaneously ensuring that specific structural and safety constraints are fully met. A distinguishing characteristic of this problem is the structural design of the cantilever beam. It is composed of five hollow cells, each featuring a square cross-section. These cells are each defined by a unique variable, while maintaining a constant thickness. Thus, there are five distinct parameters, namely, x_1, x_2, x_3, x_4 and x_5, that are subject to the optimization process. The mathematical expression that governs this problem includes a cost function that is to be minimized, and a set of constraints that must be satisfied. A schematic diagram illustrating the structural design of the cantilever beam, and providing a visual representation of the problem, is presented in Figure 11. The mathematical formulation of the problem is expressed as minimization of:

$$f(x) = 0.0624\,(x_1 + x_2 + x_3 + x_4 + x_5) \tag{16}$$

which is subjected to $g(x) = \left(\left(61/x_1^3\right) + \left(37/x_2^3\right) + \left(19/x_3^3\right) + \left(7/x_4^3\right) + \left(1/x_5^3\right) - 1\right)$ and $0.01 \le x_i \le 100$ where $i = 1, 2, 3, 4, 5$.

In endeavor to solve this optimization problem, a comprehensive and rigorous comparative analysis was performed.

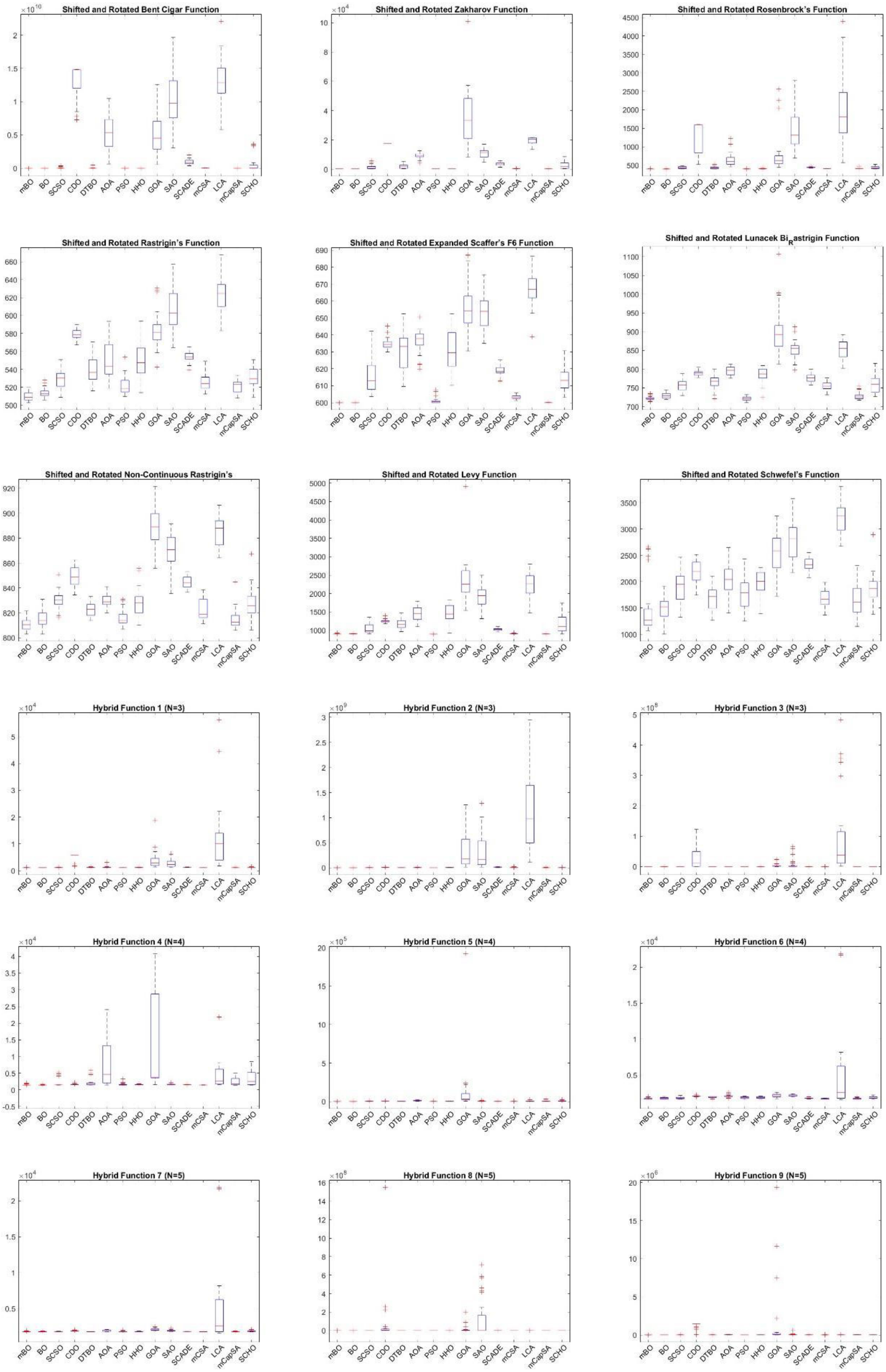

FIGURE 3. Boxplots of test functions from CEC2017 test suite (dimension = 10).

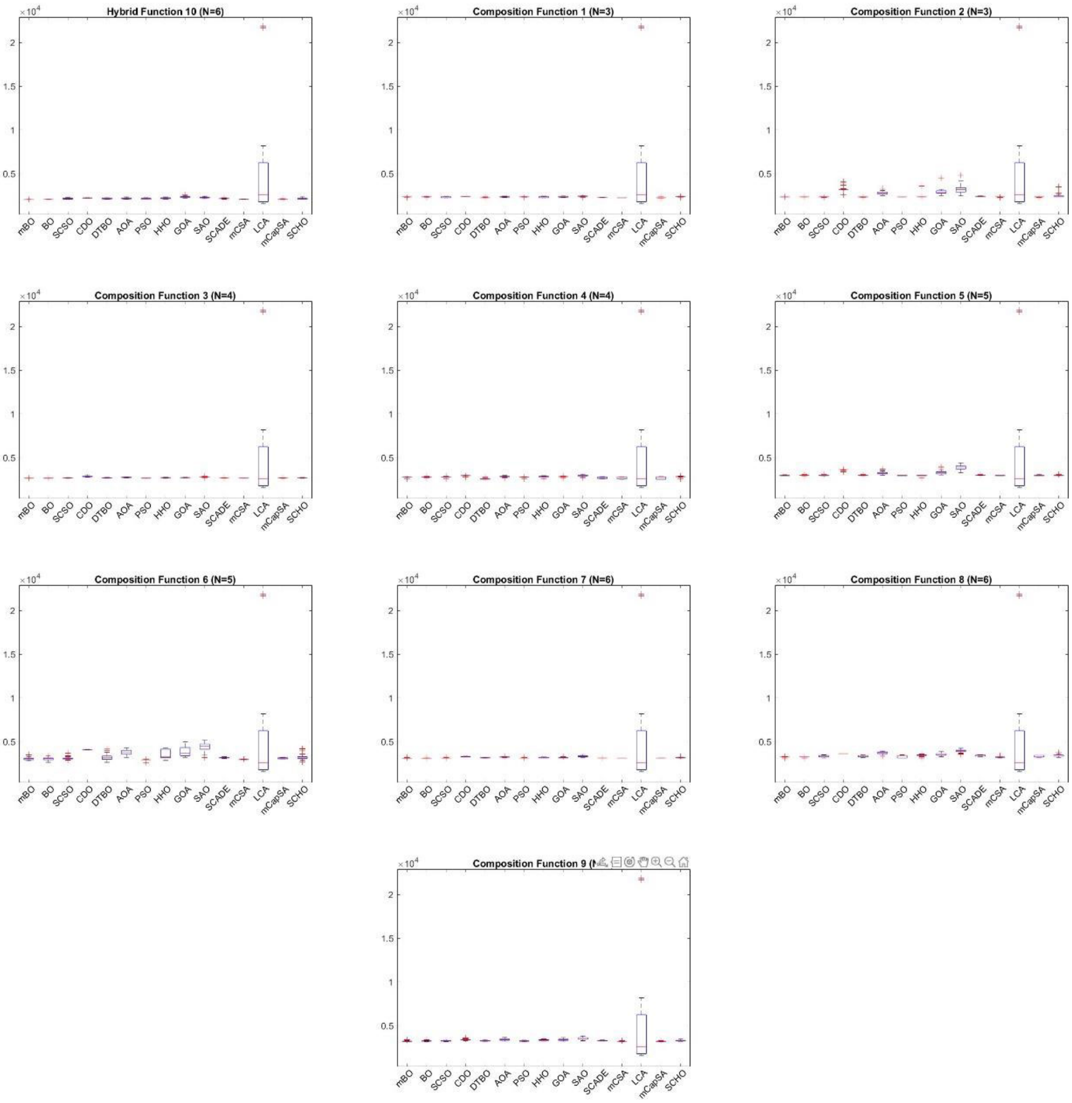

FIGURE 3. ***(Continued.)*** **Boxplots of test functions from CEC2017 test suite (dimension = 10).**

This analysis encompassed evaluating the performance and robustness of different optimization techniques, including the original BO, SCSO, CDO, DTBO, HHO, AOA, SAO, GOA, and PSO. The performance of each algorithm was determined based on the optimal values they obtained. The statistical results in Table 9 provide a comprehensive overview of the performance of various optimization algorithms for the cantilever beam design problem. Notably, the MBO stands out with the lowest minimum objective function value, minimal standard deviation, and the highest rank among all algorithms. These metrics collectively indicate the consistency and superior performance of MBO in finding optimal solutions. Additionally, the best-found solution in Table 10 reaffirms MBO's dominance, as it achieved the lowest objective function value compared to other optimizers. In contrast, while other algorithms such as BO, SCSO, and PSO demonstrated competitive results, MBO consistently outperforms them, as evidenced by its top rank and superior best-found solution, establishing its efficacy for the cantilever beam design optimization task.

Figure 12(a) presents a graphical illustration of the convergence curve of the MBO technique. This visual representation provides an empirical basis for asserting the superiority of the MBO technique. It is clear from the figure that the MBO technique converges effectively and efficiently towards the optimal solution, markedly outperforming the other algorithms under consideration. Further bolstering the superiority of the MBO technique, Figure 12(b) exhibits a boxplot depicting the performance of all considered algorithms. It is evident from this boxplot that the MBO technique not only achieves optimal solutions more

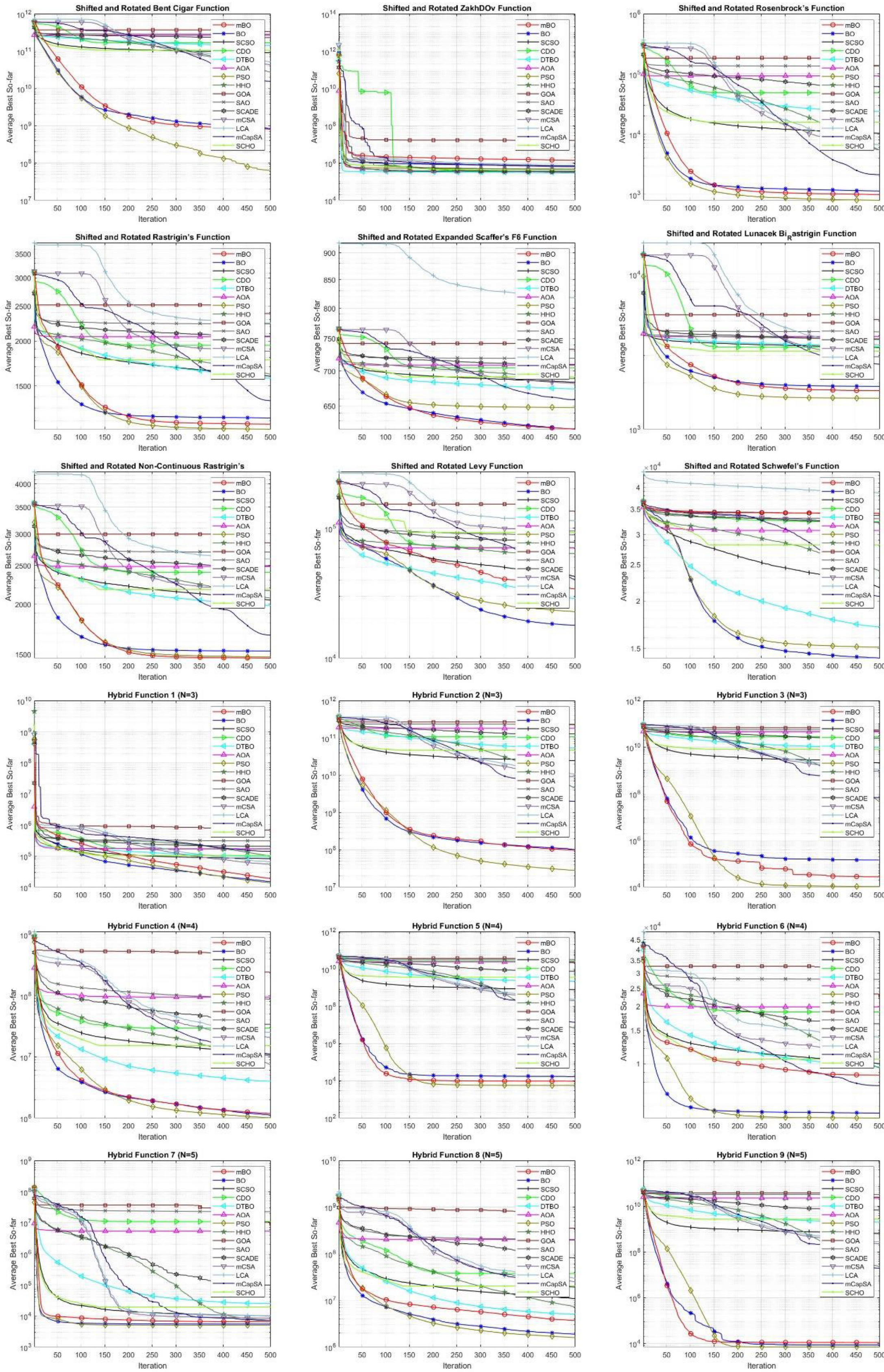

FIGURE 4. Convergence curves of test functions from CEC2017 test suite (dimension = 100).

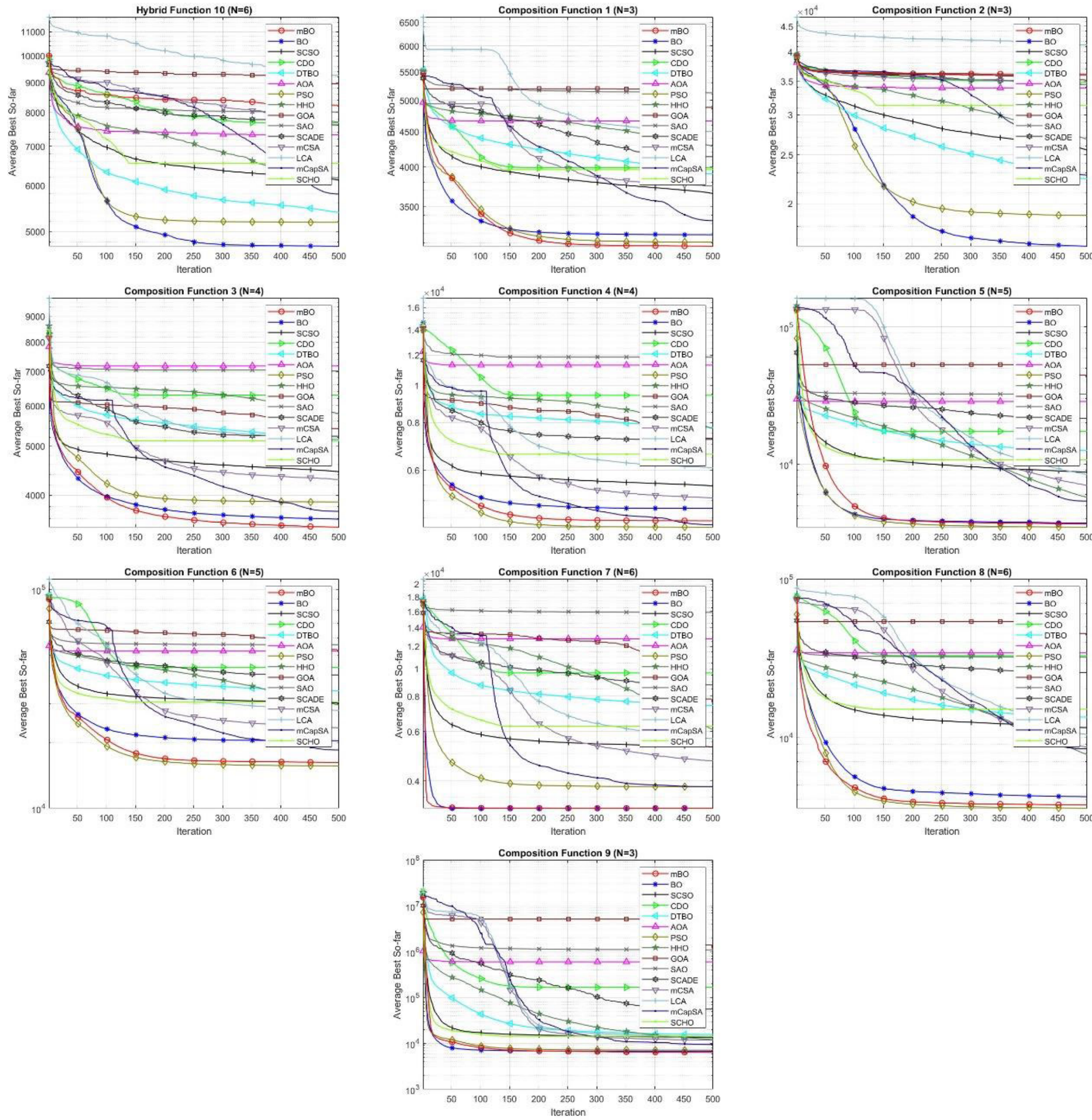

FIGURE 4. ***(Continued.)*** **Convergence curves of test functions from CEC2017 test suite (dimension = 100).**

frequently but also maintains a more consistent performance with fewer variations in comparison to other optimization algorithms. This level of consistency, characterized by a smaller interquartile range, underscores the reliability and robustness of the MBO technique, reinforcing its efficacy for this class of optimization problems.

2) INDUSTRIAL REFRIGERATION SYSTEM DESIGN

The task of designing industrial refrigeration systems is particularly complex and involves numerous design variables and constraints. With an aim to minimize a nonlinear objective function that embodies the integration of various system components. A more detailed desecration of this problem is discussed in [67].

The mathematical formulation of this industrial refrigeration system design problem is described as the minimization of (17).

$$\begin{aligned} f(x) = {} & 63098.88x_2x_4x_{12} + 5441.5x_2^2x_{12} + 115055.5x_2^{1.664}x_6 \\ & + 6172.27x_2^2x_6 + 63098.88x_1x_3x_{11} + 5441.5x_1^2x_{11} \\ & + 115055.5x_1^{1.664}x_5 + 6172.27x_1^2x_5 + 140.53x_1x_{11} \\ & + 281.29x_3x_{11} + 70.26x_1^2 + 281.29x_3^2 \\ & + 14437x_8^{1.8812}x_{12}^{0.3424}x_{10}x_{14}^{-1}x_1^2x_7x_9^{-1} \\ & + 20470.2x_7^{2.893}x_{11}^{0.316}x_1^2x_1x_3 \end{aligned} \tag{17}$$

which is subjected to

- $g_1(x) = 1.524x_7^{-1} - 1 \le 0,$
- $g_2(x) = 1.524x_8^{-1} - 1 \le 0,$
- $g_3(x) = 0.07789x_1 - 2x_7^{-1}x_9 - 1 \le 0,$
- $g_4(x) = 7.05305x_9^{-1}x_1^2x_{10}x_8^{-1}x_2^{-1}x_{14}^{-1} - 1 \le 0,$
- $g_5(x) = 0.0833x_{13}^{-1}x_{14} - 1 \le 0,$

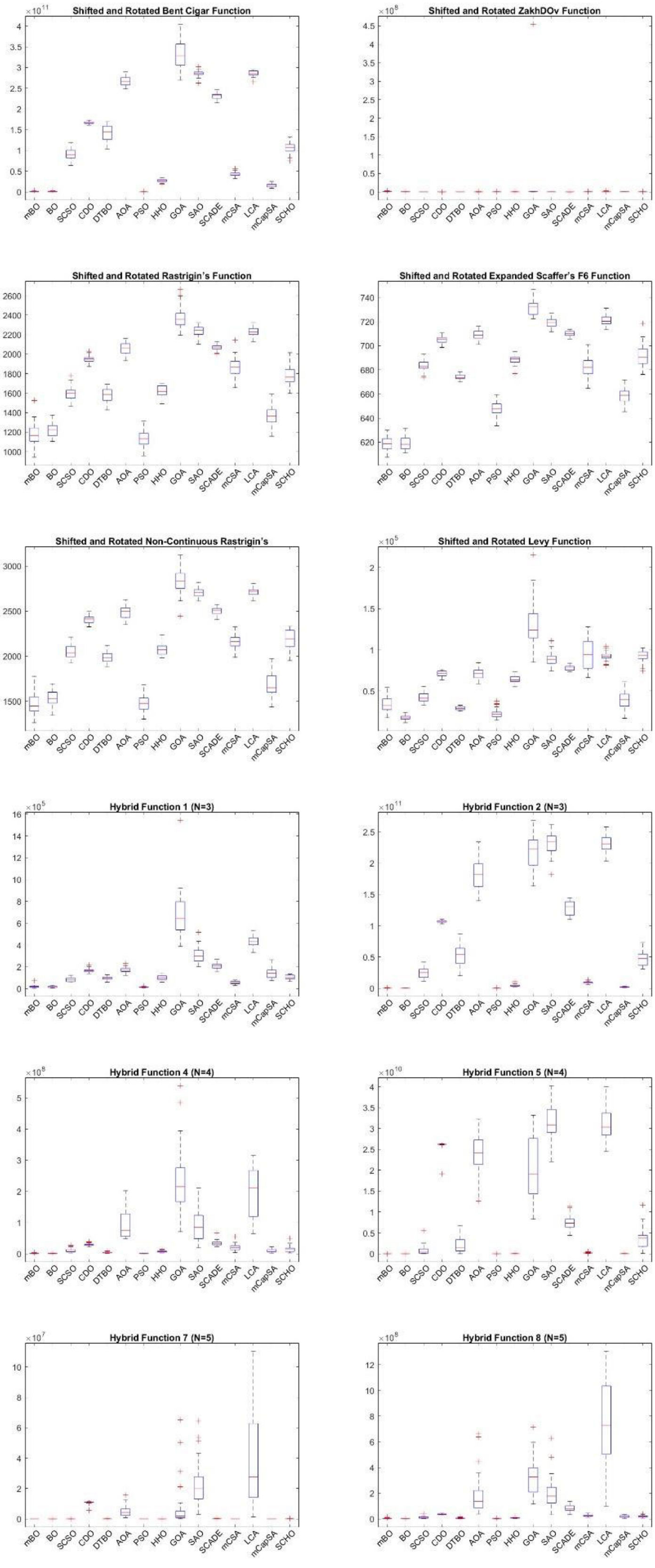

FIGURE 5. Boxplots of test functions from CEC2017 test suite (dimension = 100).

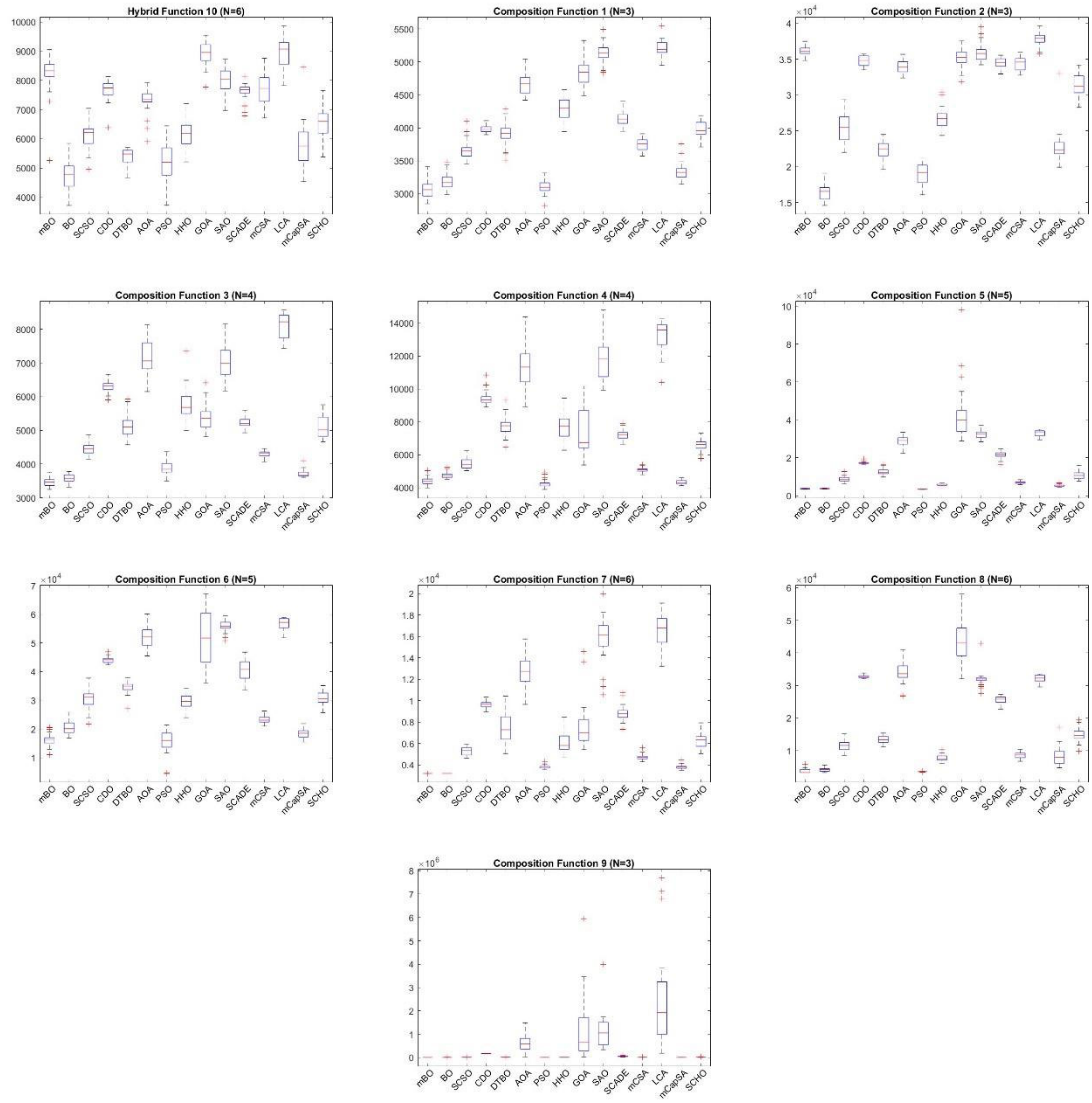

FIGURE 5. *(Continued.)* **Boxplots of test functions from CEC2017 test suite (dimension = 100).**

- $g_6(x) = 47.136x_2^{0.333}x_{12} - 1.333x_8x_{13}^{2.1195} + 62.08x_{13}^{2.1195}x_{12}^{-1}x_8^{0.2}x_{10}^{-1} - 1 \leq 0,$
- $g_7(x) = 0.04771x_8^{1.8812}x_{12}^{0.3424} - 1 \leq 0,$
- $g_8(x) = 0.0488x_9^{1.893}x_{12}^{0.316} - 1 \leq 0,$
- $g_9(x) = 0.0099x_1x_3^{-1} - 1 \leq 0,$
- $g_{10}(x) = 0.0193x_2x_4^{-1} - 1 \leq 0,$
- $g_{11}(x) = 0.0298x_1x_5^{-1} - 1 \leq 0,$
- $g_{12}(x) = 0.056x_2x_6^{-1} - 1 \leq 0,$
- $g_{13}(x) = 2x_9^{-1} - 1 \leq 0,$
- $g_{14}(x) = 2x_{10}^{-1} - 1 \leq 0,$
- $g_{15}(x) = x_{12}x_{11}^{-1} - 1 \leq 0$

with $0.01 \leq x_i \leq 5$ where $i = 1, 2, 3, \ldots, 14$.

Table 11 presents statistical results for various optimization algorithms applied to an industrial refrigeration system problem. The MBO again demonstrates notable performance, ranking third overall. MBO achieves a low minimum objective function value, indicating efficient convergence to optimal solutions. It also exhibits a relatively low standard deviation, highlighting the stability of its results. In contrast, other algorithms such as DTBO and SAO show higher variability and lower ranks. This suggests that MBO provides competitive and consistent results compared to other optimization methods.

Examining the best-found solutions in Table 12 further supports MBO's effectiveness for the refrigeration system problem. MBO attains the lowest objective function value, indicating its capability to find superior solutions. The solutions generated by MBO are characterized by low parameter values across various design variables, suggesting an efficient configuration for the refrigeration system. While some other algorithms exhibit competitive performance,

TABLE 5. Comparative statistical results on CEC2022 test suite (Dimension = 10).

Function	Metric	MBO	BO	SCSO	CDO	DTBO	AOA	PSO	HHO	GOA	SAO	SCADE	mCSA	LCA	mCapSA	SCHO
F22-01	Min	3.00E+02	3.00E+02	3.30E+02	7.94E+03	3.67E+02	7.43E+02	3.00E+02	3.00E+02	7.62E+03	4209.736	810.1844	332.5896	6277.148	300.0003	400.2764
	Max	3.00E+02	3.00E+02	6.35E+03	3.09E+06	1.91E+03	1.86E+04	3.00E+02	3.03E+02	5.64E+04	16536.14	4134.53	517.106	10802.35	300.2309	9272.352
	Mean	3.00E+02	3.00E+02	1.63E+03	1.29E+05	1.06E+03	9.09E+03	3.00E+02	3.02E+02	2.69E+04	8718.85	2590.53	400.3356	10224.06	300.0163	3563.242
	Std	4.6E-14	6.22E-13	1651.443	560199.9	671.811	4719.963	4.35E-14	0.668268	11270.2	2889.558	812.5597	54.6054	1034.048	0.042596	2686.026
	Rank	2	3	8	15	7	12	1	5	14	11	9	6	13	4	10
F22-02	Min	400	400	400.071	697.7884	400.0135	430.0954	400.0005	400.0678	466.3229	675.9374	431.1504	401.503	712.1726	407.1407	400.2338
	Max	403.9866	404.1019	487.5398	877.6525	611.8797	1719.829	470.7811	498.5789	1339.855	3555.66	490.3173	414.3872	4364.784	492.6722	608.8599
	Mean	400.5315	400.9344	427.1934	846.5223	419.1927	865.6725	406.5647	420.848	682.7758	1372.853	456.4966	409.0785	2228.777	413.9185	442.983
	Std	1.378343	1.722012	29.09221	32.2897	43.89478	322.6393	12.56433	28.72007	250.8548	567.2658	14.15188	2.601408	935.4738	21.30721	53.22324
	Rank	1	2	8	12	6	13	3	7	11	14	10	4	15	5	9
F22-03	Min	600	600	601.9024	632.0868	607.7818	624.6725	600	608.8171	627.9384	631.0359	609.122	601.3416	642.263	600.0007	602.4184
	Max	600	600.0319	641.3437	645.0853	645.6445	649.875	613.1787	657.1185	694.1513	669.5186	623.7257	606.3273	696.2944	600.5701	645.6865
	Mean	600	600.0014	615.318	636.3318	631.3873	635.6332	601.4224	628.1246	659.8935	654.3983	618.1979	603.4917	669.6646	600.0369	615.3253
	Std	1.1E-11	0.005938	10.07856	3.066115	9.537191	5.92341	3.149748	12.74038	16.83478	9.168835	3.386406	1.217682	12.25866	0.103443	9.46131
	Rank	1	2	6	12	10	11	4	9	14	13	8	5	15	3	7
F22-04	Min	803.9798	802.9849	809.089	837.0101	810.0176	810.9512	804.9748	812.9864	852.2876	840.466	830.5544	811.6275	844.0265	804.9748	820.8445
	Max	820.8941	832.8336	845.0794	862.7601	824.9182	841.7925	831.8386	843.8296	905.8719	881.9428	846.0712	840.7918	891.5984	843.778	864.794
	Mean	812.9676	814.6922	827.4601	847.2832	818.2498	829.3211	814.5595	827.1654	880.9793	863.0428	840.8505	824.3011	873.8112	818.1236	835.5662
	Std	5.679546	7.206457	8.276031	6.264564	4.115969	6.913858	6.402807	7.177303	12.0264	10.33926	3.656347	7.283647	10.88913	9.133049	10.6807
	Rank	1	3	8	12	5	9	2	7	15	13	11	6	14	4	10
F22-05	Min	900	900.6334	907.0767	1275.254	1008.681	1077.073	900	924.8897	1385.549	1251.664	937.0152	901.3411	1321.939	900	937.4303
	Max	907.8573	1012.134	1757.082	1568.136	1375.105	1669.555	902.8179	1703.683	4823.83	2165.207	1159.662	1057.564	2709.505	929.2799	1960.708
	Mean	901.2947	929.5817	1053.53	1397.241	1187.98	1302.378	900.2501	1366.615	2398.878	1676.645	1002.615	915.1981	1963.255	904.6546	1314.83
	Std	1.74182	27.63376	194.2702	75.97337	114.2829	152.3476	0.580005	186.1976	777.3149	251.0827	45.01148	28.67057	340.8342	6.102637	259.7831
	Rank	2	5	7	12	8	9	1	11	15	13	6	4	14	3	10
F22-06	Min	1826.863	1805.11	1877.091	29826191	1860.261	2101.42	1808.03	1959.344	1361183	96673.18	3395.053	2510.435	4791073	1843.337	2739.744
	Max	4578.61	13709.1	8122.438	2.89E+09	2769.165	8247.565	7670.127	7621.517	1.33E+08	5.35E+08	1120514	40719.78	2.2E+08	8110.53	34868.79
	Mean	2272.731	2393.933	4431.702	3.6E+08	2050.744	4024.974	3060.763	3788.956	26329675	38780010	304222	16354.26	1.42E+08	4872.367	9311.177
	Std	676.9541	2179.372	1854.567	6.04E+08	229.0755	1484.056	1331.003	1629.764	34240647	98261944	284597.2	10490.17	65288396	2455.376	6196.702
	Rank	2	3	7	15	1	6	4	5	12	13	11	10	14	8	9
F22-07	Min	2000	2000	2021.091	2108.303	2025.278	2048.803	2001.619	2021.737	2061.624	2051.864	2044.669	2024.557	2082.604	2004.614	2005.629
	Max	2023.611	2020.996	2105.521	2148.441	2102.977	2175.308	2049.475	2140.387	2305.624	2126.978	2079.298	2040.4	2276.579	2022.681	2115.651
	Mean	2017.463	2015.898	2043.546	2137.943	2053.509	2095.65	2026.68	2068.341	2144.875	2098.393	2062.914	2029.622	2167.425	2020.155	2044.573
	Std	7.731119	7.874175	20.55541	8.332632	18.65603	29.16379	13.26876	27.42607	50.35968	19.6991	9.516176	4.02522	51.46907	4.276495	30.06748
	Rank	2	1	6	13	8	11	4	10	14	12	9	5	15	3	7
F22-08	Min	2200.087	2200.64	2216.556	2220.534	2205.614	2225.985	2200.744	2221.628	2231.93	2228.44	2226.253	2215.182	2244.5	2201.041	2208.564
	Max	2225.82	2221.279	2232.087	2251.856	2225.078	2483.277	2339.305	2265.102	2466.451	2316.817	2236.095	2230.07	2529.432	2222.294	2347.377
	Mean	2218.048	2219.855	2225.376	2231.797	2222.146	2282.036	2231.905	2236.989	2278.68	2251.368	2230.976	2226.206	2313.024	2218.287	2233.492
	Std	8.357233	3.648489	2.966783	5.751659	4.084377	83.88575	36.44134	14.26911	55.10382	22.41633	2.238026	3.274527	72.93975	6.664319	30.37366
	Rank	1	3	5	8	4	14	9	11	13	12	7	6	15	2	10
F22-09	Min	2485.502	2485.502	2529.293	2655.315	2529.31	2631.462	2529.284	2530.004	2573.727	2651.001	2551.528	2529.333	2695.262	2529.284	2529.339
	Max	2485.502	2485.502	2661.796	2708.57	2676.216	2758.596	2676.216	2676.264	2941.619	2805.785	2642.143	2533.032	3030.406	2604.084	2742.88
	Mean	2485.502	2485.502	2566.63	2659.761	2622.728	2687.279	2534.182	2564.894	2736.38	2737.355	2588.879	2530.006	2828.9	2533.087	2600.829
	Std	1.96E-12	1E-11	37.27008	9.304682	44.50906	25.67871	26.82598	30.69067	80.9815	32.64055	22.00678	0.705293	79.82205	13.97907	45.7253
	Rank	1	2	7	11	10	12	5	6	13	14	8	3	15	4	9
F22-10	Min	2500.18	2500.222	2500.287	2643.335	2500.522	2509.74	2403.727	2500.431	2506.329	2515.139	2501.111	2500.452	2540.389	2500.262	2500.306
	Max	2500.614	2641.368	2636.065	3592.398	2631.35	3196.244	3060.152	2663.865	3867.394	3977.296	2506.947	2501.09	4872.809	2501.357	2989.433
	Mean	2500.376	2545.554	2558.983	2799.911	2532.425	2672.258	2562.943	2568.366	2647.817	2811.452	2503.229	2500.711	3285.321	2500.829	2608.918
	Std	0.109089	60.50351	63.64682	211.5373	52.88249	176.1135	113.3455	71.22918	252.3225	361.7041	1.374153	0.177156	668.3299	0.277709	154.2419
	Rank	1	6	7	13	5	12	8	9	11	14	4	2	15	3	10
F22-11	Min	2600	2600	2602.16	2872.999	2600.248	2805.781	2600	2604.096	2787.227	2858.123	2759.905	2627.97	3229.007	2600	2608.821
	Max	3000	3183.967	3105.841	3345.272	3180.319	3759.151	3000	3204.428	3845.673	4578.669	2795.444	3017.026	5271.515	2751.176	3186.877
	Mean	2676.785	2786.488	2793.534	3295.684	2755.659	3174.371	2700.061	2794.194	3145.421	3488.345	2777.661	2694.773	4131.708	2735.856	2795.774
	Std	119.5086	171.293	159.6805	121.2695	147.616	312.5721	147.4125	169.0387	296.4845	473.5836	10.60514	81.23826	583.1395	44.71139	164.3455
	Rank	1	7	8	13	5	12	3	9	11	14	6	2	15	4	10
F22-12	Min	2600	2600	2602.16	2872.999	2600.248	2921.449	2860.68	2864.566	2787.227	2858.123	2866.58	2860.306	3006.109	2861.405	2863.642
	Max	3000	3183.967	3105.841	3345.272	3180.319	3116.312	2980.613	2976.756	3845.673	4578.669	2872.539	2867.89	3635.388	2865.784	2973.303
	Mean	2663.514	2786.488	2793.534	3295.684	2755.659	3001.383	2877.138	2905.735	3145.421	3488.345	2869.923	2864.445	3196.834	2863.641	2896.873
	Std	103.4924	171.293	159.6805	121.2695	147.616	53.284	29.81626	31.16676	296.4845	473.5836	1.323487	1.916276	136.6548	1.138266	26.72336
	Rank	1	3	4	14	2	11	8	10	12	15	7	6	13	5	9
Friedman Rank		1.375	3.2083	6.75	12.5	5.9167	11	4.4167	8.25	12.9167	13.1667	8	4.9167	14.4167	4	9.1667
Mean Rank		1	2	7	12	6	11	4	9	13	14	8	5	15	3	10

MBO stands out as a robust and effective optimizer for this complex industrial optimization problem, reinforcing its superiority based on both statistical metrics and best-found solutions.

Furthermore, Figure 13 exemplifies the relatively improved rate of convergence and robustness of the proposed algorithm in minimizing the objective function and good statistical box plot performance for this problem. This study, therefore, validates the advantage of employing MBO in industrial refrigeration system design, endorsing its robust performance and enhanced solution accuracy.

3) WELDED BEAM DESIGN

The welded beam design problem is an essential task in structural engineering, which requires finding the optimal dimensions of a beam that can bear a specific load. The primary objective is to minimize the fabrication costs, which includes the material and labor costs. In tandem, it is also critical to conform to the stress and deflection limitations inherent in the design. Such requirements stem from the need to maintain the structural integrity of the beam, avoiding failures that can result from exceeding the allowable stress or deflection limits.

This problem is formulated as an optimization issue involving four design variables, presented as $x = [x_1, x_2, x_3, x_4]$, where x_1 denotes the thickness of the weld, x_2 the length of the weld, x_3 the depth of the beam, and x_4 the width of the beam. These parameters are essential components of the beam structure, influencing not only the fabrication cost but also the overall performance and reliability of the final design. The objective function, $f(x)$, is a mathematical representation of the fabrication cost that depends on the aforementioned design variables. The constraint functions, $g_i(x)$, signify the stress and deflection limits, ensuring that the final design does not compromise the beam's structural integrity. A pictorial representation of the welded beam design problem is shown in Figure 14.

The mathematical formulation of the problem is articulated as minimization of

$$f(x) = 1.10471x_1^2x_2 + 0.04811x_3x_4(14.0+x_2) \tag{18}$$

which is subjected to

- $g_1(x) = \tau(x) - \tau_{max}(x) \leq 0,$
- $g_2(x) = \sigma(x) - \sigma_{max}(x) \leq 0,$
- $g_3(x) = \delta(x) - \delta_{max}(x) \leq 0,$
- $g_4(x) = x_1 - x_4 \leq 0,$
- $g_5(x) = P - P_c(x) \leq 0,$

TABLE 6. Comparative statistical results on CEC2022 test suite (Dimension = 20).

Function	Metric	MBO	BO	SCSO	CDO	DTBO	AOA	PSO	HHO	GOA	SAO	SCADE	mCSA	LCA	mCapSA	SCHO
F22-01	Min	300	300	1809.684	24053.78	1338.604	18322.71	300	584.5336	42522.61	21217.61	16428.23	2535.269	58868.81	426.8537	4714.846
	Max	300	300.058	22430.5	26427.54	21594.85	57412.21	300.6752	8011.262	188300.1	58594.51	35512.62	9974.354	160343.6	10592.45	25410.84
	Mean	300	300.0019	10003.99	25166.51	7745.821	33106.89	300.0419	3114.249	85233.59	40936.58	27586.72	5020.403	102438.9	3498.826	14414.79
	Std	4.44E-10	0.010582	3968.606	566.5651	4261.761	11113.97	0.136345	1925.794	31897.24	8641.084	4591.083	1828.242	31772.05	2774.884	4958.95
	Rank	1	2	8	10	7	12	3	4	14	13	11	6	15	5	9
F22-02	Min	400.085	406.0729	476.118	1974.795	480.3379	1224.299	404.2873	453.029	1041.183	2175.776	618.2641	451.2524	2062.103	431.2773	463.819
	Max	479.2468	494.1482	657.6972	2135.372	946.7633	3749.003	473.594	555.3796	4532.7	5983.536	1107.168	554.5914	6160.35	506.5526	924.0057
	Mean	420.0352	430.6931	545.7733	2026.27	630.1479	2076.609	450.7118	486.3654	2354.621	3953.734	816.5207	492.7971	4243.417	460.8861	621.1151
	Std	18.35319	26.8395	52.20078	40.75985	103.7996	570.7902	16.79983	26.98175	1028.307	1048.719	98.76807	24.30335	1168.704	17.76895	128.0005
	Rank	1	2	7	11	9	12	3	5	13	14	10	6	15	4	8
F22-03	Min	600	600	628.2	650.9298	640.7107	642.2214	600.1714	639.3135	660.407	662.444	634.0166	608.0857	667.7682	600.0253	615.0695
	Max	600.0012	600.0586	667.4897	672.1196	666.483	675.9566	648.5791	673.8065	735.4857	703.38	657.1023	623.4141	714.2956	609.2618	674.6874
	Mean	600.0001	600.0028	643.1633	659.5706	655.5146	660.7346	609.8495	657.9643	694.6849	686.4689	645.5481	615.3135	696.0075	601.5345	635.9524
	Std	0.000238	0.010704	10.54838	5.341284	7.482339	7.847482	11.55994	8.353859	18.97697	10.97711	5.725768	4.088385	12.48381	2.130245	12.45906
	Rank	1	2	7	11	9	12	4	10	14	13	8	5	15	3	6
F22-04	Min	814.9244	828.8538	858.0114	919.0239	852.2808	898.0574	836.8134	865.5043	990.8612	971.5143	933.7713	874.1696	980.1626	829.1978	855.8915
	Max	907.0435	892.5307	945.536	962.4489	893.5263	969.6018	897.5057	925.4086	1073.921	1030.002	974.7912	956.7575	1032.63	897.1765	982.0217
	Mean	836.0037	850.4775	891.8467	942.0646	874.6813	934.3841	862.79	889.6893	1035.536	1004.733	956.2997	921.1006	1012.645	854.8203	898.1403
	Std	17.86869	16.54989	20.68247	11.16957	10.58848	19.60754	20.16721	14.74989	24.06347	14.61005	9.596528	18.47469	15.41218	15.66298	28.38628
	Rank	1	2	7	11	5	10	4	6	15	13	12	9	14	3	8
F22-05	Min	901.2668	959.3136	1358.015	2724.9	1764.04	1781.612	901.542	1994.645	3920.607	2965.256	2177.254	1010.432	3538.272	911.371	1717.352
	Max	1019.113	1872.2	2693.736	3706.208	2421.152	3504.181	1924.679	2987.838	13036.32	5995.918	3434.82	3714.531	5940.656	1702.403	4861.865
	Mean	933.3675	1165.093	2189.886	3214.031	2219.185	2655.236	1080.791	2630.466	7755.422	4580.195	2804.044	1861.582	4895.435	1141.18	3298.621
	Std	27.68817	204.7142	346.3462	249.4265	157.9563	355.4745	272.4285	286.8009	2403.426	727.2139	346.0071	626.0525	597.1095	173.9959	866.8097
	Rank	1	4	6	11	7	9	2	8	15	13	10	5	14	3	12
F22-06	Min	1849.929	1860.325	2206.742	8.08E+08	1940.459	12089.24	1906.906	18016.58	81758855	2.22E+08	16393832	488070.2	2.32E+09	1961.594	57840.84
	Max	40240.24	145744	24248461	5.96E+09	29123395	2.42E+09	13659.6	209971.4	4.85E+09	7.59E+09	4.56E+08	14569073	8E+09	25241.89	2.05E+08
	Mean	9209.995	10647.75	1297070	4.14E+09	1924177	5.73E+08	5109.327	87372.62	1.09E+09	4E+09	89926697	5223563	4.68E+09	15426.2	10084852
	Std	11218.27	26443.13	4434662	2.25E+09	5815418	6.58E+08	3456.322	49485.83	1.12E+09	1.67E+09	1.04E+08	3381067	1.41E+09	9977.098	37427988
	Rank	2	3	6	14	7	11	1	5	12	13	10	8	15	4	9
F22-07	Min	2025.75	2022.002	2041.436	2272.327	2066.287	2078.473	2036.724	2081.883	2179.68	2115.306	2129.834	2044.46	2231.922	2023.397	2100.777
	Max	2088.642	2167.278	2185.226	2402.398	2162.09	2410.225	2228.891	2354.727	2441.384	2392.145	2207.593	2131.837	2516.821	2158.121	2329.99
	Mean	2044.083	2071.931	2122.274	2325.575	2128.526	2197.174	2107.155	2162.476	2295.818	2225.744	2168.152	2077.6	2391.235	2056.558	2195.956
	Std	15.88481	48.41193	33.32074	27.09905	21.07048	69.5807	52.71398	55.4696	78.86891	60.17935	22.32927	19.10135	93.76585	35.90205	59.5707
	Rank	1	3	6	14	7	11	5	8	13	12	9	4	15	2	10
F22-08	Min	2220.469	2220.748	2225.843	2238.897	2224.121	2231.858	2220.454	2231.443	2299.37	2242.957	2239.922	2229.858	2518.137	2221.446	2231.673
	Max	2239.879	2401.634	2518.002	2278.344	2232.905	2690.187	2458.329	2376.398	2858.419	2751.359	2258.431	2261.926	4137.769	2282.586	2476.647
	Mean	2224.607	2256.262	2293.679	2251.042	2228.778	2395.404	2251.885	2266.171	2579.181	2449.326	2249.426	2241.543	2985.292	2230.852	2336.11
	Std	5.270479	60.528	82.49189	9.658355	1.940123	137.0418	58.72102	51.33219	137.347	157.2553	4.308485	7.650347	426.8969	16.10921	76.75855
	Rank	1	8	10	6	2	12	7	9	14	13	5	4	15	3	11
F22-09	Min	2465.344	2465.344	2491.826	2979.595	2511.505	2708.09	2480.781	2481.99	2681.59	2830.269	2538.474	2482.753	2908.171	2480.782	2490.755
	Max	2465.344	2465.344	2635.137	3604.857	2647.434	3430.958	2480.781	2521.557	4127.202	4119.395	2641.512	2515.078	4740.404	2521.412	2650.445
	Mean	2465.344	2465.344	2538.639	3442.463	2565.842	3026.955	2480.781	2491.555	3100.238	3345.162	2590.549	2491.395	3859.54	2490.969	2554.996
	Std	1.53E-11	1.87E-09	37.68212	127.733	34.96372	162.9424	2.97E-12	8.477129	333.6545	283.1911	29.39857	8.113441	479.3773	13.00799	37.97769
	Rank	1	2	7	14	9	11	3	6	12	13	10	5	15	4	8
F22-10	Min	2500.339	2401.864	2500.958	5246.699	2501.188	3078.754	2500.396	2500.837	2527.84	2923.914	2531.072	2500.998	3413.929	2500.865	2501.883
	Max	2673.678	2720.523	5831.911	6672.822	4379.725	6655.609	4908.512	4909.553	7702.861	7643.128	2595.009	4981.823	8333.409	3391.044	5573.721
	Mean	2516.763	2461.566	3650.915	6100.183	3384.768	5718.855	3310.106	3601.366	6420.033	6353.766	2557.463	2848.993	7313.429	2597.638	4204.854
	Std	49.644	78.40253	1307.043	332.684	758.6831	798.2905	773.2334	819.6918	1301.421	1409.427	16.52554	777.576	1313.589	254.5808	870.5206
	Rank	2	1	9	12	7	11	6	8	14	13	3	5	15	4	10
F22-11	Min	2900	2600	3124.101	8448.51	3286.946	6467.447	2900	2661.729	4227.515	7948.202	4867.119	3058.837	7301.855	2601.552	3243.155
	Max	3000	3000	5194.237	8533.491	7104.95	9300.103	3360.457	6930.08	10380.96	10663.4	6489.065	3448.094	10491.28	3360.529	6433.356
	Mean	2920	2910	3828.67	8489.506	4788.388	7959.667	2922.015	3144.463	7027.809	9346.961	5567.761	3312.926	9275.929	3020.861	4361.071
	Std	40.68381	71.19667	570.5025	20.0948	1120.991	781.3662	86.59875	731.1458	1731.471	648.4084	367.5874	78.00183	791.0278	201.9633	869.787
	Rank	2	1	7	13	9	12	3	5	11	15	10	6	14	4	8
F22-12	Min	2900.004	2895.757	2957.319	3437.603	2992.34	3408.921	2953.253	3004.544	2960.322	3268.438	3007.389	2954.122	3606.457	2941.579	2982.432
	Max	2900.005	2900.005	3100.824	3584.391	3451.506	4105.701	3146.928	3514.103	3521.709	4751.206	3146.682	3005.966	4593.373	3010.683	3336.639
	Mean	2900.004	2899.863	3009.635	3511.193	3141.828	3732.421	3009.165	3110.999	3130.22	3905.619	3056.06	2969.31	4145.041	2956.896	3100.235
	Std	0.000196	0.775479	31.98645	31.47289	102.972	211.0655	48.90713	104.3832	147.8506	384.8138	35.04715	12.43244	249.5641	16.74111	81.71181
	Rank	2	1	6	12	11	13	5	9	10	14	7	4	15	3	8
Friedman Rank		1.375	2.5417	7.1667	11.5833	7.4167	11.3333	3.8333	6.9167	13.0833	13.25	8.75	5.5833	14.75	3.5	8.9167
Mean Rank		1	2	7	12	8	11	4	6	13	14	9	5	15	3	10

TABLE 7. Wilcoxon's signed rank test on CEC 2022 test suite (Dimension = 10).

Functi on	MBO vs BO	MBO vs SCSO	MBO vs CDO	MBO vs DTBO	MBO vs AOA	MBO vs PSO	MBO vs HHO	MBO vs GOA	MBO vs SAO	MBO vs SCADE	MBO vs mCSA	MBO vs LCA	MBO vs mCapSA	MBO vs SCHO
F22-01	2.53E-10	1.25E-11	1.25E-11	1.25E-11	1.25E-11	5.32E-03	1.25E-11	1.25E-11	1.25E-11	1.25E-11	1.25E-11	1.25E-11	1.25E-11	1.25E-11
F22-02	3.59E-05	2.15E-10	3.02E-11	3.35E-08	3.02E-11	6.65E-10	9.76E-10	3.02E-11	3.02E-11	3.02E-11	6.7E-11	3.02E-11	3.02E-11	3.16E-10
F22-03	8.21E-01	2.22E-11	2.22E-11	2.22E-11	2.22E-11	2.22E-11	2.22E-11	2.22E-11	2.22E-11	2.22E-11	2.22E-11	2.22E-11	2.22E-11	2.22E-11
F22-04	3.79E-01	1.20E-08	3.00E-11	3.76E-04	5.55E-10	5.79E-01	2.66E-09	3.00E-11	3.00E-11	3E-11	1.72E-07	3E-11	0.012459	4.06E-11
F22-05	6.04E-10	3.29E-11	2.97E-11	2.97E-11	2.97E-11	6.04E-05	2.97E-11	2.97E-11	2.97E-11	2.97E-11	8E-10	2.97E-11	0.000767	2.97E-11
F22-06	3.18E-04	3.81E-07	3.02E-11	9.94E-01	2.20E-07	1.84E-02	2.88E-06	3.02E-11	3.02E-11	4.08E-11	4.98E-11	3.02E-11	1.73E-06	9.92E-11
F22-07	3.85E-03	1.21E-10	3.02E-11	3.02E-11	3.02E-11	9.79E-05	5.49E-11	3.02E-11	3.02E-11	3.02E-11	3.02E-11	3.02E-11	0.008684	1.07E-07
F22-08	1.71E-01	4.11E-07	1.96E-10	2.50E-03	3.02E-11	9.23E-01	5.07E-10	3.02E-11	3.02E-11	3.02E-11	3.65E-08	3.02E-11	0.56922	1.31E-08
F22-09	2.32E-05	2.52E-11	2.52E-11	2.52E-11	2.52E-11	2.53E-12	2.52E-11	2.52E-11	2.52E-11	2.52E-11	2.52E-11	2.52E-11	2.39E-11	2.52E-11
F22-10	2.28E-05	3.01E-07	3.02E-11	5.49E-11	3.02E-11	2.92E-02	8.15E-11	3.02E-11	3.02E-11	3.02E-11	1.55E-09	3.02E-11	1.86E-09	1.25E-07
F22-11	4.31E-05	1.37E-04	5.13E-11	1.30E-05	6.33E-10	1.79E-01	2.99E-06	6.33E-10	7.63E-11	1.02E-07	0.001827	2.82E-11	8.03E-06	0.000129
F22-12	1.18E-05	3.79E-05	3.74E-11	4.65E-06	1.35E-10	5.16E-09	2.29E-09	1.81E-10	4.57E-11	7.36E-09	7.36E-09	2.5E-11	7.36E-09	2.75E-09

TABLE 8. Wilcoxon's signed rank test on CEC 2022 test suite (Dimension = 20).

Functi on	MBO vs BO	MBO vs SCSO	MBO vs CDO	MBO vs DTBO	MBO vs AOA	MBO vs PSO	MBO vs HHO	MBO vs GOA	MBO vs SAO	MBO vs SCADE	MBO vs mCSA	MBO vs LCA	MBO vs mCapSA	MBO vs SCHO
F22-01	7.34E-10	3E-11	3E-11	3E-11	3E-11	3E-11	3E-11	3E-11	3E-11	3E-11	3E-11	3E-11	3E-11	3E-11
F22-02	0.002499	4.08E-11	3.02E-11	3.02E-11	3.02E-11	2E-06	7.38E-10	3.02E-11	3.02E-11	3.02E-11	2.37E-10	3.02E-11	2.02E-08	4.5E-11
F22-03	3.37E-05	3.02E-11	3.02E-11	3.02E-11	3.02E-11	3.02E-11	3.02E-11	3.02E-11	3.02E-11	3.02E-11	3.02E-11	3.02E-11	3.02E-11	3.02E-11
F22-04	0.000189	4.61E-10	3.02E-11	1.41E-09	4.07E-11	2.38E-07	4.2E-10	3.02E-11	3.02E-11	3.02E-11	4.97E-11	3.02E-11	6.73E-06	2.61E-10
F22-05	9.92E-11	3.02E-11	3.02E-11	3.02E-11	3.02E-11	0.045146	3.02E-11	3.02E-11	3.02E-11	3.02E-11	3.34E-11	3.02E-11	2.92E-09	3.02E-11
F22-06	0.807275	4.12E-06	3.02E-11	0.000239	9.92E-11	0.795846	1.46E-10	3.02E-11	3.02E-11	3.02E-11	3.02E-11	3.02E-11	0.010763	3.02E-11
F22-07	0.070127	1.33E-10	3.02E-11	4.08E-11	3.69E-11	3.35E-08	3.34E-11	3.02E-11	3.02E-11	3.02E-11	3.65E-08	3.02E-11	0.53951	3.02E-11
F22-08	0.841801	1.55E-09	3.34E-11	4.11E-07	5.49E-11	0.22823	4.18E-09	3.02E-11	3.02E-11	3.02E-11	1.17E-09	3.02E-11	0.096263	2.37E-10
F22-09	0.000431	2.99E-11	2.99E-11	2.99E-11	2.99E-11	2.24E-11	2.99E-11	2.99E-11	2.99E-11	2.99E-11	2.99E-11	2.99E-11	2.99E-11	2.99E-11
F22-10	0.145319	1.41E-09	3.02E-11	9.76E-10	3.02E-11	3.57E-06	3.16E-10	5.49E-11	3.02E-11	1.07E-07	2.39E-08	3.02E-11	3.08E-08	9.92E-11
F22-11	0.000124	2.99E-11	2.99E-11	2.99E-11	2.99E-11	0.000247	1.42E-05	2.99E-11	2.99E-11	2.99E-11	2.99E-11	2.99E-11	6.25E-06	2.99E-11
F22-12	0.304177	3.02E-11	3.02E-11	3.02E-11	3.02E-11	3.02E-11	3.02E-11	3.02E-11	3.02E-11	3.02E-11	3.02E-11	3.02E-11	3.02E-11	3.02E-11

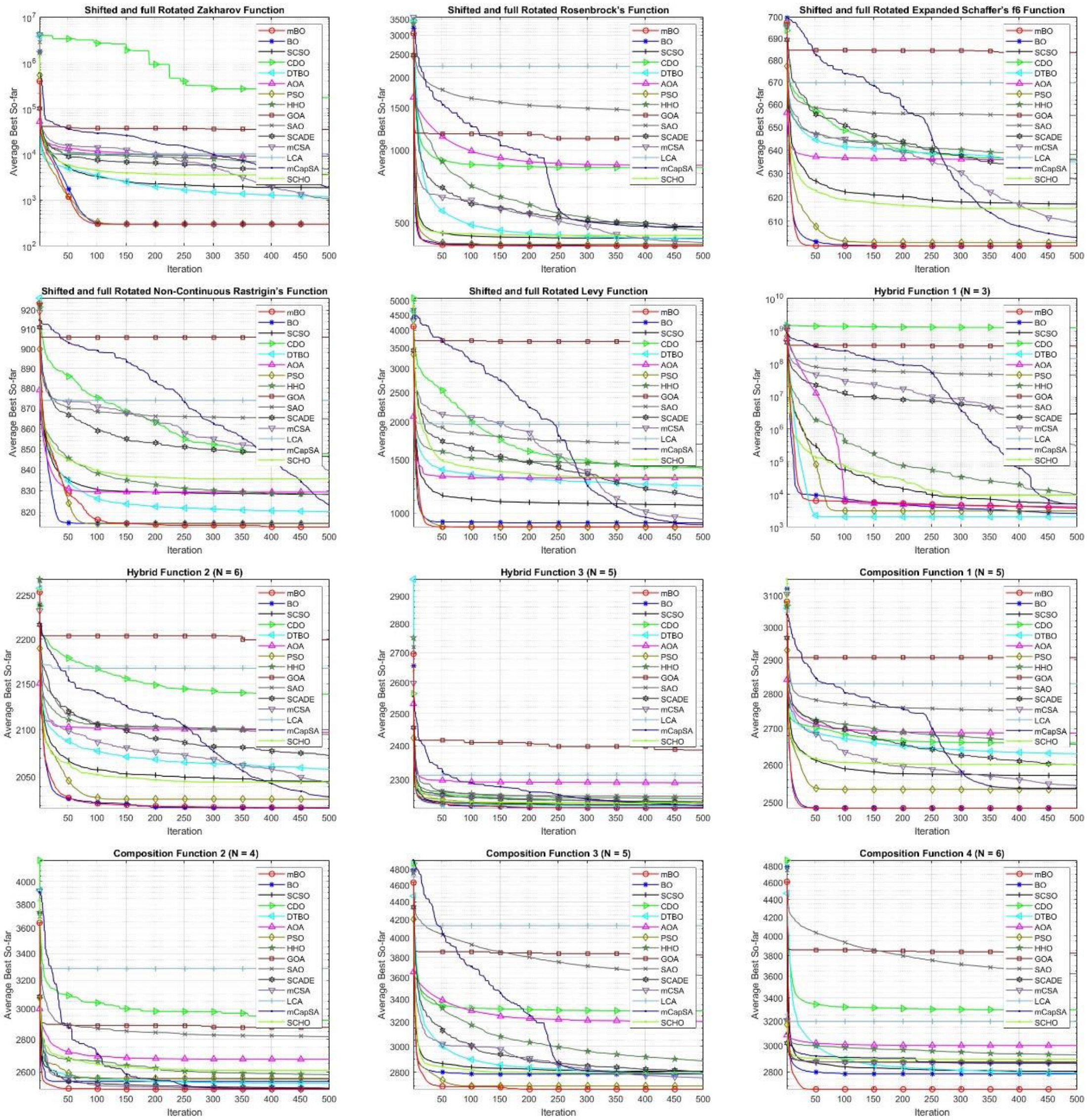

FIGURE 6. Convergence curves of test functions from CEC2022 test suite (Dimension = 10).

- $g_6(x) = 0.125 - x_1 \leq 0$
- $g_7(x) = 1.10471x_1^2x_2 + 0.04811x_3x_4(14.0 + x_2) - 5.0 \leq 0$

with $0.1 \leq x_1 \leq 2$, $0.1 \leq x_2 \leq 10$, $0.1 \leq x_3 \leq 10$ and $0.1 \leq x_4 \leq 2$.

Tables 13 and 14 present a detailed statistical analysis of the experimental results, including the optimal values identified by various optimization algorithms for this design problem. These tables also list the corresponding values of the design variables at the optimal solution. Upon analyzing these results, it becomes unequivocally clear that the MBO exhibits an enhanced ability in seeking out the optimal solution. This superior ability is evidenced in terms of the minimal objective function value and the quality of the solution, which adheres to all problem constraints.

The convergence plot, demonstrated in Figure 15(a), further substantiates the superior capability of MBO. This graphical illustration reveals the path followed by the different algorithms in their quest for the optimal solution. It shows that MBO manages to converge towards the optimal function value more rapidly, indicating a more efficient optimization process.

Such expeditious convergence is a testament to the robustness of MBO in dealing with complex optimization problems, as well as its inherent ability to bypass local optima, which often hinders the performance of conventional optimization algorithms. Further evidence of MBO's reliability and robust performance can be drawn from the boxplot in Figure 15(b). This boxplot illustrates the result distribution over multiple runs of the optimization problem, providing an insight into the algorithm's stability across multiple optimization

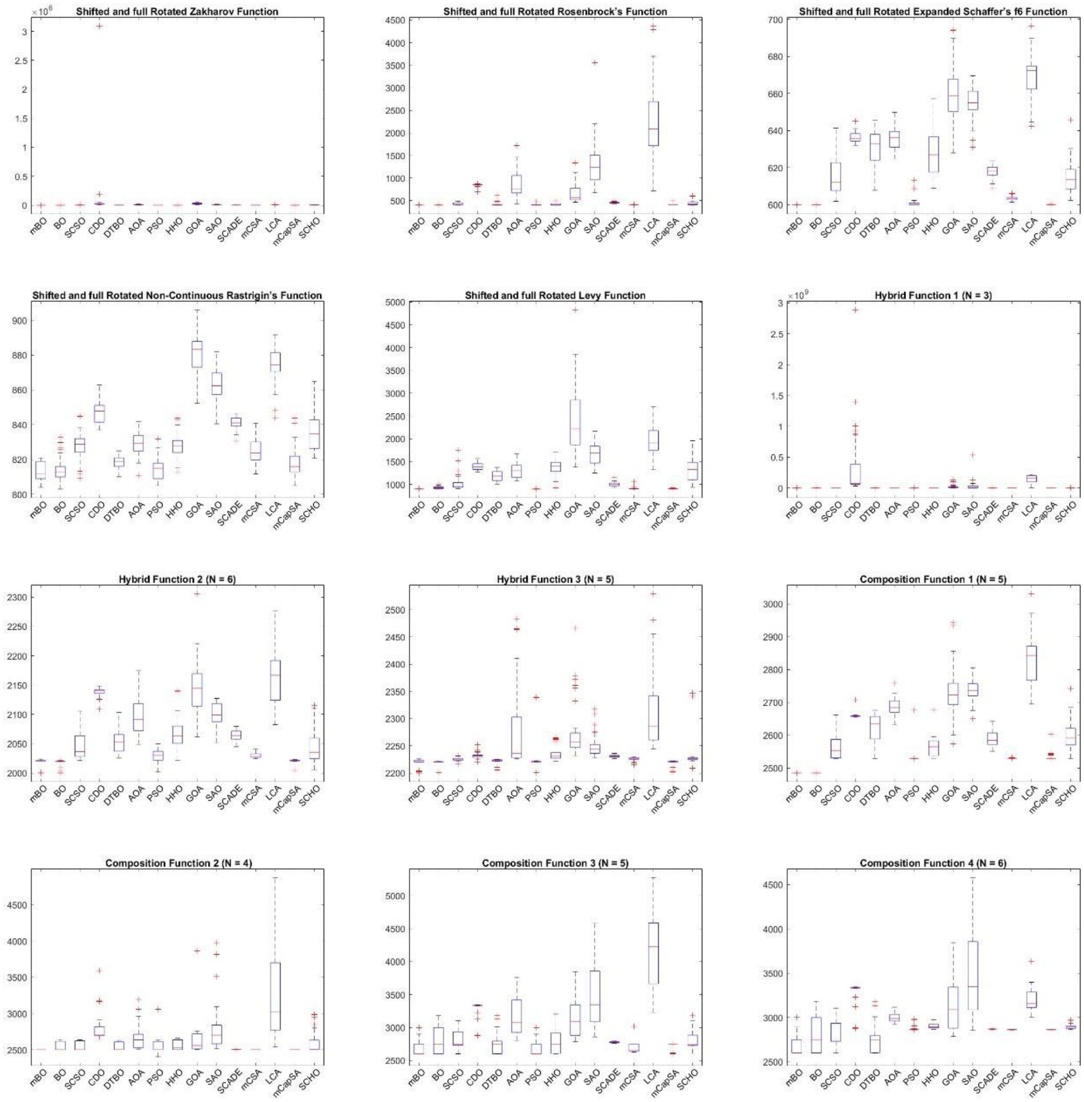

FIGURE 7. Boxplots of test functions from CEC2022 test suite (Dimension = 10).

scenarios. The tight result distribution for MBO, as seen from the boxplot, emphasizes its ability to consistently find optimal or near-optimal solutions.

4) SPEED REDUCER DESIGN

The design optimization of speed reducers has garnered substantial attention in the mechanical engineering sphere due to its critical role in modulating the speed of machines. The primary objective of this optimization is to minimize the weight of the speed reducer while ensuring compliance with the various constraints imposed by its integral components. Seven design variables play a pivotal role in this weight computation: the face width of the gear (x_1), teeth module (x_2), number of pinion teeth (x_3), length of the first shaft between bearings (x_4), length of the second shaft between bearings (x_5), and the diameters of the first (x_6) and second (x_7) shafts. A schematic overview of this problem is elucidated in Figure 16.

The mathematical formulation of the problem can be articulated as given in (19).

$$\begin{aligned} f(x) = {} & 0.7854x_1x_2^2\left(3.3333x_3^2 + 14.9334x_3 - 43.0934\right) \\ & -1.508x_1\left(x_6^2 + x_7^2\right) + 7.4777\left(x_6^3 + x_7^3\right) \\ & + 0.7854\left(x_4x_6^2 + x_5x_7^2\right) \end{aligned} \tag{19}$$

which is subjected to

- $g_1(x) = \left(27/x_1x_2^2x_3\right) - 1 \leq 0,$
- $g_2(x) = \left(397.5/x_1x_2^2x_3\right) - 1 \leq 0,$
- $g_3(x) = \left(1.93x_4^3/x_2x_3x_6^4\right) - 1 \leq 0,$
- $g_4(x) = \left(1.93x_5^3/x_2x_3x_7^4\right) - 1 \leq 0,$
- $g_5(x) = \left(1/110x_6^3\right)\sqrt{\left(745x_4/x_2x_3\right)^2 + 16.9\times10^6}$

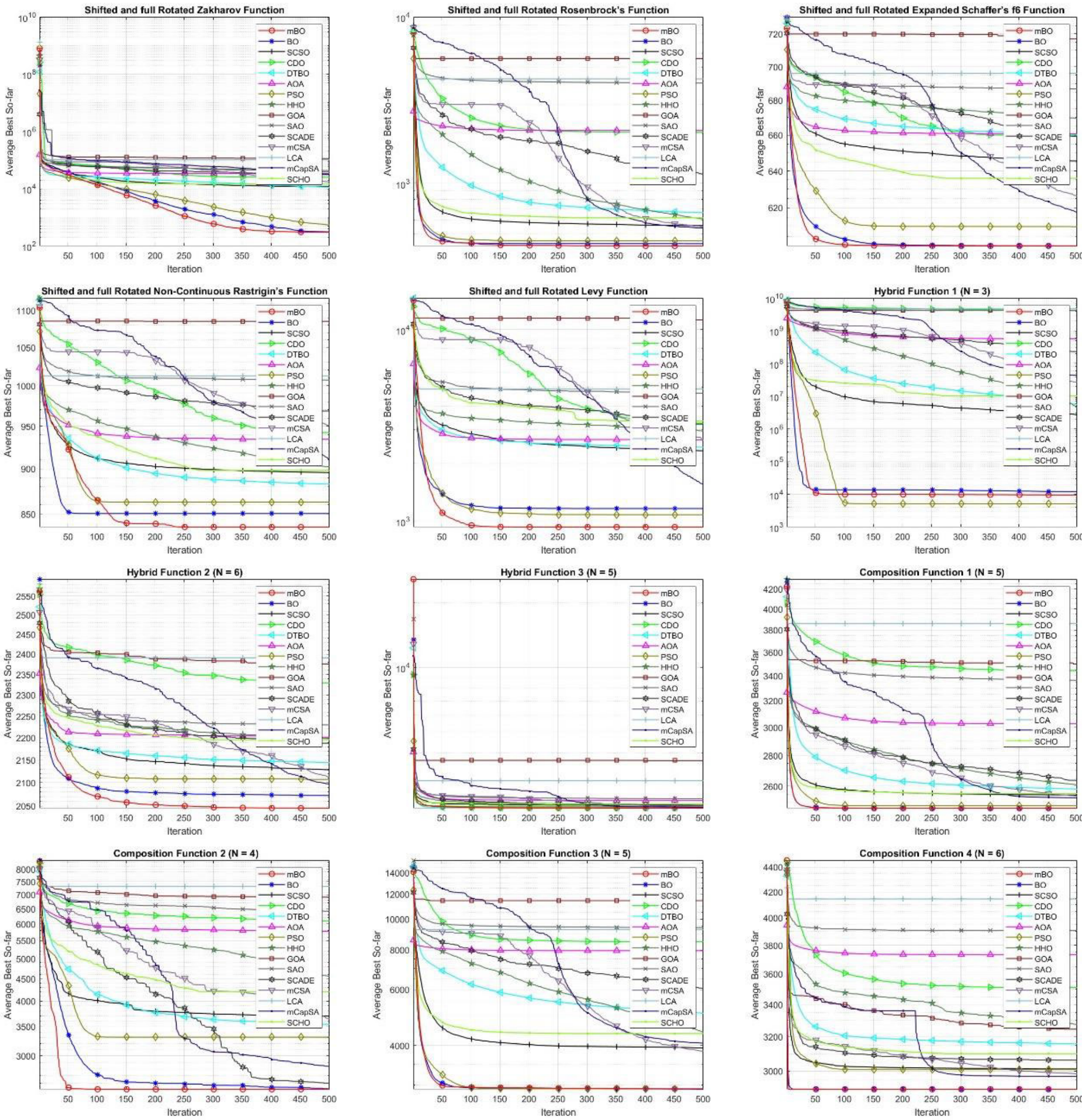

FIGURE 8. Convergence curves of test functions from CEC2022 test suite (Dimension = 20).

$-1 \leq 0,$

- $g_6(x) = \left(1/85x_7^3\right)\sqrt{\left(745x_4/x_2x_3\right)^2 + 157.5\times 10^6}$ $-1 \leq 0,$
- $g_7(x) = \left(x_2x_3/40\right) - 1 \leq 0,$
- $g_8(x) = \left(5x_2^2/x_1\right) - 1 \leq 0,$
- $g_9(x) = \left(x_1/12x_2\right) - 1 \leq 0,$
- $g_{10}(x) = \left((1.5x_6 + 1.9)/x_4\right) - 1 \leq 0,$
- $g_{11}(x) = \left((1.1x_7 + 1.9)/x_5\right) - 1 \leq 0$

with $2.6 \leq x_1 \leq 3.6$, $0.7 \leq x_2 \leq 0.8$, $2.6 \leq x_1 \leq 3.6$, $17 \leq x_3 \leq 28$, $7.3 \leq x_4 \leq 7.8$, $7.8 \leq x_5 \leq 8.3$, $2.9 \leq x_6 \leq 3.9$ and $5 \leq x_7 \leq 5.5$.

Tables 15 and 16 provide an extensive statistical analysis of our experimental findings, showcasing the optimal values achieved through various optimization algorithms for this particular design challenge. These tables also furnish the associated design variable values at these optimal solutions. Upon thorough examination of these outcomes, it becomes undeniably evident that the MBO stands out for its exceptional capacity to pinpoint the optimal solution. This heightened proficiency is evident through its ability to attain the lowest objective function value while simultaneously ensuring that all problem constraints are met with a high level of solution quality.

Examining the convergence patterns illustrated in Figure 17(a) provides a clear insight into MBO's proficiency. The convergence curve of MBO distinctly displays a sharper descent, indicating its capability to rapidly hone in on the most optimal solution. This rapid convergence is not just an indicator of speed but is a testament to the algorithm's efficiency. In real-world applications, especially in design optimization contexts, such efficiency translates to significant

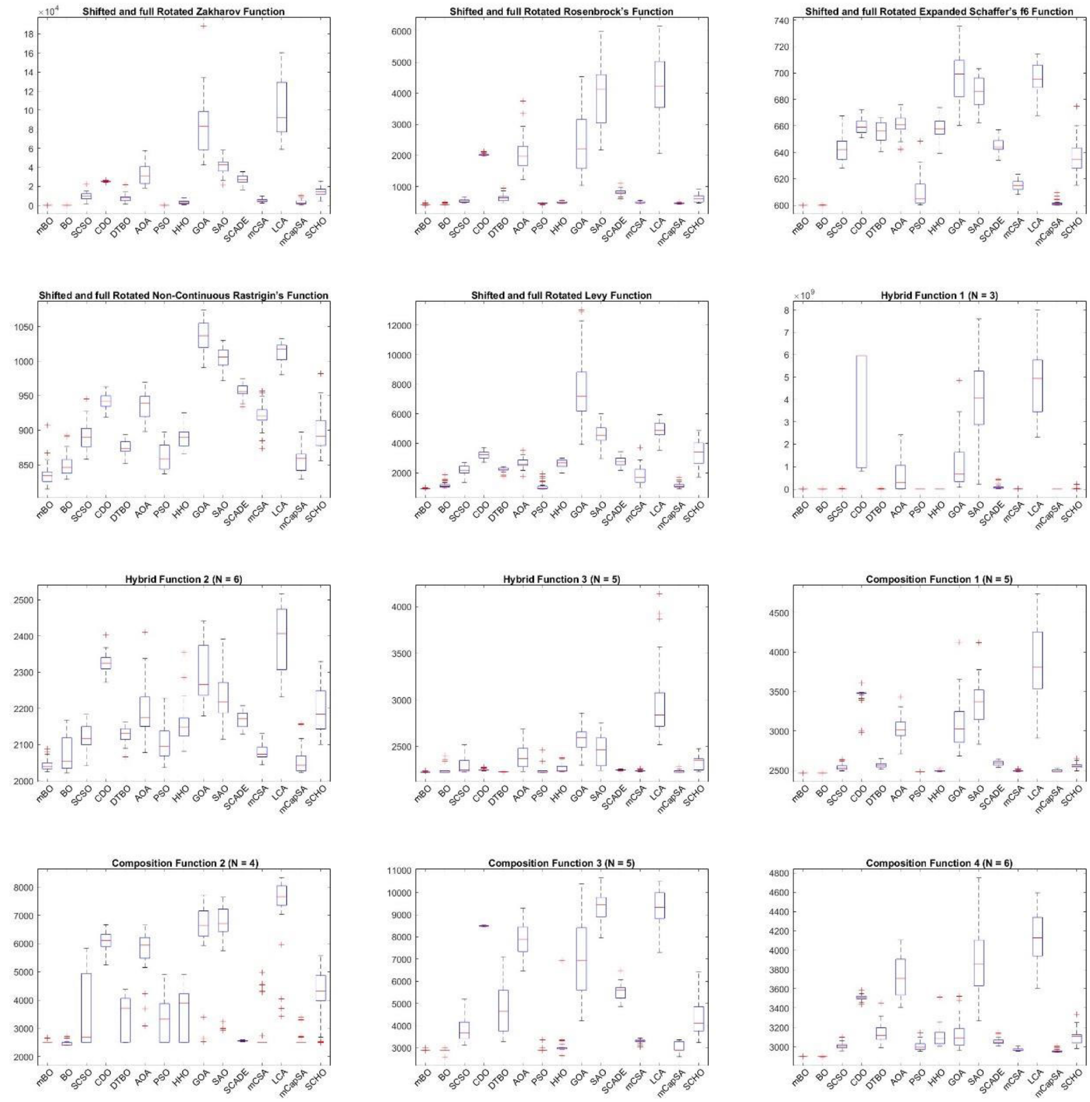

FIGURE 9. Boxplots of test functions from CEC2022 test suite (Dimension = 20).

cost and time savings, making MBO particularly suited for speed reducer design challenges. Meanwhile, an algorithm's consistency and reliability over multiple runs play an equally pivotal role, especially when considering the inherent variability in optimization problems. This dimension of MBO's performance is elucidated in Figure 17(b). The box plot therein graphically demonstrates how MBO's results cluster tightly around optimal values, with minimal spread or outliers. In academic parlance, such a tight result distribution is emblematic of an algorithm's robustness. The MBO, in comparison to other algorithms, manifests minimal variability, a crucial characteristic when considering real-world applications. Such consistency implies that the MBO can be depended upon to produce reliable and reproducible results, a trait that is indispensable in practical design optimization contexts.

5) PRESSURE VESSEL DESIGN

The conceptualization and design of a pressure vessel constitutes an intricate engineering task. This task necessitates the optimization of several design variables to meet the desired performance and safety standards. The design problem at hand contemplates four variables: the shell's thickness (x_1), the thickness of the vessel's head (x_2), the vessel's inner radius (x_3), and the vessel's length (x_4). The optimization problem's primary objective is to minimize the total cost associated with the pressure vessel's design, ensuring compliance with required specifications. Figure 18 schematically depicts this design challenge.

The Problem is mathematically formulated as:

$$f(x) = 0.6224 x_1 x_3 x_4 + 1.778 x_2 x_3^2 + 3.166 x_1^2 x_3^2 + 19.84 x_1 x_3 \quad (20)$$

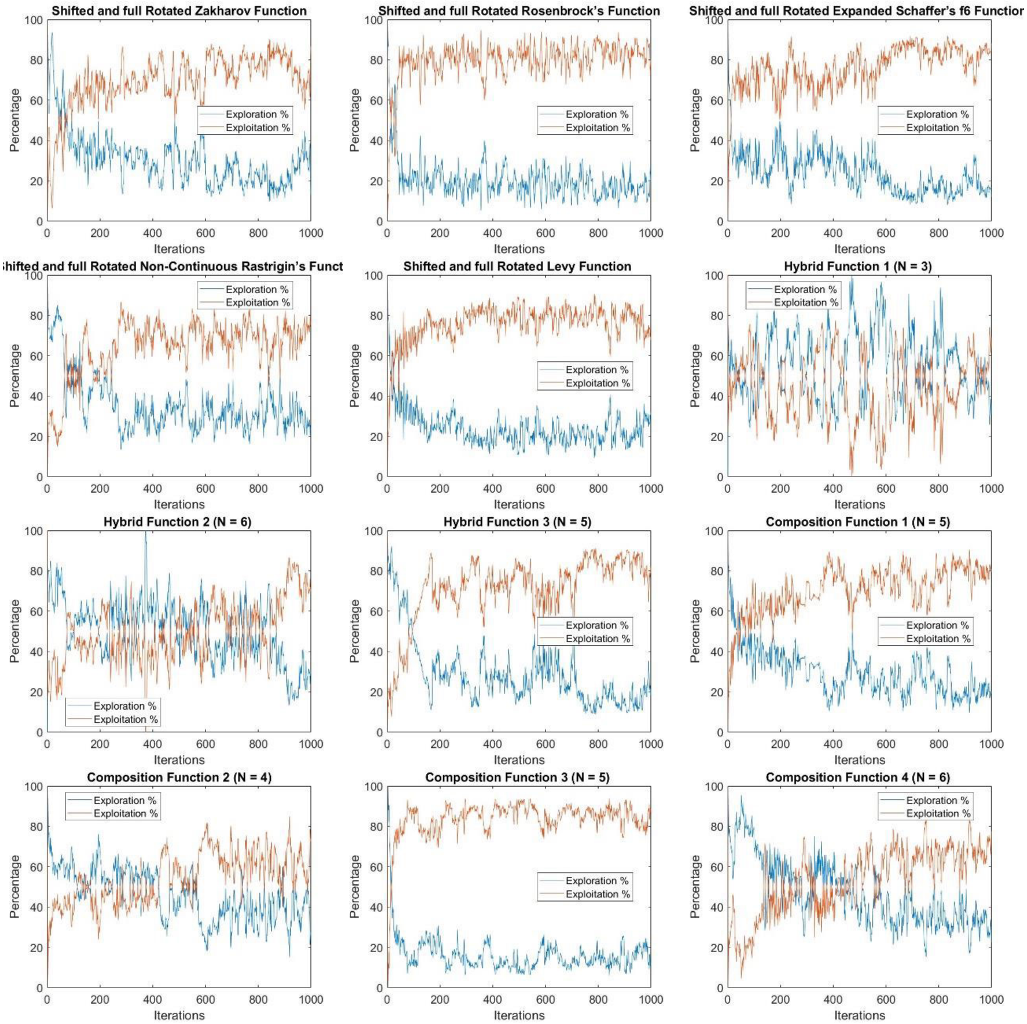

FIGURE 10. Demonstration of exploration-exploitation capability through 10-dimensional CEC 2022 test suite.

which is subjected to

- $g_1(x) = -x_1 + 0.0193x_3 \leq 0,$
- $g_2(x) = -x_2 + 0.0095x_3 \leq 0,$
- $g_3(x) = -\pi x_3^2 x_4 - \left(4\pi x_3^3/3\right) + 129600 \leq 0,$
- $g_4(x) = x_4 - 240 \leq 0$

with $0.0625 \leq x_1, x_2 \leq 99 \times 0.0625$, $10 \leq x_3, x_4 \leq 200$.

The evaluation of the performance of the MBO was carried out with respect to the problem of designing pressure vessels. The results were compared with those obtained using other established optimization algorithms. It was discovered that the MBO demonstrated a performance that was similar to other algorithms. This conclusion was drawn based on the value of the objective function. As demonstrated in Table 17, the most favorable values achieved by the different algorithms are listed, together with the associated values of the design variables. The performance of the MBO is emphasized further in Table 18.

Figure 19(a) displays the convergence plot, which clearly shows the efficiency of the MBO in converging effectively towards the a near optimal solution. The consistency of the MBO's performance across multiple iterations of the pressure vessel design problem is highlighted in the boxplot represented in Figure 19(b), as well.

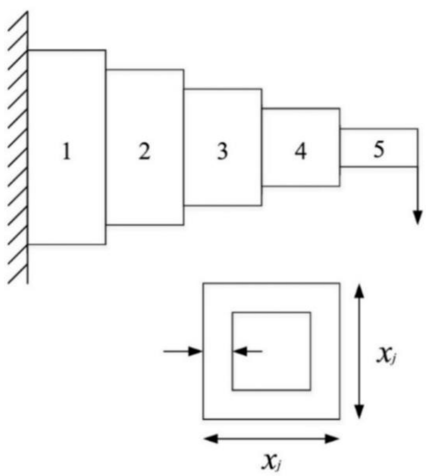

FIGURE 11. Schematic diagram of a cantilever beam design problem.

TABLE 9. Statistical results on cantilever beam design problem.

Metric	MBO	BO	SCSO	CDO	DTBO	AOA	PSO	HHO	GOA	SAO
Min	1.339956322	1.339956314	1.358543255	1.341674882	1.339957099	1.544317586	1.339957318	1.340579366	1.418964027	1.558312104
Max	1.339958921	1.340016516	1.642890392	1.368808192	1.339995298	5.067478468	1.340026383	1.346869391	5.409794131	10.84033875
Mean	1.339956795	1.339962362	1.443480398	1.356111459	1.339964183	2.279248431	1.339974147	1.34270548	2.712152394	6.036222072
Std	6.49844E-07	1.16397E-05	0.080218812	0.006693584	7.55741E-06	0.805102954	1.93225E-05	0.001409316	1.291672835	2.312211934
Rank	1	2	7	6	3	8	4	5	9	10

TABLE 10. Best found solution for each optimizer on optimal design of cantilever beam.

Optimizer	f_{best}	x_1	x_2	x_3	x_4	x_5
MBO	1.339956314	6.016042821	5.309105739	4.494576224	3.501293211	2.152640124
BO	1.358543255	6.342641781	5.205188244	4.171392322	3.350513034	2.701791137
SCSO	1.341674882	5.97197893	5.262755296	4.414740315	3.622588325	2.229137168
CDO	1.339957099	6.01891894	5.306019952	4.492971091	3.500778102	2.154982382
DTBO	1.544317586	7.177749452	8.362334936	4.451792962	2.610576451	2.146225457
AOA	1.339957318	6.015423586	5.305150431	4.496318975	3.504542561	2.152239419
PSO	1.358543255	6.342641781	5.205188244	4.171392322	3.350513034	2.701791137
HHO	1.340579366	6.045302325	5.265670754	4.576412574	3.520633793	2.075623447
GOA	1.418964027	7.146102677	5.892574138	3.508260582	3.534503085	2.658367646
SAO	1.558312104	22.51818541	66.97231923	48.25931177	7.34296399	15.97925454

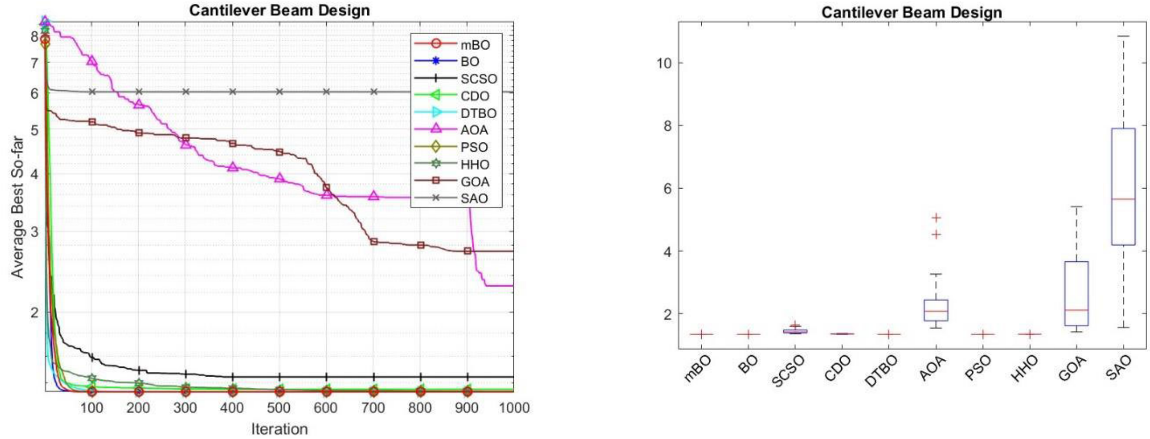

(a) (b)

FIGURE 12. Convergence curve (a) and box plot analysis (a) of cantilever beam design problem.

TABLE 11. Results on industrial refrigeration system problem.

Metric	MBO	BO	SCSO	CDO	DTBO	AOA	PSO	HHO	GOA	SAO
Min	0.032212999	0.032212999	0.194734894	0.072182432	0.190683926	4.055039359	0.032213122	0.364219008	8716.021351	14246043.85
Max	936189.4226	936189.4226	203941.852	4868329.41	2332.669785	2214137.097	936189.4226	984165.8718	65297497.01	4760296989
Mean	31206.34617	62412.66105	7243.460838	1364366.734	125.2751424	449158.7107	93618.99887	349833.4568	9506236.974	787872573.1
Std	170924.0156	237518.8604	37227.20602	1734069.944	444.406323	618984.8766	285658.1268	466964.4079	14314969.66	926033906.2
Rank	3	4	2	8	1	7	5	6	9	10

TABLE 12. Best found solution for each optimizer on optimal design of industrial refrigeration system.

Optimizer	f_{best}	x_1	x_2	x_3	x_4	x_5	x_6	x_7	x_8	x_9	x_{10}	x_{11}	x_{12}	x_{13}	x_{14}
MBO	0.032213	0.001	0.001	0.001	0.001	0.001	0.001	1.523999967	1.523999969	5	1.999999989	0.001	0.001	0.007293401	0.087555833
BO	0.194734894	0.001	0.001	0.001	0.001	0.001181252	0.003858	1.524140725	1.606981547	4.519271052	1.999978731	0.001	0.001	0.001818663	0.012425032
SCSO	0.072182432	0.001086203	0.001	0.001	0.109798891	0.004474181	0.00350113	1.569186074	1.634264613	5	2.177086733	0.002891846	0.001	0.006301236	0.070776592
CDO	0.190683926	0.001	0.001048419	0.0040825	0.011844344	0.065107928	0.012546272	1.524008025	1.524595938	3.082757573	2.100925026	0.021140538	0.018351773	0.028906279	0.346940295
DTBO	4.055039359	0.001	0.001	0.001	0.020133469	1.025840903	0.811853997	2.111029295	1.74716369	3.979592204	4.690687918	1.887293557	0.310312082	0.020133469	0.196005596
AOA	0.032213122	0.001	0.001	0.001	0.001	0.001	0.001	1.523999968	1.523999968	5	2.000021648	0.00100001	0.00100001	0.007293471	0.087556678
PSO	0.194734894	0.001	0.001	0.001	0.001	0.001181252	0.003858	1.524140725	1.606981547	4.519271052	1.999978731	0.001	0.001	0.001818663	0.012425032
HHO	0.364219008	0.001	0.001	0.005308715	0.242902941	0.010030773	0.004434824	2.861650495	2.513476696	2.024121422	2.000020634	0.001	0.001	0.006786772	0.07980364
GOA	8716.021351	0.001	0.116401458	3.365743768	0.014270413	2.575788759	1.660093911	2.99230599	3.971142701	4.629864022	4.642211445	0.001	0.001	0.001	0.001
SAO	14246043.85	4.056261437	3.897615031	3.833180435	0.341573183	0.159483329	4.162318035	3.263213144	3.984311815	0.9146728	5	0.729443384	4.060668662	4.240338102	5

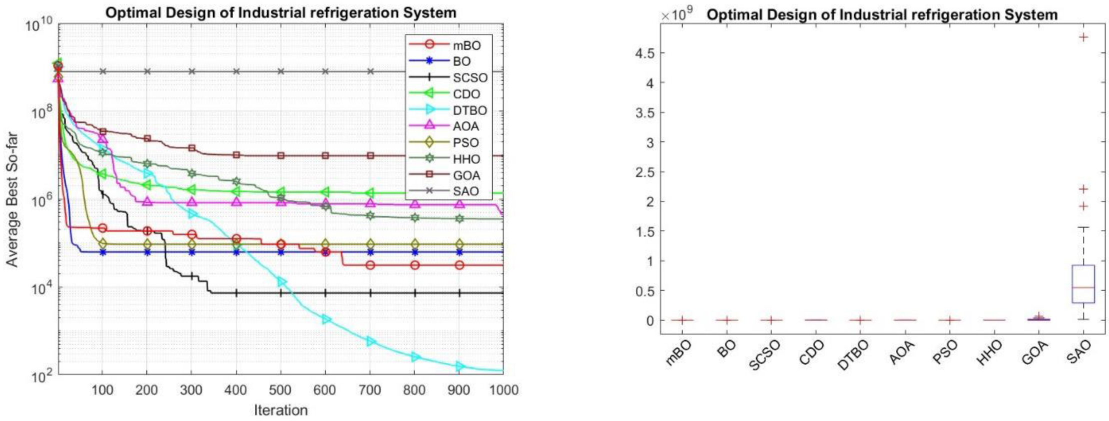

(a) (b)

FIGURE 13. Convergence curve (a) and box plot analysis (b) of industrial refrigeration system problem.

TABLE 13. Results on welded beam problem.

Metric	MBO	BO	SCSO	CDO	DTBO	AOA	PSO	HHO	GOA	SAO
Min	1.724851850	1.72485185	1.786992446	1.755813099	1.724921444	1.827742449	1.724851861	1.790459174	1.873233442	1.792206765
Max	1.724851876	1.974449424	3.852053109	1.879417336	1.767367416	2.70007125	2.175585383	2.682967349	5.826183841	4.036101787
Mean	1.724851855	1.744473057	2.445143082	1.825101621	1.72805348	2.37827792	1.81649051	2.025108715	3.158859153	2.995644832
Std	6.0555E-09	0.064606991	0.577102667	0.0311289	0.008987208	0.187315828	0.135139952	0.210771494	1.08569924	0.596868516
Rank	1	3	8	5	2	7	4	6	10	9

TABLE 14. Best found solution for each optimizer on optimal design of optimal design of welded beam.

Optimizer	f_{best}	x_1	x_2	x_3	x_4
MBO	1.72485185	0.205730318	3.470474072	9.03662391	0.20572964
BO	1.786992446	0.21639172	3.313302273	8.875822253	0.21852951
SCSO	1.755813099	0.195414059	3.68018653	9.118883667	0.206352202
CDO	1.724921444	0.205717765	3.47094278	9.036549864	0.205734751
DTBO	1.827742449	0.209280148	3.496817186	9.241034866	0.21321312
AOA	1.724851861	0.205730281	3.470474833	9.036624019	0.205729639
PSO	1.786992446	0.21639172	3.313302273	8.875822253	0.21852951
HHO	1.790459174	0.173239315	4.308508152	9.096589182	0.20563089
GOA	1.873233442	0.247534637	3.010067892	8.239709975	0.247587617
SAO	1.792206765	2.000000000	0.932642296	1.496869031	0.644415481

6) MULTI-PRODUCT BATCH PLANT DESIGN

The multi-product batch plant design problem initiates with the announcement of a customer's order, which signifies a single product type. Each customer's order corresponds to a distinct product, with the batch size remaining constant throughout the manufacturing process. Every order is assigned specific release and due dates. Each manufacturing stage possesses its unique processing units, which are exclusively operational at that stage. The optimization problem aims to minimize the make-span while accounting for other constraints such as the sequence of unit assignment orders, due and release dates, and storage considerations. The details regarding the problem formulation of this design can be found in [68].

In an evaluation comparing the MBO algorithm with other methods, the MBO outperforms most of its competitors in minimizing the make-span and complying with constraints. The comparison is based on the mean and standard deviation statistical measures. Detailed results are illustrated in Tables 19 and 20. Figure 20 reveals the convergence behavior and box plot analysis of the MBO and its competitors, with the MBO demonstrating a robust and efficient convergence to

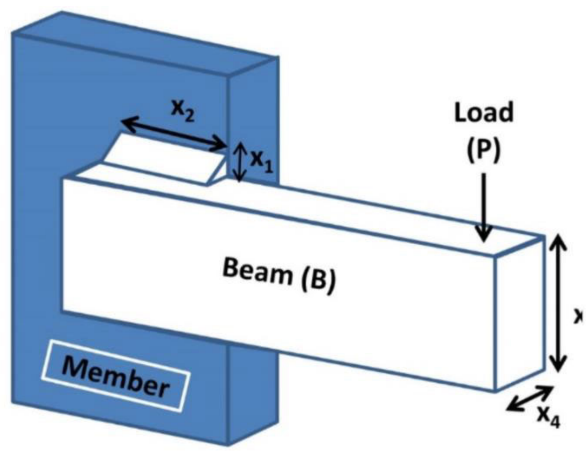

FIGURE 14. Schematic diagram of welded beam design problem.

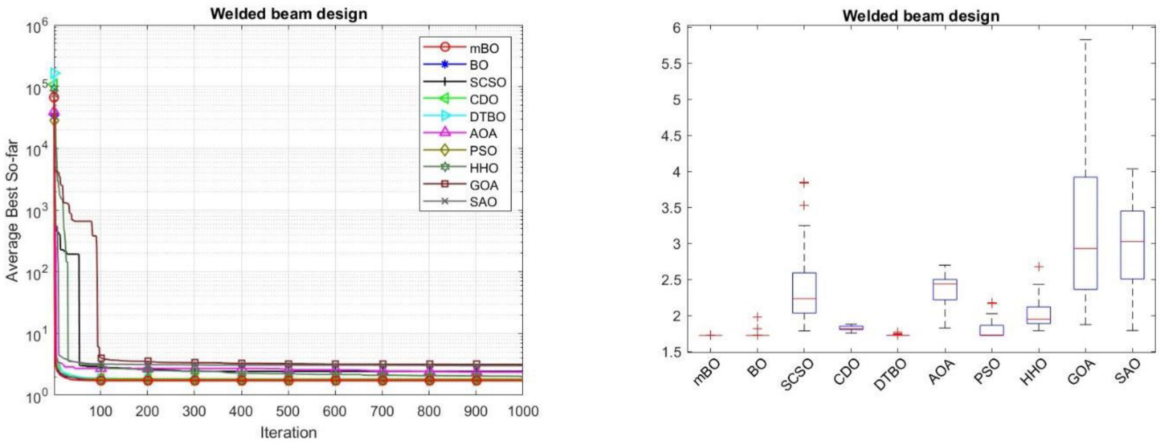

(a) (b)

FIGURE 15. Convergence curve (a) and box plot analysis (b) of welded beam design problem.

TABLE 15. Results on speed reducer problem.

Metric	MBO	BO	SCSO	CDO	DTBO	AOA	PSO	HHO	GOA	SAO
Min	2993.634258	2993.634258	3000.818329	3052.927298	2993.859854	3092.033581	2993.634258	2994.197106	3034.44679	3230.902096
Max	2993.634258	2993.634258	6981.798027	3169.842698	3005.663497	3228.354736	2993.634258	4307.675559	8843.277026	8071.253528
Mean	2993.634258	2993.634258	3810.69955	3094.338809	2999.639962	3154.919614	2993.634258	3146.587351	4425.906754	4153.676151
Std	4.62521E-13	5.97113E-13	1110.949119	33.4362738	3.844957096	45.47206623	2.67037E-13	259.75656	1503.484913	956.0171643
Rank	1	2	8	5	4	7	3	6	10	9

TABLE 16. Best found solution for each optimizer on optimal design of speed reducer.

Optimizer	f_{best}	x_1	x_2	x_3	x_4	x_5	x_6	x_7
MBO	2993.634258	3.497599094	0.7	17	7.3	7.713534975	3.350055806	5.285631196
BO	3000.818329	3.496125282	0.7	17	7.936068457	7.761740302	3.351138548	5.285662262
SCSO	3052.927298	3.6	0.7	17	7.3	8.3	3.361237746	5.292188806
CDO	2993.859854	3.497589193	0.7	17	7.303557852	7.722295157	3.349989164	5.285748314
DTBO	3092.033581	3.6	0.7	17	7.3	8.3	3.48826099	5.300639588
AOA	2993.634258	3.497599093	0.7	17	7.3	7.713534978	3.350055806	5.285631196
PSO	3000.818329	3.496125282	0.7	17	7.936068457	7.761740302	3.351138548	5.285662262
HHO	2994.197106	3.497970152	0.7	17	7.3	7.732422653	3.350520977	5.285312291
GOA	3034.44679	3.571421499	0.701485961	17	7.64934698	7.714520868	3.353149236	5.288426322
SAO	3230.902096	3.6	2.6	3.56545261	2.843730138	2.951026886	3.314186891	2.715052645

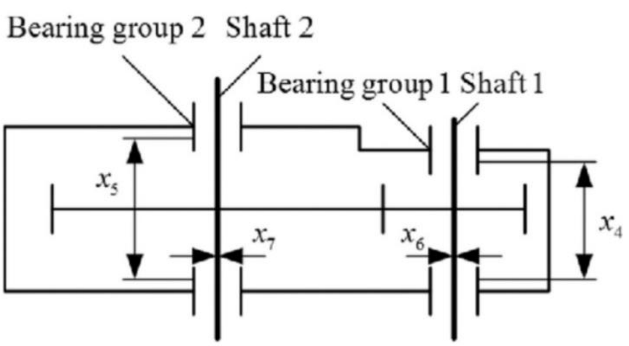

FIGURE 16. Schematic diagram of speed reducer design problem.

the optimal solution. The results underline the proficiency of the MBO in addressing the multi-product batch plant design problem, underscoring its potential in complex engineering design optimization challenges.

7) THREE-BAR TRUSS DESIGN

This engineering optimization problem depends on two design variables: the cross-sectional areas of bars 1 and 3 (x_1) and bar 2 (x_2). The main goal of this optimization task is to minimize the total weight of the truss structure. This design process is also subject to manufacturing constraints, including stress, deflection, and buckling limits. The three-bar truss design problem can be mathematically formalized as minimization of:

$$f(x) = \left(2\sqrt{2}\,x_1 + x_2\right) \cdot l \tag{21}$$

which is subjected to

- $R_1(x) = \left(\sqrt{2}\,x_1 + x_2\right) \Big/ \left(\sqrt{2}\,x_2\left((1 + 2x_1x_2)/P\right)\right) - \sigma \leq 0,$
- $R_2(x) = (x_2) \Big/ \left(\sqrt{2}\,x_1\left((1 + 2x_1x_2)/P\right)\right) - \sigma \leq 0,$
- $R_3(x) = \left((x_2) \Big/ \left(\sqrt{2}\,x_2 + x_1\right)\right)(1/P) - \sigma \leq 0.$

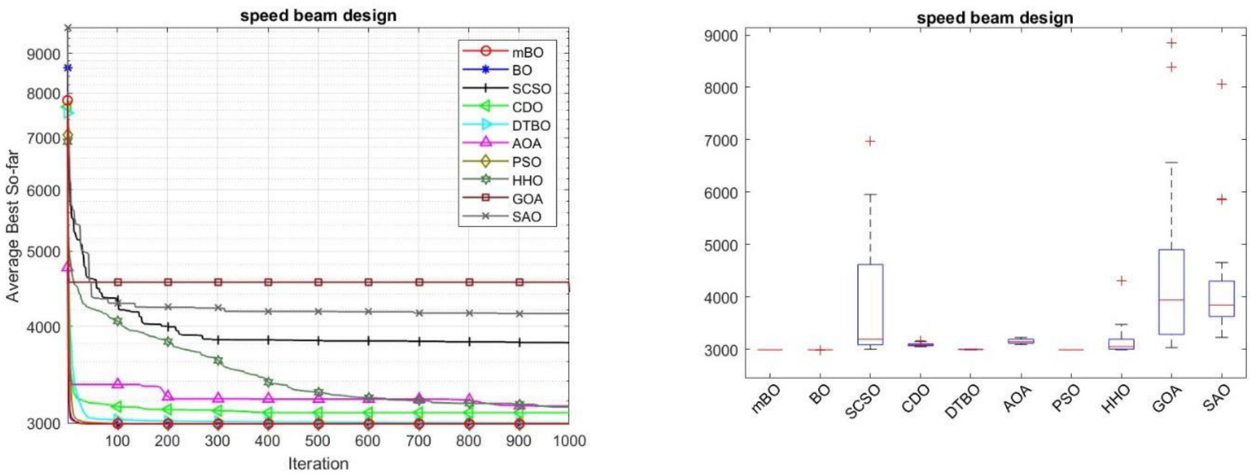

FIGURE 17. Convergence curve (a) and box plot analysis (b) of speed reducer design problem.

TABLE 17. Results on pressure vessel problem.

Metric	MBO	BO	SCSO	CDO	DTBO	AOA	PSO	HHO	GOA	SAO
Min	5870.123977	5870.123977	6039.51034	5982.48268	5893.263821	6908.027685	5876.941025	6046.190655	7411.902278	7710.968222
Max	5870.123977	7301.195546	12016.49739	6374.407342	6829.3285	15959.65864	6898.221838	7464.369158	40809.83036	23390.17534
Mean	5870.123977	5917.826362	7613.320956	6171.90542	6389.415008	9798.143802	6242.954501	6530.49134	16388.74875	13266.0776
Std	2.19185E-11	261.2767267	1090.403713	96.7761142	258.8080998	1953.989137	248.7349066	399.0298802	8315.391397	3334.069309
Rank	1	2	7	3	5	8	4	6	10	9

TABLE 18. Best found solution for each optimizer on optimal design of pressure vessel.

Optimizer	f_{best}	x_1	x_2	x_3	x_4
MBO	200	0.774549094	0.383203859	40.31961872	5870.123977
BO	166.3092073	0.819111378	0.418800194	42.95497256	6039.51034
SCSO	200	0.790006219	0.381008716	40.35491885	5982.48268
CDO	190.8091432	0.787685541	0.389951063	40.99488362	5893.263821
DTBO	200	0.769060932	0.379011772	41.25717088	6908.027685
AOA	197.203016	0.778476425	0.385079475	40.52190845	5876.941025
PSO	166.3092073	0.819111378	0.418800194	42.95497256	6039.51034
HHO	158.7634141	0.835827022	0.43012259	43.61014254	6046.190655
GOA	98.84784599	1.083653014	0.572747632	50	7411.902278
SAO	5.133646976	2.527901755	5.801291717	1.559886276	7710.968222

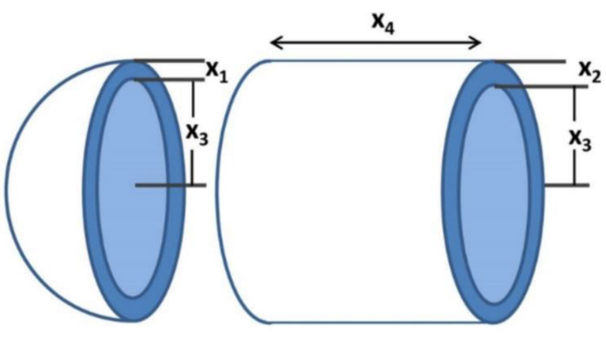

FIGURE 18. Schematic diagram of pressure vessel design problem.

Here, $x = [x1,x2]$ represent the design variables and are bounded as $0 \leq x1,x2 \leq 1$, $l = 100cm$, $P = 2KN/cm^2$ and $\sigma = 2KN/cm^2$.

Evaluation of the performance of the MBO was conducted against other notable algorithms in tackling the three-bar truss design problem. As per Table 21, the results indicate the MBO produced competitive results. The results show MBO was ranked second marginally behind HHO. Furthermore, Table 22 displays the promising variable values obtained by the MBO.

The comparative results in Table 22 underline the significance of the outcomes achieved by the MBO. Figure 21, on the other hand, illustrates the convergence behaviors of all the algorithms together with box plot analysis. Apart from SAO, which demonstrated premature convergence, all algorithms, including the MBO, exhibit similar convergence behavior towards the optimal solution. This set of results underscores the applicability and potency of the MBO in resolving complex optimization challenges in engineering design, illus-

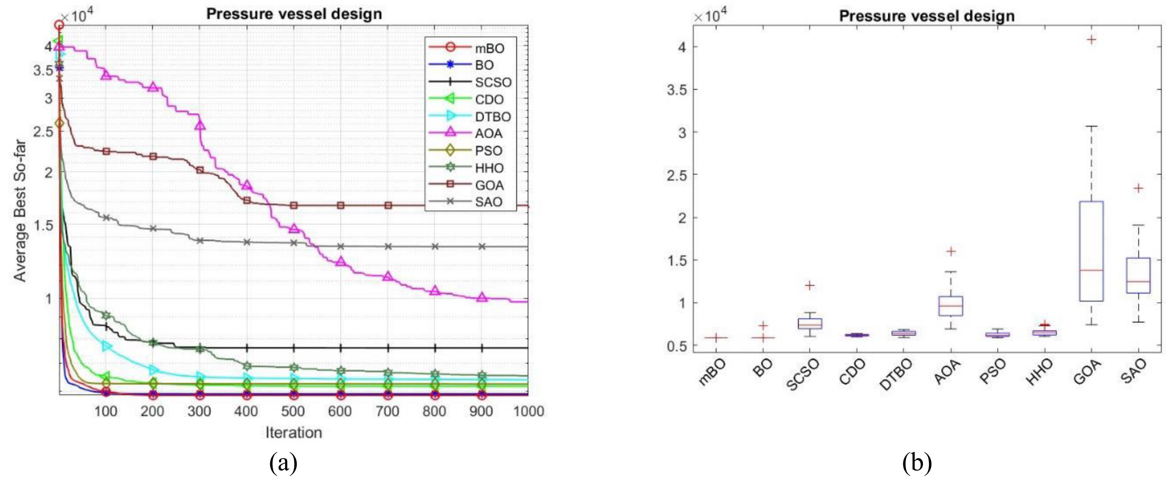

FIGURE 19. Convergence curve (a) and box plot analysis (b) of pressure vessel design problem.

TABLE 19. Results on multi-product batch plant design problem.

Metric	MBO	BO	SCSO	CDO	DTBO	AOA	PSO	HHO	GOA	SAO
Min	53638.90875	53650.70862	71922.31155	55185.49477	53640.1684	61148.57829	58506.0273	64778.06172	125170.1717	80120.89474
Max	66524.47923	71206.31488	348036840.1	71869.09789	74528.78789	75311.88766	71888.25657	90866.09212	47076277056	62776576306
Mean	59003.95388	59915.63046	56910823.18	60793.15118	61253.02059	67834.20267	61126.70911	74008.66858	3387482972	5119492390
Std	2511.100214	3389.287717	107140436.6	4118.938375	6642.884369	4023.977029	4792.113211	6004.124556	10317177553	12622897034
Rank	1	2	8	3	5	6	4	7	9	10

TABLE 20. Best found solution for each optimizer on optimal design of multi-product batch plant.

Optimizer	f_{best}	x_1	x_2	x_3	x_4	x_5	x_6	x_7	x_8	x_9	x_{10}
MBO	53650.708	0.51	0.51	0.51	960.57233	1440.8686	1317.7640	19.999856	16	238.90708	120.68905
BO	71922.311	1.5015956	1.5491555	0.51	723.89947	950.37770	886.56935	9.9882838	7.9947248	126.02175	73.556297
SCSO	55185.494	0.5159157	0.51	1.0944423	1031.2174	1461.1949	1401.2978	20	16	264.36330	111.06939
CDO	53640.168	0.5314267	0.5533582	0.6057438	963.19880	1444.7691	1309.7799	19.999841	15.999721	234.95954	123.31132
DTBO	61148.578	1.2009034	0.51	0.5502146	1265.2416	1779.3476	1572.1873	20	16	216.20158	157.03484
AOA	58506.027	1.8471407	1.9787795	0.6979384	479.38732	719.08099	663.02217	9.9998972	7.9999333	121.39266	59.150499
PSO	71922.311	1.5015956	1.5491555	0.51	723.89947	950.37770	886.56935	9.9882838	7.9947248	126.02175	73.556297
HHO	64778.061	1.7130520	1.5870872	1.1884228	524.30930	743.48044	1127.8208	9.9996105	8.0015610	150.05320	48.292759
GOA	125170.17	1.6385723	3.1110432	2.2668705	1145.7167	1248.9442	1296.4393	7.3161146	15.463408	140.06310	125.61797
SAO	80120.894	2.3244552	2.9001007	1.4359986	2.2091862	1.3937152	0.7920866	3.3411211	1.5030927	3.4199131	2.6397905

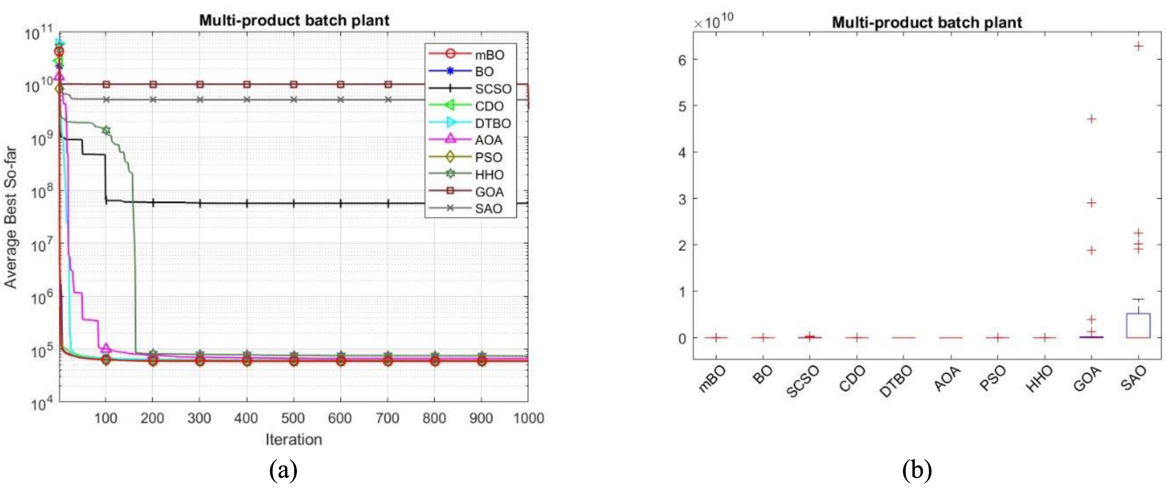

FIGURE 20. Convergence curve (a) and box plot analysis (b) of multi-product batch plant problem.

TABLE 21. Results on three-bar truss design problem.

Metric	MBO	BO	SCSO	CDO	DTBO	AOA	PSO	HHO	GOA	SAO
Min	263.8914911	263.8914911	263.8916052	263.8930202	263.8914912	264.053266	263.8914911	263.8915107	263.8914934	264.498931
Max	263.8914911	263.8914911	273.6139818	264.132097	263.8915532	282.8427125	263.8914931	264.484128	265.4966095	308.104155
Mean	263.8914911	263.8914911	264.8650814	263.9722302	263.8914986	266.7424364	263.8914912	264.0010432	264.2229931	274.0035172
Std	1.10708E-13	1.08162E-13	1.908696033	0.059718328	1.21452E-05	5.565890172	3.60964E-07	0.128725158	0.477901611	9.827148714
Rank	1	2	8	5	4	9	3	6	7	10

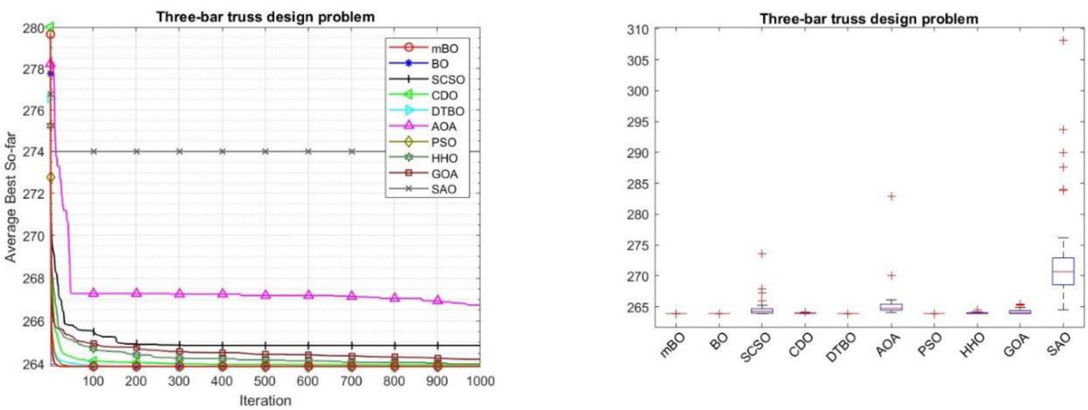

(a) (b)

FIGURE 21. Convergence curve (b) and box plot analysis (c) of three bar truss design problem.

TABLE 22. Best found solution for each optimizer on optimal design of three-bar truss problem.

Optimizer	f_{best}	x_1	x_2
MBO	263.8914911	0.788649119	0.408234832
BO	263.8916052	0.789037647	0.407134769
SCSO	263.8930202	0.789685237	0.405348301
CDO	263.8914912	0.788658213	0.408209223
DTBO	264.053266	0.798563719	0.381853375
AOA	263.8914911	0.78864912	0.408234829
PSO	263.8916052	0.789037647	0.407134769
HHO	263.8915107	0.788485951	0.408696537
GOA	263.8914934	0.788593071	0.408393389
SAO	264.498931	1	0.733031688

trating its potential for robust and reliable real-world implementations.

VI. CONCLUSION AND FUTURE WORKS

This study introduced a modified version of the bonobo optimizer, incorporating a new exploration stage, Gaussian local mutation, a restart strategy, and a random contraction strategy to enhance exploration and exploitation capabilities. Inspired by the unique social and reproductive behaviors of bonobos, the original bonobo optimizer had already demonstrated promise in solving optimization problems. The improvements made in MBO aimed at addressing specific challenges and further elevating its performance. The evaluation of MBO commenced with a rigorous benchmarking process using the CEC 2017 (10 and 100-dimensional) and CEC 2022 (10 and 20-dimensional) test suites, comparing its performance against established nature-inspired algorithms. The results indicated that MBO showcased remarkable efficiency. For instance, in the 10-dimensional CEC 2022 test suite, MBO achieved highly significant p-values of 2.53E-10 against BO, 1.25E-11 against SCSO, CDO, DTBO, AOA, and other algorithms on Function F22-01. Similarly, in higher dimensions, such as 20, MBO continued to outperform competitors, achieving significant p-values across functions like F22-01 and F22-02. The algorithm's robust performance can be attributed to its accelerated convergence rate, stability across diverse functions, good exploration-exploitation behavior, and adaptability to high-dimensional and complex solution spaces. Building upon this benchmarking foundation, MBO was then applied to seven real-world engineering optimization problems, spanning diverse domains such as structural design, refrigeration system design, and mechanical engineering. Across these challenges, MBO consistently outperformed its counterparts, exhibiting superior convergence rates and solution quality. The contributions of this work extend beyond showcasing MBO's proficiency in optimization tasks. The deliberate improvement strategy, involving accelerated convergence, stability across diverse functions, and adaptability to high-dimensional spaces, positions MBO as a reliable and efficient tool for addressing challenging engineering optimization problems. The study not only demonstrates the algorithm's enhanced performance but also provides insights into the systematic improvements that contributed to its success.

While the MBO has exhibited notable improvements in this study, there are avenues for further exploration and enhancement. Continued refinement of the algorithm parameters and strategies could lead to even better performance in specific problem domains. Fine-tuning could involve a systematic exploration of parameter spaces and their impacts on convergence and solution quality. Investigating the potential benefits of hybridizing MBO with other optimization algorithms could result in a more versatile and powerful optimization tool. Combining strengths from different algorithms might enhance overall performance across a broader range of problems. Incorporating mechanisms for dynamic adaptation of algorithm parameters during runtime could improve MBO's adaptability to evolving problem landscapes. Dynamic adaptation strategies could enhance the algorithm's ability to navigate changing optimization scenarios. Exploring methods to parallelize MBO and enhance its scalability can be crucial for handling larger and more complex optimization problems. Leveraging parallel computing resources could further boost the algorithm's efficiency. In conclusion, while MBO has shown promising results, ongoing research and development efforts can refine its capabilities and extend its applicability to a broader spectrum of optimization challenges.

ACKNOWLEDGMENT

This work was supported by Princess Nourah bint Abdulrahman University, Riyadh, Saudi Arabia, through the Researchers Supporting Project PNURSP2024R407. We would like to express our sincere gratitude to Ajman University for their generous support in covering the full Article Processing Charge (APC) for our publication in the IEEE Access Journal.

REFERENCES

[1] S. Ekinci, D. Izci, E. Eker, L. Abualigah, C.-L. Thanh, and S. Khatir, "Hunger games pattern search with elite opposite-based solution for solving complex engineering design problems," *Evolving Syst.*, vol. 15, no. 3, pp. 939–964, Jun. 2024, doi: 10.1007/s12530-023-09526-9.

[2] W. Zhao, L. Wang, Z. Zhang, H. Fan, J. Zhang, S. Mirjalili, N. Khodadadi, and Q. Cao, "Electric eel foraging optimization: A new bio-inspired optimizer for engineering applications," *Expert Syst. Appl.*, vol. 238, Mar. 2024, Art. no. 122200, doi: 10.1016/j.eswa.2023.122200.

[3] L. W. Theng et al., "Salak image classification method based deep learning technique using two transfer learning models," in *Classification Applications With Deep Learning and Machine Learning Technologies* (Studies in Computational Intelligence), vol. 1071, L. Abualigah Ed. Cham, Switzerland: Springer, 2023, doi: 10.1007/978-3-031-17576-3_4.

[4] D. Izci, S. Ekinci, and A. G. Hussien, "Effective PID controller design using a novel hybrid algorithm for high order systems," *PLoS ONE*, vol. 18, no. 5, May 2023, Art. no. e0286060, doi: 10.1371/journal.pone.0286060.

[5] Y. Tikhamarine, D. Souag-Gamane, A. Najah Ahmed, O. Kisi, and A. El-Shafie, "Improving artificial intelligence models accuracy for monthly streamflow forecasting using grey wolf optimization (GWO) algorithm," *J. Hydrol.*, vol. 582, Mar. 2020, Art. no. 124435, doi: 10.1016/j.jhydrol.2019.124435.

[6] N. Zhang, C. Li, R. Li, X. Lai, and Y. Zhang, "A mixed-strategy based gravitational search algorithm for parameter identification of hydraulic turbine governing system," *Knowledge-Based Syst.*, vol. 109, pp. 218–237, Oct. 2016, doi: 10.1016/j.knosys.2016.07.005.

[7] Y. Li, X. Chen, Y. An, Z. Zhao, H. Cao, and J. Jiang, "Integrating machine layout, transporter allocation and worker assignment into job-shop scheduling solved by an improved non-dominated sorting genetic algorithm," *Comput. Ind. Eng.*, vol. 179, May 2023, Art. no. 109169, doi: 10.1016/j.cie.2023.109169.

[8] S. Ekinci, H. Çetin, D. Izci, and E. Köse, "A novel balanced arithmetic optimization algorithm-optimized controller for enhanced voltage regulation," *Mathematics*, vol. 11, no. 23, p. 4810, Nov. 2023, doi: 10.3390/math11234810.

[9] S. Ekinci, C. Budak, D. Izci, and V. Gider, "An atom search optimization approach for IIR system identification," *Int. J. Model. Simul.*, pp. 1–17, Nov. 2023, doi: 10.1080/02286203.2023.2287968.

[10] M. E.-S.-M. Essa, M. Elsisi, M. S. Elsayed, M. F. Ahmed, and A. M. Elshafeey, "An improvement of model predictive for aircraft longitudinal flight control based on intelligent technique," *Mathematics*, vol. 10, no. 19, p. 3510, Sep. 2022, doi: 10.3390/math10193510.

[11] S. Ekinci, D. Izci, M. R. Al Nasar, R. A. Zitar, and L. Abualigah, "Logarithmic spiral search based arithmetic optimization algorithm with selective mechanism and its application to functional electrical stimulation system control," *Soft Comput.*, vol. 26, no. 22, pp. 12257–12269, Nov. 2022, doi: 10.1007/s00500-022-07068-x.

[12] H. Ali, S. Das, and A. Akbar Shaikh, "Investigate an imperfect green production system considering rework policy via teaching-learning-based optimizer algorithm," *Expert Syst. Appl.*, vol. 214, Mar. 2023, Art. no. 119143, doi: 10.1016/j.eswa.2022.119143.

[13] R. J. Kuo, M. F. Luthfiansyah, N. A. Masruroh, and F. Eva Zulvia, "Application of improved multi-objective particle swarm optimization algorithm to solve disruption for the two-stage vehicle routing problem with time windows," *Expert Syst. Appl.*, vol. 225, Sep. 2023, Art. no. 120009, doi: 10.1016/j.eswa.2023.120009.

[14] S. Ekinci, D. Izci, L. Abualigah, A. G. Hussien, C.-L. Thanh, and S. Khatir, "Revolutionizing vehicle cruise control: An elite opposition-based pattern search mechanism augmented INFO algorithm for enhanced controller design," *Int. J. Comput. Intell. Syst.*, vol. 16, no. 1, p. 129, Aug. 2023, doi: 10.1007/s44196-023-00304-8.

[15] J. Too and A. R. Abdullah, "Chaotic atom search optimization for feature selection," *Arabian J. Sci. Eng.*, vol. 45, no. 8, pp. 6063–6079, Aug. 2020, doi: 10.1007/s13369-020-04486-7.

[16] D. Izci, E. Köse, and S. Ekinci, "Feedforward-compensated PI controller design for air–fuel ratio system control using enhanced weighted mean of vectors algorithm," *Arabian J. Sci. Eng.*, vol. 48, no. 9, pp. 12205–12217, Sep. 2023, doi: 10.1007/s13369-023-07724-w.

[17] D. Izci, "A novel modified arithmetic optimization algorithm for power system stabilizer design," *Sigma J. Eng. Natural Sci.*, vol. 40, no. 3, pp. 529–541, 2022, doi: 10.14744/sigma.2022.00056.

[18] J. Wang, C. Zhan, S. Li, Q. Zhao, J. Liu, and Z. Xie, "Adaptive variational mode decomposition based on archimedes optimization algorithm and its application to bearing fault diagnosis," *Measurement*, vol. 191, Mar. 2022, Art. no. 110798, doi: 10.1016/j.measurement.2022.110798.

[19] W. Zhao, K. Wang, Y. Ju, L. Fan, H. Cao, Y. Yang, L. Shu, Z. Feng, R. Cui, X. Guo, and L. Wang, "Quantification of the asynchronous gas diffusivity in macro-/micropores using a Nelder-Mead simplex algorithm and its application on predicting desorption-based indexes," *Fuel*, vol. 332, Jan. 2023, Art. no. 126149, doi: 10.1016/j.fuel.2022.126149.

[20] L. Nurbekyan, W. Lei, and Y. Yang, "Efficient natural gradient descent methods for large-scale PDE-based optimization problems," *SIAM J. Sci. Comput.*, vol. 45, no. 4, pp. A1621–A1655, Aug. 2023, doi: 10.1137/22m1477805.

[21] J. Liao, G. Qiu, Y. Huang, and V. Khadkikar, "Lagrange multiplier based control method to optimize efficiency for four-switch buck-boost converter over whole operating range," *IEEE Trans. Ind. Electron.*, vol. 71, no. 1, pp. 822–833, Jan. 2024, doi: 10.1109/TIE.2023.3250745.

[22] B. A. Hassan and I. A. R. Moghrabi, "A modified secant equation quasi-Newton method for unconstrained optimization," *J. Appl. Math. Comput.*, vol. 69, no. 1, pp. 451–464, Feb. 2023, doi: 10.1007/s12190-022-01750-x.

[23] K. Li, X. Yan, and Y. Han, "Multi-mechanism swarm optimization for multi-UAV task assignment and path planning in transmission line inspection under multi-wind field," *Appl. Soft Comput.*, vol. 150, Jan. 2024, Art. no. 111033, doi: 10.1016/j.asoc.2023.111033.

[24] J. O. Agushaka, A. E. Ezugwu, and L. Abualigah, "Dwarf mongoose optimization algorithm," *Comput. Methods Appl. Mech. Eng.*, vol. 391, Mar. 2022, Art. no. 114570, doi: 10.1016/j.cma.2022.114570.

[25] K. Rajwar, K. Deep, and S. Das, "An exhaustive review of the metaheuristic algorithms for search and optimization: Taxonomy, applications, and open challenges," *Artif. Intell. Rev.*, vol. 56, no. 11, pp. 13187–13257, Nov. 2023, doi: 10.1007/s10462-023-10470-y.

[26] W. Zhao, L. Wang, Z. Zhang, S. Mirjalili, N. Khodadadi, and Q. Ge, "Quadratic interpolation optimization (QIO): A new optimization algorithm based on generalized quadratic interpolation and its applications to real-world engineering problems," *Comput. Methods Appl. Mech. Eng.*, vol. 417, Dec. 2023, Art. no. 116446, doi: 10.1016/j.cma.2023.116446.

[27] L. Abualigah, M. A. Elaziz, P. Sumari, Z. W. Geem, and A. H. Gandomi, "Reptile search algorithm (RSA): A nature-inspired meta-heuristic optimizer," *Expert Syst. Appl.*, vol. 191, Apr. 2022, Art. no. 116158, doi: 10.1016/j.eswa.2021.116158.

[28] K. Wang, M. Guo, C. Dai, Z. Li, C. Wu, and J. Li, "An effective metaheuristic technology of people duality psychological tendency and feedback mechanism-based inherited optimization algorithm for solving engineering applications," *Expert Syst. Appl.*, vol. 244, Jun. 2024, Art. no. 122732, doi: 10.1016/j.eswa.2023.122732.

[29] M. Dehghani, Z. Montazeri, E. Trojovská, and P. Trojovský, "Coati optimization algorithm: A new bio-inspired metaheuristic algorithm for solving optimization problems," *Knowl.-Based Syst.*, vol. 259, Jan. 2023, Art. no. 110011, doi: 10.1016/j.knosys.2022.110011.

[30] A. S. Joshi, O. Kulkarni, G. M. Kakandikar, and V. M. Nandedkar, "Cuckoo search optimization—A review," *Mater. Today, Proc.*, vol. 4, no. 8, pp. 7262–7269, 2017, doi: 10.1016/j.matpr.2017.07.055.

[31] S. Ekinci and D. Izci, "Enhanced reptile search algorithm with Lévy flight for vehicle cruise control system design," *Evol. Intell.*, vol. 16, no. 4, pp. 1339–1351, Aug. 2023, doi: 10.1007/s12065-022-00745-8.

[32] A. Kirimtat, M. F. Tasgetiren, O. Krejcar, O. Buyukdagli, and P. Maresova, "A multi-objective optimization framework for functional arrangement in smart floating cities," *Expert Syst. Appl.*, vol. 237, Mar. 2024, Art. no. 121476, doi: 10.1016/j.eswa.2023.121476.

[33] D. Karakatsanis and N. Theodossiou, "Smart hydropower water distribution networks, use of artificial intelligence methods and metaheuristic algorithms to generate energy from existing water supply networks," *Energies*, vol. 15, no. 14, p. 5166, Jul. 2022, doi: 10.3390/en15145166.

[34] M. Ragab, E. B. Ashary, W. H. Aljedaibi, I. R. Alzahrani, A. Kumar, D. Gupta, and R. F. Mansour, "A novel metaheuristics with adaptive neuro-fuzzy inference system for decision making on autonomous unmanned aerial vehicle systems," *ISA Trans.*, vol. 132, pp. 16–23, Jan. 2023, doi: 10.1016/j.isatra.2022.04.006.

[35] V. Sharma and A. K. Tripathi, "A systematic review of meta-heuristic algorithms in IoT based application," *Array*, vol. 14, Jul. 2022, Art. no. 100164, doi: 10.1016/j.array.2022.100164.

[36] G. Hu, Y. Guo, G. Wei, and L. Abualigah, "Genghis khan shark optimizer: A novel nature-inspired algorithm for engineering optimization," *Adv. Eng. Informat.*, vol. 58, Oct. 2023, Art. no. 102210, doi: 10.1016/j.aei.2023.102210.

[37] D. H. Wolpert and W. G. Macready, "No free lunch theorems for optimization," *IEEE Trans. Evol. Comput.*, vol. 1, no. 1, pp. 67–82, Apr. 1997, doi: 10.1109/4235.585893.

[38] P. Sharma and S. Raju, "Metaheuristic optimization algorithms: A comprehensive overview and classification of benchmark test functions," *Soft Comput.*, vol. 28, no. 4, pp. 3123–3186, Oct. 2023, doi: 10.1007/s00500-023-09276-5.

[39] L. Velasco, H. Guerrero, and A. Hospitaler, "A literature review and critical analysis of metaheuristics recently developed," *Arch. Comput. Methods Eng.*, vol. 31, no. 1, pp. 125–146, Jul. 2023, doi: 10.1007/s11831-023-09975-0.

[40] A. K. Das and D. K. Pratihar, "Bonobo optimizer (BO): An intelligent heuristic with self-adjusting parameters over continuous spaces and its applications to engineering problems," *Int. J. Speech Technol.*, vol. 52, no. 3, pp. 2942–2974, Feb. 2022, doi: 10.1007/s10489-021-02444-w.

[41] L. Deng and S. Liu, "Snow ablation optimizer: A novel metaheuristic technique for numerical optimization and engineering design," *Expert Syst. Appl.*, vol. 225, Sep. 2023, Art. no. 120069, doi: 10.1016/j.eswa.2023.120069.

[42] A. Seyyedabbasi and F. Kiani, "Sand cat swarm optimization: A nature-inspired algorithm to solve global optimization problems," *Eng. With Comput.*, vol. 39, no. 4, pp. 2627–2651, Aug. 2023, doi: 10.1007/s00366-022-01604-x.

[43] H. A. Shehadeh, "Chernobyl disaster optimizer (CDO): A novel meta-heuristic method for global optimization," *Neural Comput. Appl.*, vol. 35, no. 15, pp. 10733–10749, May 2023, doi: 10.1007/s00521-023-08261-1.

[44] M. Dehghani, E. Trojovská, and P. Trojovský, "A new human-based metaheuristic algorithm for solving optimization problems on the base of simulation of driving training process," *Sci. Rep.*, vol. 12, no. 1, p. 9924, Jun. 2022, doi: 10.1038/s41598-022-14225-7.

[45] A. A. Heidari, S. Mirjalili, H. Faris, I. Aljarah, M. Mafarja, and H. Chen, "Harris hawks optimization: Algorithm and applications," *Future Gener. Comput. Syst.*, vol. 97, pp. 849–872, Aug. 2019, doi: 10.1016/j.future.2019.02.028.

[46] F. A. Hashim, K. Hussain, E. H. Houssein, M. S. Mabrouk, and W. Al-Atabany, "Archimedes optimization algorithm: A new metaheuristic algorithm for solving optimization problems," *Appl. Intell.*, vol. 51, no. 3, pp. 1531–1551, Mar. 2021, doi: 10.1007/s10489-020-01893-z.

[47] A. T. Salawudeen, M. B. Mu'azu, Y. A. Sha'aban, and A. E. Adedokun, "A novel smell agent optimization (SAO): An extensive CEC study and engineering application," *Knowl.-Based Syst.*, vol. 232, Nov. 2021, Art. no. 107486, doi: 10.1016/j.knosys.2021.107486.

[48] Y. Meraihi, A. B. Gabis, S. Mirjalili, and A. Ramdane-Cherif, "Grasshopper optimization algorithm: Theory, variants, and applications," *IEEE Access*, vol. 9, pp. 50001–50024, 2021, doi: 10.1109/ACCESS.2021.3067597.

[49] R. Poli, J. Kennedy, and T. Blackwell, "Particle swarm optimization," *Swarm Intell.*, vol. 1, no. 1, pp. 33–57, Oct. 2007, doi: 10.1007/s11721-007-0002-0.

[50] H. Nenavath and R. K. Jatoth, "Hybridizing sine cosine algorithm with differential evolution for global optimization and object tracking," *Appl. Soft Comput.*, vol. 62, pp. 1019–1043, Jan. 2018, doi: 10.1016/j.asoc.2017.09.039.

[51] M. A. Tolba, E. H. Houssein, M. H. Ali, and F. A. Hashim, "A new robust modified capuchin search algorithm for the optimum amalgamation of DSTATCOM in power distribution networks," *Neural Comput. Appl.*, vol. 36, no. 2, pp. 843–881, Jan. 2024, doi: 10.1007/s00521-023-09064-0.

[52] E. H. Houssein, D. Oliva, N. A. Samee, N. F. Mahmoud, and M. M. Emam, "Liver cancer algorithm: A novel bio-inspired optimizer," *Comput. Biol. Med.*, vol. 165, Oct. 2023, Art. no. 107389, doi: 10.1016/j.compbiomed.2023.107389.

[53] R. R. Mostafa, A. A. Ewees, R. M. Ghoniem, L. Abualigah, and F. A. Hashim, "Boosting chameleon swarm algorithm with consumption AEO operator for global optimization and feature selection," *Knowl.-Based Syst.*, vol. 246, Jun. 2022, Art. no. 108743, doi: 10.1016/j.knosys.2022.108743.

[54] T. Kano, "An ecological study of the pygmy chimpanzees (*Pan paniscus*) of Yalosidi, Republic of Zaire," *Int. J. Primatol.*, vol. 4, no. 1, pp. 1–31, Mar. 1983, doi: 10.1007/bf02739358.

[55] F. B. M. D. Waal, "Bonobo sex and society," *Sci. Amer.*, vol. 272, no. 3, pp. 82–88, Mar. 1995, doi: 10.1038/scientificamerican0395-82.

[56] P. S. Meilinger, R. Wrangham, D. Peterson, L. H. Keeley, and J. Keegan, "Demonic males: Apes and the origins of human violence," *J. Mil. Hist.*, vol. 61, no. 3, p. 598, Jul. 1997, doi: 10.2307/2954037.

[57] T. Kano, "Male rank order and copulation rate in a unit-group of bonobos at Wamba, Za?re," in *Great Ape Societies*, L. F. Marchant, W. C. McGrew, and T. Nishida, Eds., Cambridge, U.K.: Cambridge Univ. Press, 1996, pp. 135–145, doi: 10.1017/CBO9780511752414.012.

[58] A. K. Das and D. K. Pratihar, "A new bonobo optimizer (BO) for real-parameter optimization," in *Proc. IEEE Region Symp. (TENSYMP)*, Jun. 2019, pp. 108–113, doi: 10.1109/TENSYMP46218.2019.8971108.

[59] S. Ekinci and D. Izci, "Enhancing IIR system identification: Harnessing the synergy of gazelle optimization and simulated annealing algorithms," *e-Prime Adv. Electr. Eng., Electron. Energy*, vol. 5, Sep. 2023, Art. no. 100225, doi: 10.1016/j.prime.2023.100225.

[60] Y. Duan, C. Liu, S. Li, X. Guo, and C. Yang, "Manta ray foraging and Gaussian mutation-based elephant herding optimization for global optimization," *Eng. With Comput.*, vol. 39, no. 2, pp. 1085–1125, Apr. 2023, doi: 10.1007/s00366-021-01494-5.

[61] S. Song, P. Wang, A. A. Heidari, M. Wang, X. Zhao, H. Chen, W. He, and S. Xu, "Dimension decided Harris hawks optimization with Gaussian mutation: Balance analysis and diversity patterns," *Knowl.-Based Syst.*, vol. 215, Mar. 2021, Art. no. 106425, doi: 10.1016/j.knosys.2020.106425.

[62] A. Taheri, K. RahimiZadeh, and R. V. Rao, "An efficient balanced teaching-learning-based optimization algorithm with individual restarting strategy for solving global optimization problems," *Inf. Sci.*, vol. 576, pp. 68–104, Oct. 2021, doi: 10.1016/j.ins.2021.06.064.

[63] M. Zhang, Q. Wu, H. Chen, A. A. Heidari, Z. Cai, J. Li, E. M. Abdelrahim, and R. F. Mansour, "Whale optimization with random contraction and Rosenbrock method for COVID-19 disease prediction," *Biomed. Signal Process. Control*, vol. 83, May 2023, Art. no. 104638, doi: 10.1016/j.bspc.2023.104638.

[64] D. Izci, S. Ekinci, E. Eker, and M. Kayri, "Augmented hunger games search algorithm using logarithmic spiral opposition-based learning for function optimization and controller design," *J. King Saud Univ. Eng. Sci.*, vol. 36, no. 5, pp. 330–338, Jul. 2024, doi: 10.1016/j.jksues.2022.03.001.

[65] M. Abdel-Basset, R. Mohamed, S. A. A. Azeem, M. Jameel, and M. Abouhawwash, "Kepler optimization algorithm: A new metaheuristic algorithm inspired by Kepler's laws of planetary motion," *Knowl.-Based Syst.*, vol. 268, May 2023, Art. no. 110454, doi: 10.1016/j.knosys.2023.110454.
[66] M. Abdel-Basset, D. El-Shahat, M. Jameel, and M. Abouhawwash, "Exponential distribution optimizer (EDO): A novel math-inspired algorithm for global optimization and engineering problems," *Artif. Intell. Rev.*, vol. 56, no. 9, pp. 9329–9400, Sep. 2023, doi: 10.1007/s10462-023-10403-9.
[67] N. Andrei, "Nonlinear optimization applications using the GAMS technology," in *Springer Optimization and Its Applications*, vol. 81. Boston, MA, USA: Springer, 2013, doi: 10.1007/978-1-4614-6797-7.
[68] F. Verbiest, T. Cornelissens, and J. Springael, "A matheuristic approach for the design of multiproduct batch plants with parallel production lines," *Eur. J. Oper. Res.*, vol. 273, no. 3, pp. 933–947, Mar. 2019, doi: 10.1016/j.ejor.2018.09.012.

MAALI ALABDULHAFITH (Member, IEEE) was born in Saudi Arabia, in September 1985. She received the Doctor of Philosophy (Ph.D.) degree in computer science from Dalhousie University, Halifax, Canada, in 2017. In 2014, she joined the College of Computer and Information Science (CCIS), Princess Noura University (PNU), as a Lecturer and was promoted to an Assistant Professor, in 2018. Her research interests include machine learning, data analytics, emerging wireless technology, and technology applications in health care. Currently, she is the Director of Data Management and Performance Measurement with CCIS, PNU, overlooking and managing the strategy of the college.

HARSHIT BATRA is currently pursuing the Graduate degree with the Department of Computer Science & Engineering, Netaji Subhas University of Technology, Dwarka, New Delhi, India. He also conducted research with the Centre of Excellence in AI, Netaji Subhas University of Technology. Currently, he is the Chief Technology Officer of Anup Capital.

NAGWAN M. ABDEL SAMEE received the B.S. degree in computer engineering from Ein Shams University, Egypt, in 2000, and the M.S. degree in computer engineering and the Ph.D. degree in systems and biomedical engineering from Cairo University, Egypt, in 2008 and 2012, respectively. Since 2013, she has been an Assistant Professor with the Information Technology Department, CCIS, Princess Nourah bint Abdulrahman University, Riyadh, Saudi Arabia. Her research interests include data science, machine learning, bioinformatics, and parallel computing. His awards and honors include the Takafull Prize (Innovation Project Track), Princess Nourah Award in Innovation, Mastery Award in Predictive Analytics (IBM), Mastery Award in Big Data (IBM), and Mastery Award in Cloud Computing (IBM).

MOHAMMED AZMI AL-BETAR (Member, IEEE) received the Ph.D. degree in artificial intelligence from Universiti Sains Malaysia (USM), in 2010. He was a Postdoctoral Research Fellow with USM, for three years, and invited as a Visiting Researcher two times. He is currently the Head of the Artificial Intelligence Research Center (AIRC), Ajman University, where he has been a full-time Faculty Member with the Master of Artificial Intelligence (MSAI) Program, since 2020. He is also the Head of the Evolutionary Computation Research Group (ECRG). He has more than 15 years of teaching experience in higher education institutions. He has taught several courses in computer science and artificial intelligence fields. He has published more than 175 scientific publications in high-quality and well-reputed journals and conferences. He ranked in Stanford's study of the world's top 2% of scientists. His main research interests include scheduling and optimization.

AMMAR ALMOMANI received the Ph.D. degree from Universiti Sains Malaysia (USM) in 2013. Currently, he is an academic member of the Computer Information Science (CIS) program, Bachelor of Cybersecurity at the Higher Colleges of Technology (HCT), Sharjah, UAE. He has received numerous international awards and supervises several Ph.D. students from the U.K., and Malaysia. He has demonstrated experience in writing and securing grants and contracts with various universities. He has published over 150 articles, conference papers, and books, with most being in Scopus Q1, Q2, and WoS journals. His work includes ten patents from Germany and India. His research interests include cybersecurity based on artificial intelligence, and his research record includes 90 Scopus articles. He has over 100,000 readers and followers on ResearchGate.

DAVUT IZCI received the B.Sc. degree in electrical and electronic engineering from Dicle University, Türkiye, and the M.Sc. degree in mechatronics and the Ph.D. degree in microsystem from Newcastle University, England, U.K. He is currently an Associate Professor working on optimization, control system design, sensing applications, energy harvesting, microsystems development and applications of metaheuristic optimization techniques to different control systems, and real-world engineering problems. He has published more than 100 articles in prestigious international journals. He is also a member of the Editorial Board in *e-Prime Journal* (Elsevier) and serves as a reviewer for several top tier journals in the field of metaheuristics, artificial intelligence, and control systems. He is recognized as one of the world's top 2% scientists by Elsevier and Stanford University.

SERDAR EKINCI received the B.Sc. degree in control engineering and the M.Sc. and Ph.D. degrees in electrical engineering from Istanbul Technical University (ITU), in 2007, 2010, and 2015, respectively. He is currently an Associate Professor with the Department of Computer Engineering, Batman University, Türkiye. His research interests include electrical power systems, stability, control technology, and the applications of metaheuristic optimization algorithms to various control systems.

FATMA A. HASHIM received the M.Sc. degree in biomedical engineering from the Biomedical Engineering Department, Helwan University, "optic disc detection in retinal fundus images," in 2014. She studied in the ITI "System Development Department," in 2009. Her research interests include image processing, signal processing, bioinformatics, optimization, and metaheuristics. Along with her career, she was a technical reviewer and an editorial board member for several international journals. She has more than 20 scientific research papers published in prestigious international journals in the topics of medical imaging processing, bioinformatics, machine learning and its applications. Her research interests include image processing, signal processing, artificial intelligence, bioinformatics, optimization, and metaheuristics. She is serving as a Reviewer for several journals, including: *Knowledge-Based Systems*, *Applied Soft Computing*, and *Engineering Applications of Artificial Intelligence*. She is participating as an Editor of *Applied Soft Computing*, *Information Sciences*, *Journal of Ophthalmological Diseases*, and *Journal of Electronic Research and Application*.